

Mechanistic studies of the electrochemical reduction of the cadmium ion

Studies over het mechanisme van de elektrochemische reduktie van het cadmium ion

(met een samenvatting in het Nederlands)

Proefschrift

ter verkrijging van de graad van Doctor aan de
Rijksuniversiteit te Utrecht, op gezag van de
Rector Magnificus Prof.dr. J.A. van Ginkel,
ingevolge het besluit van het college van deka-
nen in het openbaar te verdedigen op maandag
18 maart 1991 des morgens te 10.30 uur.

door

Machiel Saakes

geboren op 13 september 1960 te Waalwijk.

Promotor : Prof.dr. J.H. Sluyters

Co-promotor : Dr. M. Sluyters-Rehbach

Aan mijn ouders

VOORWOORD

Bij het afronden van dit proefschrift wil ik iedereen van harte bedanken die in enigerlei opzicht heeft bijgedragen aan de totstandkoming ervan.

In het bijzonder wil ik daarbij aandacht voor de volgende medewerkers.

In de eerste plaats mijn promotor Prof. dr. J.H. Sluyters.

Hooggeleerde Sluyters, beste Jan, het is mij altijd een voorrecht en genoeg geweest onder jouw inspirerende leiding te hebben mogen werken. Vooral je heldere ideeën over het doel van mijn verrichte werkzaamheden heb ik als erg nuttig ervaren.

In de tweede plaats mijn co-promotor Dr. M. Sluyters-Rehbach. Zeer geleerde Sluyters-Rehbach, beste Greet, jouw theoretische inbreng en waardevolle suggesties met betrekking tot de uitwerking van de verrichte experimenten zijn essentieel geweest voor het uiteindelijke resultaat. Met name ook voor je hulp bij het laatste hoofdstuk ben ik je dankbaar.

Voorts wil ik van de gelegenheid gebruik maken een aantal medewerkers te bedanken die werkzaam waren in de werkgroep Elektrochemie ten tijde van mijn bijvak en aansluitende promotie-aanstelling.

In de eerste plaats de vorige "generatie" promovendi te weten Kees van Velzen, Gert-Jan Brug en Ad van den Eeden.

Voorts een aantal mede promovendi.

Allereerst mijn kamergenoten: Wim Mulder, met wie ik op plezierige wijze talrijke fysieke en chemische zaken heb besproken en Ricardo Souto met wie ik samen heb gewerkt aan een tweetal publikaties. Verder Jack Wijenberg die twee jaar later in dienst trad.

De assistentie van Jacques Oostveen op experimenteel gebied heb ik zeer gewaardeerd.

Uiteraard is elektrochemisch werk alleen mogelijk met een geschikte elektronische ondersteuning. Daarvoor bedank ik de medewerkers van de afdeling elektronica en met name Harry van der Wildt, B. Goes en G. van Vliet, die altijd paraat stonden.

Daarnaast ben ik dank verschuldigd aan Igno Dur vanwege zijn glasmaesterlijke bijdrage.

Voor het typewerk van hoofdstuk 2, 3 en 4 wil ik Marina Uit de Bulten en Margaret de Groot hartelijk danken. Theo Schroote verzorgde op accurate wijze de tekeningen. De overige medewerkers van het Van 't Hoff laboratorium hebben zorg gedragen voor een uitstekend klimaat om in te mogen werken.

Voor de mogelijkheden geboden bij de afronding van mijn proefschrift ben ik de Directie van de Hoofdgroep Maatschappelijke Technologie van TNO te Delft mijn dank verschuldigd. Daarbij wil ik Els Zwart bedanken voor de typografische verzorging van de resterende hoofdstukken.

Tenslotte wens ik mijn opvolger Stefan veel succes toe en wil ik mijn vrienden bedanken voor de prettige tijd tijdens en na mijn Utrechtse universitaire tijd.

The following chapters of this thesis have been published in or will be submitted to the *Journal of Electroanalytical Chemistry and Interfacial Electrochemistry* :

Chapter 2

The mechanism of the reduction of cadmium ions at a dropping mercury electrode from NaClO₄ base electrolyte solutions with varied water activity

M. Saakes, M. Sluyters-Rehbach and J.H. Sluyters,
J.Electroanal.Chem., 259 (1989)265-284.

Chapter 3

The reaction pathway of the Cd(II) reduction in mixed (0.8-x)M NaClO₄ + xM NaF base electrolytes

M. Saakes, M. Sluyters-Rehbach, R.M. Souto and J.H. Sluyters,
J.Electroanal.Chem., 264 (1989)217-234.

Chapter 4

The inhibition of Cd(II) reduction at the DME from aqueous 1 M NaClO₄ by sucrose

M. Saakes, M. Sluyters-Rehbach and J.H. Sluyters,
J.Electroanal.Chem., 282 (1990)161-174.

Chapter 5

The investigation of the adsorptive behaviour of electroactive species by means of demodulation voltammetry

M. Saakes, M. Sluyters-Rehbach and J.H. Sluyters,
J.Electroanal.Chem., to be submitted.

Chapters 2, 3 and 4 have been reproduced from the *Journal of Electroanalytical and Interfacial Electrochemistry* with permission from the copyright holder, Elsevier Sequoia S.A.

CONTENTS

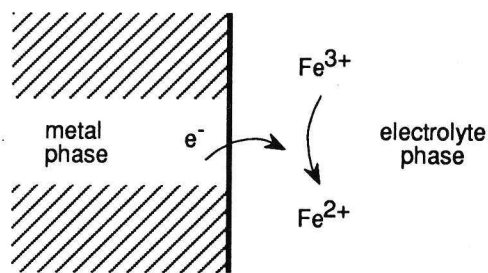
	page
1. GENERAL INTRODUCTION	13
2. THE MECHANISM OF THE REDUCTION OF CADMIUM IONS AT A DROPPING MERCURY ELECTRODE FROM NaClO ₄ BASE ELECTROLYTE SOLUTIONS WITH VARIED WATER ACTIVITY	21
3. THE REACTION PATHWAY OF THE Cd(II) REDUCTION IN MIXED (0.8-X)M NaClO ₄ + X M NaF BASE ELECTROLYTES	41
4. THE INHIBITION OF Cd(II) REDUCTION AT THE DME FROM AQUEOUS 1 M NaClO ₄ BY SUCROSE	59
5. THE INVESTIGATION OF THE ADSORPTIVE BEHAVIOUR OF ELECTROACTIVE SPECIES BY MEANS OF DEMODULATION VOLTAMMETRY	73
SUMMARY	99
SAMENVATTING	103
CURRICULUM VITAE	107

CHAPTER 1

GENERAL INTRODUCTION

In a metal electrical conduction proceeds via transport of electrons and in an electrolyte via movement of ions. Necessarily at the interface between a metallic phase and an electrolyte special processes have to occur, so-called electrode processes, if an electric current passes the interface.

An overall electrode process can be pictured intuitively as follows:



representing the reduction of a ferric ion to a ferrous ion by an electron emerging from the metal:



This model suffices to understand the two basic and classical laws of electrochemistry, which are

- (i) Faraday's law, saying that there is a stoichiometry also in electrochemical reactions and
- (ii) Nernst's law expressing the equilibrium condition for an electrochemical reaction.

Although the stoichiometry can be difficult to be unravelled in the case of complex electrode reactions, there is no reason to assume any basic difficulties in connection with Faraday's law. Also Nernst's law as it is derived either from thermodynamic arguments or via kinetics is inviolable, provided that it is realized that solutions do not behave ideal which especially for charged particles necessitates to assume the existence of interactions that express themselves in the form of complications like activity coefficients, ion pairing, incomplete dissociation, complexation, solvation etc. Although quantitatively such compli-

cations on Nernst's law can be considerable, the underlying effects, however complex they may be, still can be considered as understood in principle.

On the contrary, the processes that occur on an atomic scale at the phase boundary between the electrolyte and the metal when an electric current passes the interface are basically less well understood. This is not surprising, because the comprehension of a process is always developed less than the concomitant equilibrium. A clear example in chemistry is the mass action law that describes chemical equilibrium quite well with an equilibrium constant, while the theory of chemical reaction rate still mainly has to manage with much less securely founded concepts like activation energy, frequency factor, collisional cross section and the like.

In electrochemical kinetics the process is still further complicated because essentially there the process is the transfer of an electron, the movement of which, because of its low mass, should be described by quantum mechanics. Such theories have been developed since the earliest days of quantum mechanics and in fact a calculation of the rate of the proton reduction by Gurney [1] in 1931 was one of the earliest applications of quantum mechanics.

Such basic theories on electron transfer as yet have found little application and mostly experimental results have been interpreted in terms of the Butler-Volmer theory [2], that actually states that for an electron transfer the "normal" Eyring theory of the activated state should hold with the extension that the activation free energy of the electron transfer process as a first approximation should be linearly dependent on the potential difference E traversed by the electron:

$$G_{\text{act}} = G_{\text{act}}(E=0) + \alpha FE$$

Such a linear relationship explains the empirical linear relationship between the electrode potential and the logarithm of the faradaic current j_F discovered as early as 1905 by Tafel [3]. The proportionality constant α is the so called transfer coefficient, that is inversely proportional to the Tafel slope, $b = dE/d \ln j_F = -RT/\alpha F$. As yet the transfer coefficient is a not too well understood parameter that because an activation energy cannot be negative always should obey the condition $0 < \alpha < 1$.

Connecting the Butler-Volmer theory with the above-mentioned basic theories seems to indicate that α should be close to 0.5 and should weakly and linearly depend on the electrode potential (Marcus' theory [4]).

Experimental justification and confirmation as yet is missing because no electrode reaction seems to exist the mechanism of which indeed consists above suspicion of one single electron transfer solely. A potential dependence of the transfer coefficient as it is predicted by

Marcus' theory will be small as compared with the effect resulting from a complex mechanism of the electrode reaction. For example, if the one-electron transfer process discussed above is both preceded and followed by a (potential independent) heterogeneous chemical reaction step, i.e. if a so called CEC mechanism prevails, the overall reduction rate constant, k_f , will obey the relationship

$$\frac{1}{k_f} = \frac{1}{B_0} + \frac{\exp\left(\frac{\alpha F}{RT} (E-E^0)\right)}{A_1} + \frac{\exp\left(\frac{F}{RT} (E-E^0)\right)}{B_1}$$

where E^0 is the standard potential, and B_0 , A_1 and B_1 are constants. Clearly, going from far positive to far negative potentials, the "overall" or "operational transfer coefficient", defined as

$$- (RT/F) d \ln k_f/dE$$

will vary from unity to zero. For this reason it will be hardly possible to prove Marcus' theory by experiment, even with a favourable choice of the electrode reaction and while applying the best experimental techniques.

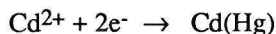
So the best that can be done at the moment seems to be to acquire data on suitable model electrode reactions and to analyse these data on the assumption that transfer coefficients of single electron transfers always are equal to 0.5, independent of electrode potential. Indeed it seems that analyses of experimental data starting with this assumption lead to good quantitative agreement with some appropriate mechanism. This has been the guiding principle for a number of years in our laboratory [5-14] and it will do so in this thesis as well.

The nature of the mechanism of an electrode reaction can be found from the potential dependence of its reduction rate constant. This rate constant has to be known with the highest possible accuracy and in the widest possible potential range. To that end the impedance technique [5] and the demodulation technique [6] have been developed with which it appeared possible to achieve the accuracy needed.

From the potential dependence of the reduction rate constant, obtained via these techniques, it was found that next to the electron transfer(s) the presence of additional steps in the mechanism had to be assumed, the rate constant of which is independent of electrode potential. These steps were found in the reduction of Cd^{2+} in different base electrolyte solutions [7-10] and also in the reduction of Fe^{3+} -oxalate [11] at mercury electrodes. The nature of these steps is still not clear, though it has been speculated that they should be

identified with the creation of a configuration at the interface that is necessary for the probability of electron transfer to acquire an appreciable value [10,11].

In this thesis it is attempted to study the model electrode reaction



that earlier [7-10] has been found to proceed via a CEE mechanism, i.e. the reaction rate is controlled by successively a heterogeneous chemical step and two single electron transfer steps, at varied circumstances.

It is well known that especially cations in aqueous solution are hydrated. Because ultimately the reduction product is a cadmium atom dissolved in the mercury phase, necessarily the cadmium ion has to lose its hydration shell and it is of interest to see the sequence in which this happens during the electrochemical reduction. We will do this following an earlier study on the Zn^{2+} reduction by Andreu, Sluyters-Rehbach and Sluyters [12] by varying water activity. The cadmium ion reduction is more complex because of the presence of the additional preceding chemical step that did not occur in the Zn^{2+} reduction. It will be shown that the loss of hydration water indeed occurs in steps, that proceed immeasurably fast, and that consequently cannot be identified with the co-rate determining chemical step.

In the presence of fluoride ions the cadmium ions are present in the form of several complexes with F^{-} ions that in principle all could contribute to the faradaic process simultaneously. The question then arises to what extent these parallel processes contribute and also what could be the sequence in which fluoride ions are lost and electrons accepted. It turns out to be possible to assess the preferred pathway by studying the process quantitatively at varied F^{-} concentration and at constant ionic strength.

Another way to learn more about electrode processes is to see how their rate is influenced by additives that are adsorbed at the electrode-electrolyte interface. The effect can be catalysis as well as inhibition. Now that it is well known that the Cd^{2+} reduction proceeds in three steps that all are accessible to experimental study, it is worthwhile to see the effect of an additive on all steps separately, rather than the effect on the overall process as is customary.

The catalysis of the Cd^{2+} reduction by thiourea has been unravelled lately by Souto, Sluyters-Rehbach and Sluyters [13, 14]. Here as an example we shall report the inhibition of this electrode process by sucrose adsorbed on the mercury electrode.

An electrochemical charge transfer process can also be complicated by adsorption of the electroactive species at the electrode-electrolyte interface. An example of reactant adsorption is the reduction of Cd^{2+} in the presence of Br^- or I^- [15] which has been studied with impedance voltammetry. In this case the reduction of the Cd^{2+} species proceeds reversibly which means that only the adsorption and the diffusive properties of the Cd^{2+} species are investigated. In the last chapter of this thesis a theoretical treatment is reported on the potentialities of the demodulation technique for the study of processes with reactant adsorption. From this theoretical study, taking the adsorption coefficient β_0 either potential dependent or potential independent and assuming a Langmuir adsorption isotherm, a high sensitivity is found for the value of β_0 which makes the demodulation technique a very suitable and valuable method to study in detail heterogeneous redox reactions complicated by reactant adsorption.

In chemical kinetics it is usual to assume the presence of several steps in a mechanism. Generally then one of these steps is considered to be "the" rate-determining step. In electrochemical kinetics it is possible to analyse a mechanism quantitatively in more detail, so that the rate constants of several, or even all, of the steps in the mechanism can be obtained simultaneously. This is feasible because in different potential ranges the preponderance of the different steps varies.

In order to successfully unravel such an electrode reaction because of the large number of adjustable parameters and also because of the interference by the double layer capacitance at the interface and the ohmic resistance in the cell it is necessary that experimental data are obtained with utmost precision. This can be done with the present-day equipment and with the suitable techniques, i.e. impedance voltammetry and demodulation voltammetry. On the other hand these techniques are capable of precise data only if applied to model systems.

Therefore studies like these are only possible if the symmetry of the electrode system is such that a perfectly homogeneous current density exists. On a macro-scale this can best be realized with a spherical electrode and on a micro-scale with a mercury electrode which is perfectly smooth. Also the electrode surface should be completely free from contaminants. These requirements imply the use of a dropping mercury electrode, that in fact is the only electrode with which a sufficiently high accuracy can be attained.

Although this is a restriction that causes this work to be somewhat remote from applications, on the other hand it teaches us about the laws of nature, and gives an indication what to expect in more complex practical systems.

References

1. R.W. Gurney, Proc.Roy.Soc., A, 134(1931)137; 136(1932)378.
2. T. Erdey-Grüz and M. Volmer, Z.Physik.Chem., 150A(1930)203.
J.A.V. Butler, Trans.Faraday Soc., 19(1924)729; 19(1924)734.
3. J. Tafel, Z.Physik.Chem., 50(1905)641.
4. R.A. Marcus, J.Chem.Phys., 43(1965)679.
5. C.P.M. Bongenaar, M. Sluyters-Rehbach and J.H. Sluyters, J.Electroanal.Chem., 109
(1980) 23.
6. J. Struys, M. Sluyters-Rehbach and J.H. Sluyters, J.Electroanal.Chem., 146 (1983)
263.
7. C.P.M. Bongenaar, A.G. Remijnse, M. Sluyters-Rehbach and J.H. Sluyters, J.Electroanal.Chem., 111 (1980) 139.
8. J. Struys, M. Sluyters-Rehbach and J.H. Sluyters, J.Electroanal.Chem., 171 (1984)
177.
9. R.M. Souto, M. Sluyters-Rehbach and J.H. Sluyters, J.Electroanal.Chem., 201 (1986)
33.
10. R.M. Souto, M. Saakes, M. Sluyters-Rehbach and J.H. Sluyters, J.Electroanal.Chem.,
245 (1987) 167.
11. J. Struys, M. Sluyters-Rehbach and J.H. Sluyters, J.Electroanal.Chem., 146 (1983)
263.
12. R. Andreu, M. Sluyters-Rehbach, A.G. Remijnse and J.H. Sluyters, J.Electroanal.
Chem., 175 (1984) 251.
13. R.M. Souto, M. Sluyters-Rehbach and J.H. Sluyters, J.Electroanal.Chem., 201 (1986)
33

14. R.M. Souto, M. Sluyters-Rehbach and J.H. Sluyters, *J.Electroanal.Chem.*, 245 (1987) 167.
15. E. Fatas-Lahoz, M. Sluyters-Rehbach and J.H. Sluyters, *J.Electroanal.Chem.*, 136 (1982) 59.

CHAPTER 2

THE MECHANISM OF THE REDUCTION OF CADMIUM IONS AT A DROPPING MERCURY ELECTRODE FROM NaClO_4 BASE ELECTROLYTE SOLUTIONS WITH VARIED WATER ACTIVITY

The reduction of Cd(II) to Cd(Hg) has been studied by means of demodulation voltammetry in a wide potential range and at various water activities using NaClO_4 as the base electrolyte. From this study it is concluded that the reduction proceeds according to:

- (i) fast loss of 12.5 water molecules in a preceding equilibrium;
- (ii) a slow "chemical" step, which is not a desolvation;
- (iii) slow transfer of the first electron;
- (iv) fast loss of four water molecules;
- (v) slow transfer of the second electron; and
- (vi) fast loss of the remaining nine water molecules.

These results and the values of the rate constants obtained are compared with results obtained earlier on the reduction of Zn(II) .

(I) INTRODUCTION

In an earlier paper from this laboratory [1] it was shown that from a determination of the kinetics of the Zn(II) reduction at varied water activity, desolvation steps can be demonstrated to exist. As a result, it was concluded that the Zn(II) reduction proceeds according to a cEcE mechanism, where c stands for a fast desolvation step and E for a rate-determining electron transfer. Both the rate constants of the electron transfers and the number of water molecules involved in the desolvation steps were obtained. It was also found that identifying the reaction plane with the outer Helmholtz plane led to an overestimation of the Frumkin correction and that supposing the reaction plane to be situated 0.28 nm more remote from the electrode gives a good result.

The multi-step character of the Cd(II) reduction has also been demonstrated [2,3]. The potential dependence of the forward (reduction) rate constant could be explained only on the assumption of the existence of a co-rate-determining potential-independent ("chemical") step, thus a CEE mechanism. Such a behaviour has been found both in fluoride and in perchlorate base electrolytes. Similar, as yet unexplained "chemical" steps have been found to exist in the mechanism of some other electrode reactions [4-6]. Their presence is puzzling and the elucidation of their nature highly desirable. One might speculate that these "chemical" steps could be identified with a slow desolvation of the reactant, or rather that they represent the slow development of a conformation which allows an electron to be transferred. In order to collect arguments we have set out to perform experiments on the Cd(II) reduction under varied circumstances to see their influence on the chemical step. Variation of the water activity following the route in ref. 1 seems to be a good choice.

Sodium perchlorate is a suitable base electrolyte because of its low tendency to form complexes, its high solubility, because water activities of its aqueous solutions are known [7] and because the double-layer data needed are available from the literature [8-11]. The reduction rate of cadmium ions from concentrated perchlorate solutions, however, is so high that first-order ac methods are inappropriate and demodulation voltammetry has to be applied [3]. With the latter method, the potential-dependent rate constant is not obtained directly, because the ac frequency is not varied. Instead, it requires a mathematical fit of an experimental demodulation voltammogram and a theoretical expression derived on the assumption that a chosen mechanism applies, double-layer corrections included. So double-layer corrections cannot be made afterwards, as was usual in our mechanistic studies hitherto.

(II) EXPERIMENTAL

(II.1) General

All experiments were performed in a three-electrode cell configuration. The working electrode was a dropping mercury electrode made from a drawn-out capillary. A mercury pool served as the counter-electrode and the reference electrode was a sodium chloride saturated calomel electrode (SSCE) connected to the cell via a salt bridge filled with the cell solution. All solutions were prepared from freshly twice-distilled water and p.a. chemicals, and freed from oxygen by passing argon through them. The cell was thermostated at $25.0 \pm 0.1^\circ\text{C}$ and all measurements were made 4 s after drop birth.

(II.2) Dc measurements

In order to obtain the value of the diffusion coefficients of the Cd(II) ion in the 0.2-7.0 M NaClO₄ base electrolytes, sampled dc voltammograms were measured with the network analyser system described earlier [12]. The calculations are described in Section (III.2).

(II.3) *Ac measurements*

The values of the differential double-layer capacitance in the 0.2–7.0 *M* NaClO₄ solutions were measured at 1020 Hz with the network analyser system described earlier [12].

(II.4) *Demodulation measurements*

Demodulation voltammograms were measured with the instrument described in ref. 13. The HF current density used was about 0.35 A cm⁻² and the low and high frequencies were chosen at 122 Hz and 100 kHz, respectively. The bulk concentration of Cd(II) was 1 mM throughout. The mercury drops were knocked off with an electromagnetic hammer with a 4 s interval. The surface area of the drop was about 0.02 cm².

(III) DATA ANALYSIS AND RESULTS

(III.1) *Double-layer data*

The double-layer capacities obtained as a function of the potential (referred to the SSCE) were integrated using literature data for the potential of zero charge [1], leading to the charge density σ^M on the electrode.

In order to calculate the potential profile in the diffuse double layer it is necessary to estimate the charge density σ^1 of specifically adsorbed ClO₄⁻ ions as a function of σ^M . The specific adsorption of the perchlorate ion has been studied by several authors [8–11], from which we chose the study by Parsons and Payne [11] as being the most appropriate one for our purpose. The data available in ref. 11 are σ^1 vs. $\ln a_{\pm}$ and σ^1 vs. σ^M plots for HClO₄ solutions at concentrations of 0.01–3.7 *M*. Extrapolation to higher concentrations, i.e. to 5 and 7 *M*, could be performed with reasonable reliability both from plots of σ^1 vs. concentration and from plots of $-\sigma^1$

TABLE 1

Specifically adsorbed amounts in $\mu\text{C cm}^{-2}$ of ClO₄⁻ as a function of c_{NaClO_4} and σ^M . The possible systematic error is less than 0.5 at $c_{\text{NaClO}_4} < 3$ *M*, ca. 0.5 at $c_{\text{NaClO}_4} = 5$ *M* and ca. 1.5 at $c_{\text{NaClO}_4} = 7$ *M* (see text)

$\sigma^M / \mu\text{C cm}^{-2}$	$c_{\text{NaClO}_4} / \text{mol l}^{-1}$							
	0.2	0.5	0.8	1	2	3	5	7
-8	-0.6	-2.4	-2.2	-2.8	-5.8	-8.8	-14	-21
-6	-0.8	-2.7	-3.2	-4.0	-7.7	-11.2	-18	-24
-4	-1.6	-3.6	-4.6	-5.5	-9.7	-13.5	-20	-28
-2	-2.8	-4.9	-6.3	-7.3	-11.8	-15.8	-23	-31
0	-4.3	-6.6	-8.2	-9.2	-13.9	-18.0	-26	-33
2	-6.1	-8.5	-10.2	-11.2	-15.9	-20.0	-28	-36
4	-7.9	-10.6	-12.1	-13.1	-17.8	-21.9	-30	-38
6	-9.8	-12.8	-13.8	-14.8	-19.6	-23.5	-32	-40
8	-11.6	-14.8	-15.3	-16.3	-21.1	-25.0	-33	-42

vs. $\ln(\sigma^1/a_{\text{HClO}_4})$, the latter giving fairly straight lines, at least at $-8 < \sigma^M < 8 \mu\text{C cm}^{-2}$ which is the region we are interested in. Moreover, the rather rough assumption has been made that the amount of specific ClO_4^- adsorption is the same for HClO_4 and NaClO_4 at the same concentration and the same charge density. The underlying arguments are: (i) the single ion activity coefficient of the ClO_4^- ion will not depend too much on the nature of the cation; (ii) the C_d vs. E data for NaClO_4 (this work) show characteristics similar to those for HClO_4 [11]; (iii) for our purpose it is sufficient to have the relative change in the diffuse layer potentials going from 0.2 to 7 M NaClO_4 .

The values of σ^1 used for our calculations are listed in Table 1. From $\sigma^M + \sigma^1$, the potentials ϕ_2 at the outer Helmholtz plane (OHP) were derived in the usual manner assuming validity of the Gouy–Chapman–Stern theory [14]:

$$\phi_2 = \left(\frac{2RT}{F} \right) \sinh^{-1} \left[\frac{\sigma^M + \sigma^1}{(8RT\epsilon c_b)^{1/2}} \right] \quad (1)$$

where c_b is the bulk concentration of NaClO_4 and ϵ is the permittivity of the solvent. In view of the arguments to be discussed in Section (III.3), the potential $\phi_{1\text{H}_2\text{O}}$ pertaining to a plane 0.28 nm outside the OHP was also calculated using

$$\phi_{1\text{H}_2\text{O}} = - \frac{4RT}{F} \tanh^{-1} \left[\tanh \left(\frac{F\phi_2}{4RT} \right) \exp(-\kappa d_{\text{H}_2\text{O}}) \right] \quad (2)$$

with

$$\kappa = (2F^2 c_b / \epsilon RT)^{1/2} \quad (3)$$

and $d_{\text{H}_2\text{O}} = 2.8 \times 10^{-8}$ cm.

The results of these calculations are represented as a function of the applied potential in Figs. 1 and 2. Comparing these figures, it can be seen that the diffuse

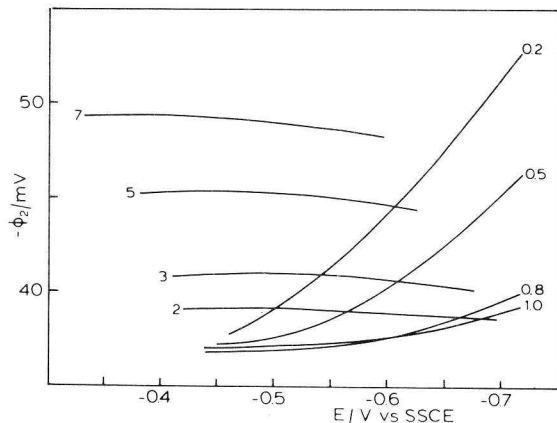


Fig. 1. Value of $-\phi_2$ vs. the electrode potential for 0.2–7.0 M NaClO_4 . Numbers indicate the molarity of NaClO_4 .

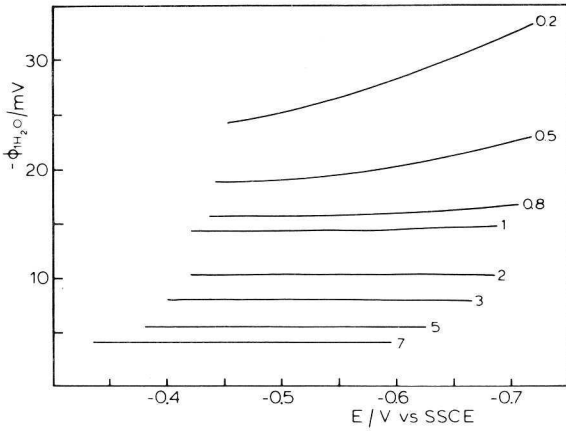


Fig. 2. Value of $-\phi_{\text{H}_2\text{O}}$ vs. the electrode potential for 0.2–7.0 M NaClO_4 . Numbers indicate the molarity of NaClO_4 .

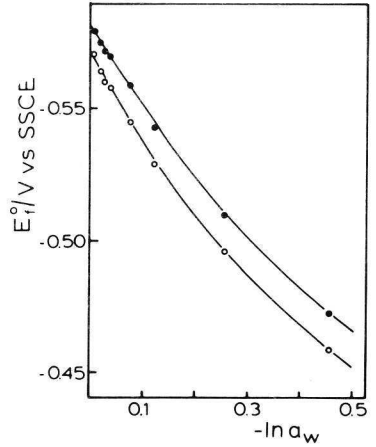


Fig. 3. Formal standard potential E_f° as a function of the water activity a_w . (●) Obtained from the kinetic analysis; (○) the same, but corrected for the salt concentration effects (see text).

layer potential drops rather sharply going from the OHP to the plane at a distance of the diameter of one water molecule from the OHP.

(II.2) The overall process

From the limiting current in the dc polarograms the diffusion coefficient D_{O} was derived using the Ilković equation corrected for sphericity with the expression proposed by Newman [15]. The values are tabulated in Table 2.

Because the demodulation voltammograms are very sensitive to the reversible half-wave potential, its value, $E_{1/2}^r$, was obtained from the analysis of the kinetics described in Section (III.3), for each NaClO_4 concentration. Combination of the

TABLE 2

Values of D_{ox} , $E_{1/2}^r$, E_f° and $-\ln a_w$ at the NaClO_4 concentrations applied

	$c_{\text{NaClO}_4}/\text{mol l}^{-1}$							
	0.2	0.5	0.8	1.0	2.0	3.0	5.0	7.0
E_f°/mV vs. SSCE	-579	-575	-572	-570	-559	-543	-510	-472
$E_{1/2}^r/\text{mV}$ vs. SSCE	-577	-573	-570	-567	-555	-539	-505	-464
$10^6 D_{\text{ox}}/\text{cm}^2 \text{s}^{-1}$	8.3	8.3	8.0	7.3	6.3	5.7	4.5	3.3
$-\ln a_w$ [1]	0.0070	0.0171	0.0260	0.0346	0.0747	0.122	0.254	0.454

$E_{1/2}^r$ values and the D_O values, with $D_R = 10.7 \times 10^{-6} \text{ cm}^2 \text{ s}^{-1}$ taken from the literature [2] gives the formal standard potential, E_f° , according to

$$E_f^\circ = E_{1/2}^r + RT/nF \ln(D_O/D_R)^{1/2} \quad (4)$$

The results for $E_{1/2}^r$ and E_f° are also collected in Table 2, together with the logarithm of the water activity at the various salt concentrations, taken from the literature [1].

The variation of E_f° with the NaClO_4 concentration reflects the variation in the activity of the dissolved Cd(II) , or rather the variation in its molar activity coefficient y_O . According to the theory of electrolyte solutions, there are three factors influencing y_O , namely

- (i) the electrostatic interaction with Na^+ and ClO_4^- ions (Debye-Hückel effect);
- (ii) the change in the mole fraction of Cd(II) when the amount of added salt increases; and
- (iii) the decrease in water activity with increasing NaClO_4 concentration.

The three effects lead to the following expression for E_f° [16-18]:

$$\begin{aligned} E_f^\circ &= E^\circ + (RT/nF) \ln y_O - (RT/nF) \ln y_R \\ &= E^\circ + \frac{RT}{nF} \left\{ \ln f_O^{\text{DH}} + \ln \frac{m_O}{c_O} - \ln[1 + 0.018(2 - h_S)m_S] \right\} \\ &\quad - \frac{RT}{nF} h_O \ln a_w - \frac{RT}{nF} \ln y_R \end{aligned} \quad (5)$$

where f_O^{DH} is the Debye-Hückel activity coefficient of Cd(II) , m_O is the molality of Cd(II) , c_O is the concentration of Cd(II) , $h_S (= h_{\text{Na}^+} + h_{\text{ClO}_4^-})$ is the hydration number of NaClO_4 , m_S is the molality of NaClO_4 , h_O is the hydration number of Cd(II) , a_w is the water activity and y_R is the activity coefficient of Cd(Hg) , assumed to be constant.

If the term in brackets can be calculated as a function of c_{NaClO_4} , it is possible to calculate the hydration number h_O from the relation between E_f° and $-\ln a_w$. The term in brackets (actually the activity coefficient of the hydrated Cd(II) ion) contains obvious quantities, except for the hydration number h_S , of the salt. Usually it is assumed that $h_{\text{ClO}_4^-}$ equals zero, so that $h_S = h_{\text{Na}^+}$. Inspection of the literature [16] shows that experimental values of h_{Na^+} range from 1 to 7, and a rational choice is difficult to make. Therefore we followed the procedure proposed by Chai-fu Pan [19], in which h_{Na^+} is derived from the experimentally obtained a_w values by an iterative numerical calculation. This procedure resulted in $h_{\text{Na}^+} = 2.1$, a value close to the integer number 2, accepted by Jacobsen and Skou [18] as the value giving the best internal consistency for a plot of a_w against the mole fraction of free water in NaClO_4 solutions.

In Table 3 we give a survey of the relative significance of the three contributions to the correction term, which has to be subtracted from E_f° . The correction term is also listed.

TABLE 3

Values of the terms constituting the "correction term" in brackets in eqn. (5), and the resulting corrected formal standard potentials

$c_{\text{NaClO}_4}/\text{mol l}^{-1}$	$\ln f_{\text{O}}^{\text{DH}}$	$\ln m_{\text{O}}/c_{\text{O}}$	$-\ln[1 + 0.018(2 - h_s)m_s]$	Corr. term/ mV	$E_f^\circ - \text{corr. term}$ /mV vs. SSCE
0.2	-0.631	0.010	0.0004	-8.0	-571.0
0.5	-0.844	0.027	0.0009	-10.5	-564.5
0.8	-0.962	0.044	0.0015	-11.8	-560.2
1.0	-1.019	0.054	0.0019	-12.4	-557.6
2.0	-1.193	0.111	0.0040	-13.8	-545.2
3.0	-1.291	0.171	0.0064	-14.3	-528.7
5.0	-1.407	0.305	0.0123	-14.0	-496.0
7.0	-1.478	0.450	0.0200	-12.9	-459.1

In Fig. 3, both E_f° and $E_f^\circ - (\text{correction term})$ have been plotted against $-\ln a_w$. Linear relationships exist up to $-\ln a_w = 0.15$, which corresponds with about 3.5 M NaClO₄. The slopes of these lines give the hydration number for the Cd(II) ion: $h_{\text{O}} = 22.9 \pm 1$ (not corrected) and $h_{\text{O}} = 25.5 \pm 1$ (corrected). Evidently, beyond 3.5 M NaClO₄ the hydration number of Cd(II) decreases gradually down to about 11.7 at 7 M NaClO₄, indicating desolvation at low water activity. A similar effect was observed with the Zn(II) ion [1]. It may be noted here that in the calculation of h_{O} for Zn(II), a similar effect of the correction term, which was neglected in the cited works [1,18], has to be expected.

The variation of y_{O} with the salt concentration will also play a role in the interpretation of the rate equation accepted for charge transfer. For a linear reaction mechanism we usually write

$$-j_{\text{F}} = nFk_{\text{f}} [c_{\text{O}} - c_{\text{R}} \exp(\varphi)] \quad (6)$$

with

$$\varphi = (nF/RT)(E - E_f^\circ) \quad (7)$$

This means that the activity coefficient y_{O} has been incorporated in k_{f} . In terms of activities, the rate equation should read

$$-j_{\text{F}} = nFk_{\text{f}}^* [y_{\text{O}}c_{\text{O}} - y_{\text{R}}c_{\text{R}} \exp(\varphi^*)] \quad (8)$$

with

$$\varphi^* = (nF/RT)(E - E^\circ) = \varphi + \ln(y_{\text{O}}/y_{\text{R}}) \quad (9)$$

Evidently we have

$$k_{\text{f}} = k_{\text{f}}^* y_{\text{O}} = k_{\text{f}}^* \left(\frac{f_{\text{O}}^{\text{DH}}(m_{\text{O}}/c_{\text{O}})}{1 + 0.018(2 - h_s)m_s} \right) a_w^{-h_{\text{O}}} \quad (10)$$

This will be discussed further in Section (III.4).

(III.3) The kinetic analysis

The analysis of the phase-sensitive demodulation voltammograms was conducted on the basis of the mathematical descriptions given earlier [3,4,13,20,21], i.e. using the theoretical expressions for the in-phase (I_{LF}) and the quadrature (Q_{LF}) components:

$$I_{LF} - [S_C] = \{[S_F] - [S_C]\} \frac{a_L^*(a_L^* + 1)}{(p_L + 1)^2 + (a_L^* + 1)^2} \quad (11)$$

$$Q_{LF} = -\{[S_F] - [S_C]\} \frac{a_L^*(p_L + 1)}{(p_L + 1)^2 + (a_L + 1)^2} \quad (12)$$

where

$$a_L^* = (2\omega_L)^{-1/2} \sigma^{-1} (C_d + C_{ex}) \quad (\text{see ref. 13})$$

$$p_L = (2\omega_L)^{1/2} p' \quad (\omega_L = \text{low frequency})$$

and

$$p' = (2D_O)^{1/2} [1 + (D_O/D_R)^{1/2} \exp(\varphi)]^{-1} k_f^{-1} \quad (13)$$

The values of the virtual voltage source $[S_C]$ that originates from the non-linearity of the double-layer charging process, were as usual calculated numerically from the double-layer capacity data (Section III.1). The virtual voltage source $[S_F]$ originating from the non-linearity of the faradaic process [20,21] contains the parameter

$$p_H = (2\omega_H)^{1/2} p' \quad (\omega_H = \text{high frequency})$$

and the operational transfer coefficient α defined by

$$\alpha = -d \ln k_f / d\varphi \quad (14)$$

The experimental data for I_{LF} and Q_{LF} as a function of the dc potential were analysed by comparing them with calculated voltammograms based on the mechanistic model to be discussed below. The fitting procedure was essentially a least-squares routine, followed by a graphical comparison of the experimental and the calculated voltammograms. The number of adjustable parameters was kept as small as feasible. Usually the analysis at a certain NaClO_4 concentration was repeated for several values of the reversible half-wave potential $E_{1/2}^r$, which occurs in both p' and σ . Selecting the run with the minimum sum of least squares enabled $E_{1/2}^r$ to be determined with a precision better than ± 1 mV.

Because the faradaic contribution $[S_F]$ contains both the rate constant k_f and its derivative with respect to potential, it is necessary to adopt a mechanism which prescribes the potential dependence of k_f . In our earlier work, also on the Cd(II) reduction [3], it was shown that the demodulation method is quite selective as

regards the type of mechanism, and the so-called CEE mechanism was found to apply exclusively both in 0.5 M HClO₄ and in 1 M KF as the supporting electrolyte. This mechanism is confirmed at all the NaClO₄ concentrations studied in the present work, again taking the transfer coefficients of the electrochemical steps equal to 0.5 and assuming the chemical step to be potential independent.

In earlier publications it has been shown that for such a mechanism the apparent standard rate constant, k_f , of the overall reaction should depend on the potential according to [2,3]

$$\frac{1}{k_f} = \frac{1}{k_{s,0}^c} + \frac{\exp \frac{1}{4}\varphi}{k_{s,1}} + \frac{\exp \frac{3}{4}\varphi}{k_{s,2}} \quad (15)$$

where φ is given by eqn. (7).

Here, we wish to introduce the possibility of applying a non-specific double-layer correction. This can be done by modifying eqn. (15) to

$$\frac{\exp\left[-\frac{zF}{RT}\phi_r\right]}{k_f} = \frac{1}{k_f^t} = \frac{1}{k_{s,0}^c} + \frac{\exp \frac{1}{4}\varphi'}{k_{s,1}} + \frac{\exp \frac{3}{4}\varphi'}{k_{s,2}} \quad (16)$$

with

$$\varphi' = \frac{2F}{RT}(E - E^\circ - \phi_r) \quad (17)$$

Here, z denotes the charge of the reacting Cd(II) species ($z = 2$ in the present case of a non-complexing base electrolyte) and the exponential in the left-hand side of eqn. (16) is in fact the Boltzmann part of the double-layer correction. ϕ_r is the potential of the reaction plane towards which the reactant has to move prior to the first reaction step.

The computer fits were made with expressions (16) and (17) for k_f substituted into eqns. (11)–(13). This was done with three choices of the value of ϕ_r :

(i) $\phi_r = 0$, leading to "apparent" values of the rate constants $k_{s,0}^c$, $k_{s,1}$ and $k_{s,2}$ (cf. eqn. 15);

(ii) $\phi_r = \phi_2$; then the analysis is based on the supposition that the reaction plane coincides with the outer Helmholtz plane, the distance of nearest approach of the Na⁺ ion. This is liable to lead to an overestimation of the double-layer correction because the (hydrated) Cd(II) ion is larger than the Na⁺ ion [1,22–25]. Therefore it is reasonable also to try:

(iii) $\phi_r = \phi_{1H_2O}$, which implies that the reaction plane is chosen 0.28 nm more remote from the electrode surface.

The three ways of fitting appeared to be equally successful, regardless of the value that was assigned to the reversible half-wave potential, $E_{1/2}^r$, as explained above. As an example, we report Figs. 4a and 4b pertaining to case (iii), $\phi_r = \phi_{1H_2O}$. At first sight, the equal quality of the fits is amazing. The reason for it is that both ϕ_2 and ϕ_r change only weakly with potential in the potential range used, so that the form of the right-hand side of eqn. (16) is retained, even though ϕ_r has a considerable value.

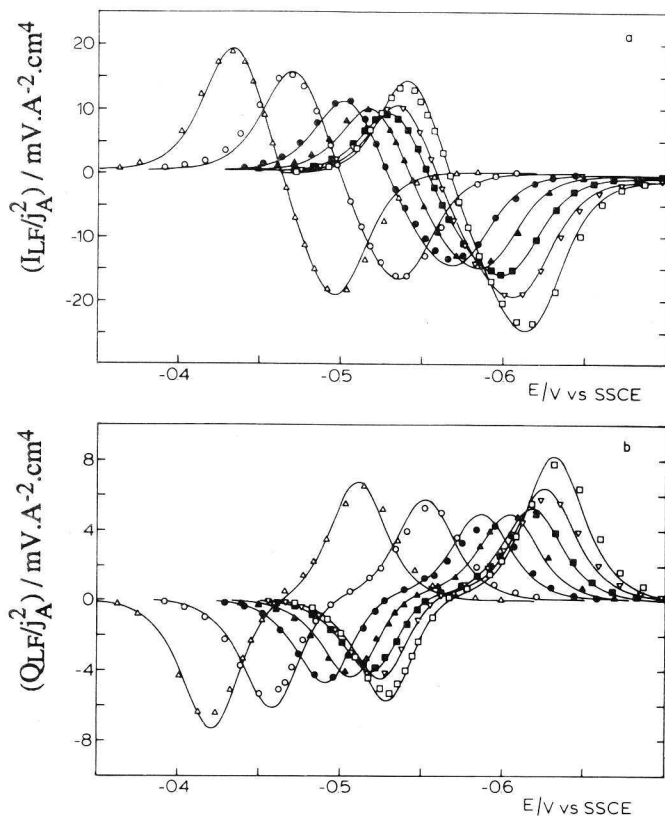


Fig. 4. Normalized in-phase (a) and quadrature (b) component vs. the electrode potential for 0.2 M (\square), 0.5 M (∇), 1.0 M (\blacksquare), 2.0 M (\blacktriangle), 3.0 M (\bullet), 5.0 M (\circ) and 7.0 M (\triangle) NaClO_4 . For experimental conditions see text.

The standard rate constants for the three steps, obtained as the adjusted parameters in the fits, are reported in Table 4, for the three choices of the reaction plane and at the eight concentrations of NaClO_4 . These standard rate constants pertain to the formal standard potential E_f° of the Cd(II) reduction reaction at the appurtenant base electrolyte concentration. The values of $k_{s,0}^c$, $k_{s,1}$ and $k_{s,2}$ for case (iii) were used to construct Fig. 5, where $\ln k_f + (zF/RT)\phi_r$ is plotted against $E - \phi_r$ in order to visualize the potential dependence of k_f as well as the effect of the salt concentration.

(III.4) The relation to the water activity

The analysis in this section will be based on the idea that water is repelled from the hydration shell around the cadmium ion in separate stages, as was found to occur in the case of the Zn(II) reduction [1]. The standard rate constants in Table 4 cannot be used directly for this purpose, because they are referred to different standard potentials E_f° pertaining to the different NaClO_4 concentrations. A fair

TABLE 4

Values of $k_{s,0}^c$, $k_{s,1}$ and $k_{s,2}$ for $\phi_r = 0$, ϕ_2 and ϕ_{1H_2O} at given $NaClO_4$ concentration and formal standard potential. The accuracy of these results is typically ± 3 in the last digit

c_{NaClO_4} /mol l ⁻¹	E_f° /mV vs. SSCE	$\phi_r = 0$			$\phi_r = \phi_2$			$\phi_r = \phi_{1H_2O}$		
		$k_{s,0}^c$	$k_{s,1}$	$k_{s,2}$	$k_{s,0}^c$	$k_{s,1}$	$k_{s,2}$	$k_{s,0}^c$	$k_{s,1}$	$k_{s,2}$
0.2	-579	5.0	0.94	8.3	0.10	0.114	5.9	0.88	0.26	10
0.5	-575	2.1	1.28	10	0.06	0.189	6.7	0.60	0.48	8.3
0.8	-572	3.7	0.83	10	0.18	0.079	4.0	1.0	0.34	5.5
1.0	-570	4.0	0.79	10	0.26	0.092	6.7	1.7	0.35	5.0
2.0	-559	10	0.75	6.6	0.20	0.077	3.0	1.8	0.42	5.5
3.0	-543	25	0.81	5.2	0.5	0.075	2.5	5	0.52	4.0
5.0	-510	∞	1.43	6.6	2	0.099	3.3	17	1.05	5.9
7.0	-472	∞	17	20	10	0.267	17	∞	20	20

comparison can be made only by converting the reported data to one common reference potential, for which we have arbitrarily chosen the standard potential in 1 M $NaClO_4$, -0.570 V (vs. SSCE), thus ignoring liquid junction potentials [1]. The conversions were made by calculating the values of

$$k_{s,1} \exp\left[\frac{\alpha_1 F}{RT}(E_f^\circ + 0.570)\right] = "k_{s,1}" \quad (18)$$

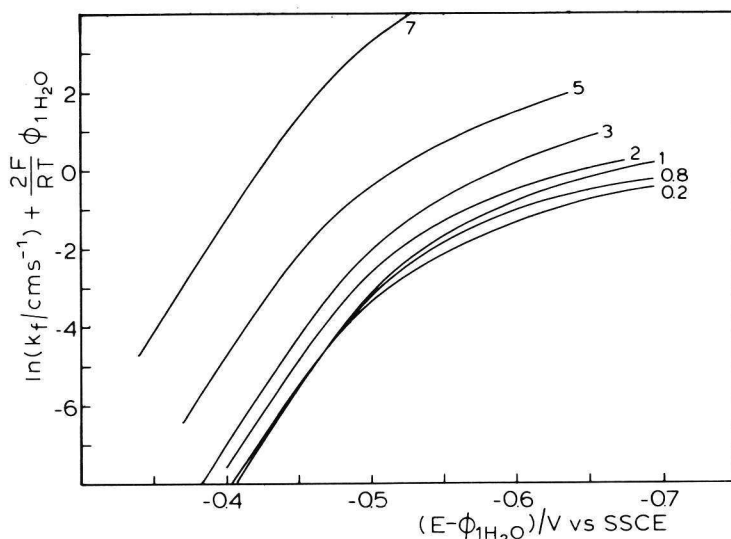


Fig. 5. Value of $\ln k_f + (2F/RT)\phi_{1H_2O}$ vs. $E - \phi_{1H_2O}$ for 0.2-7.0 M $NaClO_4$. Numbers indicate the molarity of $NaClO_4$.

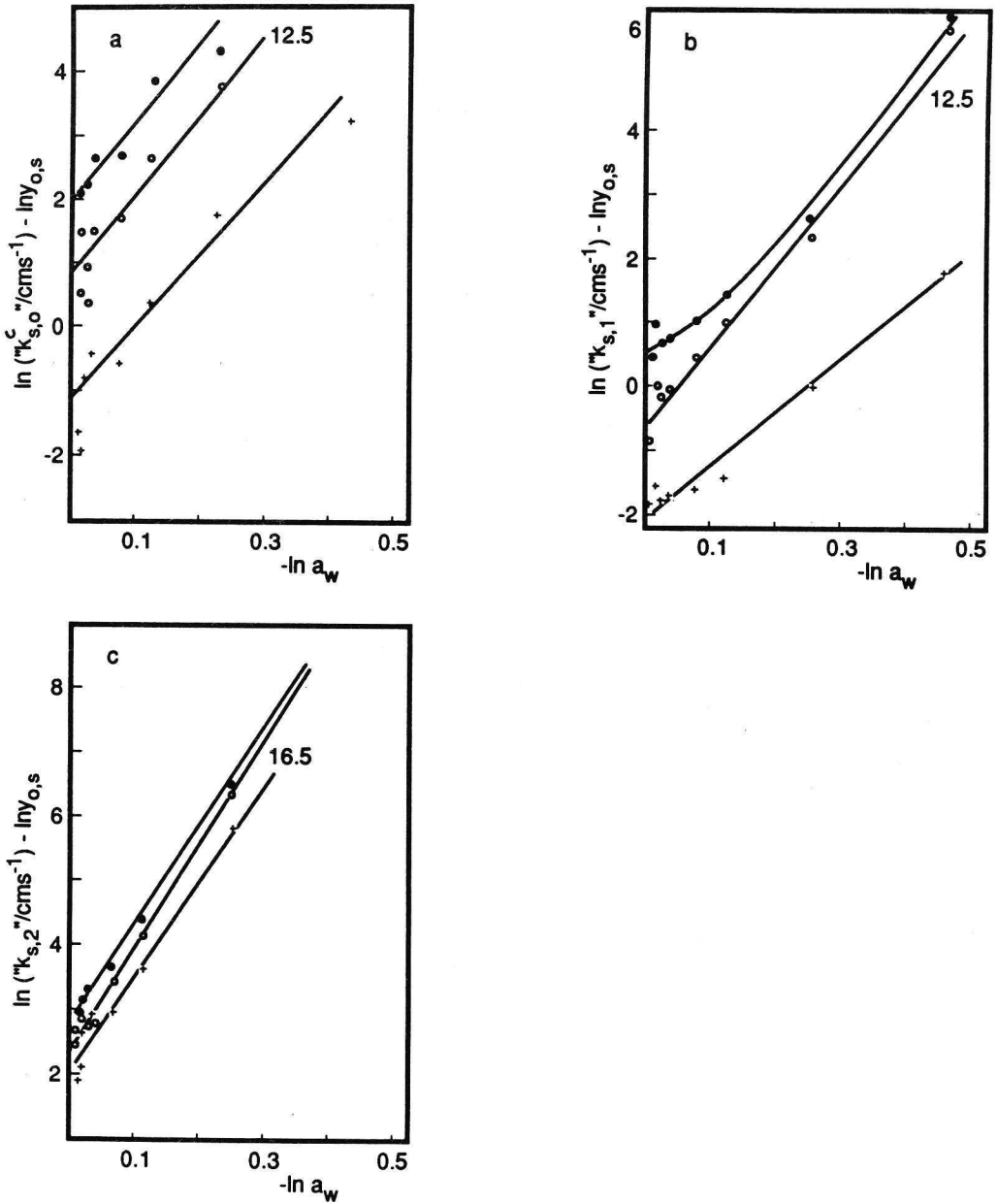


Fig. 6. Values of (a) $\ln "k_{s,0}^c"$, (b) $\ln "k_{s,1}"$ and (c) $\ln "k_{s,2}"$ as a function of $-\ln a_w$, calculated with eqns. (18) and (19), and corrected for the quantity expressed by eqn. (21). Symbols used are (●) for $\phi_r = 0$, (+) for $\phi_r = \phi_2$ and (○) for $\phi_r = \phi_{1H_2O}$ (see text).

and

$$k_{s,2} \exp \left[\frac{(\alpha_2 + 1)F}{RT} (E_f^\circ + 0.570) \right] = "k_{s,2}" \quad (19)$$

for the first and second electron-transfer steps, respectively. The $k_{s,0}^c$ values represent the potential-independent rate of the preceding chemical reaction step, and therefore require no conversion.

The parameters thus obtained are to be plotted as their logarithms vs. the logarithm of the water activity. The slopes of such plots should yield the number x_i of water molecules released in all steps that precede the relevant step:

$$\ln("k_{s,i}") = \text{const.} - x_i \ln a_w \quad (20)$$

However, here the other effects due to the variation of the NaClO_4 concentration (see Section III.2) should also be taken into account. In Appendix I it will be shown that this implies subtraction of the correction term

$$\ln y_{O,S} = \ln f_O^{\text{DH}} + \ln \frac{m_O}{c_O} - \ln [1 + 0.018(2 - h_s)m_s] \quad (21)$$

i.e. the correction term listed in Table 3, from all the $\ln("k_{s,i}")$ values. The effect of the correction is to change the x_i values to the amount of 2 to 3. It may be noted that its significance is so small because the contributions of f_O^{DH} and m_O/c_O tend to compensate each other, and moreover $h_s \approx 2$.

The corrected $\ln("k_{s,i}")$ vs. $-\ln a_w$ plots are represented in Figs. 6a–6c. The next step is to interpret these results in terms of a stepwise dehydration, according to eqn. (20) above. For ease of survey this will be discussed in seven separate points.

(i) As far as is reasonable, straight lines have been drawn in Figs. 6a–6c, which, taking into consideration Fig. 3, are meaningful only up to ca. 4 M NaClO_4 or $-\ln a_w \approx 0.2$.

(ii) The accuracies with which the kinetic data on the steps are obtained are very different. This can be made evident by comparing the terms in eqn. (16) after substitution of the rate constants from Table 4. It then becomes clear that $k_{s,1}$ and $k_{s,2}$ have been obtained with a far better accuracy than $k_{s,0}^c$, and, correspondingly, " $k_{s,1}$ " and " $k_{s,2}$ " are more reliable.

(iii) As in the earlier study from this laboratory on the Zn(II) reduction [1], the present results justify situating the reaction plane at the $\phi_{1\text{H}_2\text{O}}$ plane; this choice yields straight lines and the differences with the uncorrected data become small at low water activity. Therefore the discussion to follow will be restricted to the results calculated with the $\phi_{1\text{H}_2\text{O}}$ double-layer correction.

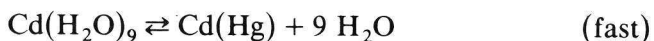
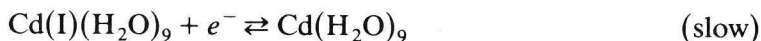
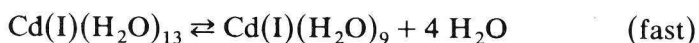
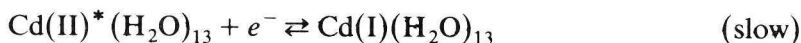
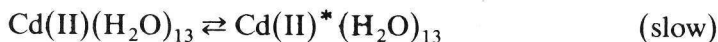
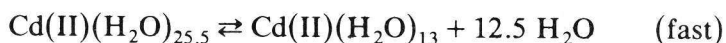
(iv) Also the rate constant $k_{s,0}^c$ of the "chemical" step is found to depend on the water activity (Fig. 6a). This can be explained only on the assumption of the presence of a reaction preceding the "chemical" step, in which 12.5 ± 2 water molecules are released in a fast equilibrium. This newly discovered dehydration step can be either homogeneous or heterogeneous.

(v) Also the slope in Fig. 6b amounts to 12.5 water molecules. This indicates that the product of the chemical step is reduced directly without altering its interaction with the solvent.

(vi) The slope in Fig. 6c corresponds to 16.5 ± 1 water molecules, so the second electron transfer appears to be preceded by a fast dehydration with $16.5 - 12.5 = 4 \pm 1$ water molecules.

(vii) The total number of water molecules found in the mechanism up to the last step is 16.5 ± 1 , which is less than the number, 25.5, found to be involved in the overall reaction (see Fig. 3 and Section III.2). This difference indicates that after the second electron transfer nine more water molecules are released.

On the basis of these results it can be concluded that the reduction of Cd(II) ions at mercury from NaClO₄ base electrolyte proceeds via the following mechanism:



Regarding the overall accuracy of the method, we believe that all the steps found exist, although the numbers of water molecules involved are subject to some uncertainty, mainly due to the uncertainty in the rate constant of the "chemical" step, which is rather fast.

(IV) DISCUSSION

The analysis in the preceding section is based on the following premises:

- (i) The reduction proceeds via the C₀E₁E₂ mechanism.
- (ii) The double-layer effect due to the variation of the NaClO₄ concentration is only non-specific.
- (iii) The remaining effect, after the double-layer correction, is completely related to bulk solution interactions.
- (iv) The idea of progressive dehydration of Cd(II) during its stepwise reduction.

(i) Very recently, a paper from this laboratory was published [26] in which the Cd(II) reduction at Hg from mixtures of $(1 - x) M \text{ KF} + x M \text{ KCl}$ was studied. From that work it was concluded that the mechanism in that medium should be characterized as C₀E₁C₁E₂C₂, i.e. two more rate-controlling "chemical steps" are revealed, because the Cl⁻ ion catalyses the preceding chemical step and the first electron transfer dramatically. From Figs. 4a and 4b in the present work, the impression is obtained that also here the fit to the CEE mechanism is less

satisfactory at the highest salt concentrations, and that possibly more chemical steps are involved. However, the discrepancy is too small to draw any solid conclusion in this direction.

Comparing again with the catalysis by chloride, which is supposed to be related to the specific Cl^- adsorption, it should be recognized that in the potential range of interest (-0.4 to -0.8 V vs. SSCE) the ClO_4^- ion is also specifically adsorbed. It is unlikely, however, that the accelerating effect observed would be analogous to that of the Cl^- ion. For example, the overall rate constant measured in 1 M KCl is about 8 times higher than in 1 M NaClO_4 , whereas the specific surface excesses of Cl^- and ClO_4^- are of the same order of magnitude.

(ii) The validity of eqns. (1)–(3), used to calculate the potential ϕ_r of the reaction planes and thus to account for the double-layer effect, is, of course, very questionable. The GCS theory is said to hold for electrolyte concentrations only below 0.01 M [14,27,28], but seems “to work”, especially for correcting kinetic data, up to 1 M electrolyte concentration [29,30]. This is probably partly due to the lesser importance of the correction at higher concentrations, where the diffuse layer is more compressed.

With regard to this point, it can be argued that in the present study, and in the previous one on the Zn(II) reduction [1], the variation of the apparent rate constant is clearly related to the combined effects of the variation in ϕ_r and in a_w . From Fig. 6 it can be deduced that the two effects are counteracting, leading to the shallow minima in the individual rate constants at about 1 M NaClO_4 . In view of the double-layer studies referred to [8–11], there is no doubt that ϕ_r should have a negative sign in the potential region of our interest, leaving only its value as a function of the NaClO_4 concentration to be estimated.

More sophisticated theories for the diffuse double layer and improvements to the GCS theory have been proposed and reviewed [27,28], but to our knowledge they have never been applied in the study of charge-transfer processes. In future work this should certainly be tried, in order to improve the understanding of many “other effects”. For the work presented here, it should be noted that any error in the value of ϕ_r will influence the “true” individual rate constants almost to the same extent, because its major effect is reflected by the factor $\exp[-zf\phi_r]$ on the left-hand side of eqn. (16). It seems reasonable, therefore, to conclude that $\phi_r = \phi_2$ would lead to an overestimation of the double-layer effect, and to adopt $\phi_r = \phi_{1\text{H}_2\text{O}}$ as the better choice for the time being.

(iii) A similar discussion may be raised regarding the actual item on which this paper is focused, i.e. the bulk solution effect of the non-complexing electrolytes, NaClO_4 . The treatment in terms of the hydration numbers is also “classical” in comparison with more modern theories of solvents and of solutions. However, their use in reaction schemes like the general one in the Appendix helps to simplify the formalism. This seems all right, as long as one realizes that the hydration number is a measure of the extent of interaction between an ion and the solvent molecules surrounding it. Therefore, its value is not necessarily an integer, in contrast to the coordination number in the case of complexation by a ligand.

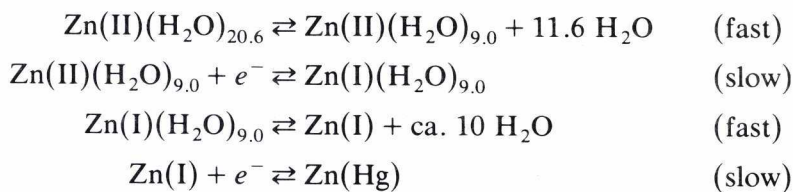
TABLE 5

Comparison of the mechanisms of Cd(II) and Zn(II) reductions regarding the numbers of water molecules released and the rate constants of the rate-determining steps (at 1 M NaClO₄ concentration and corrected for $\phi_{4\text{H}_2\text{O}}$)

Step	Cd		Zn	
	H ₂ O molecules	Rate constant /cm s ⁻¹	H ₂ O molecules	Rate constant /cm s ⁻¹
Dehydration	-12.5		-11.6	
“Chemical” step		1.43		∞
First electron transfer		0.32		0.0013
Dehydration	-4		-10	
Second electron transfer		4.0		0.048
Dehydration	-9		0	
Total number of H ₂ O	-25.5		-20.6	

In the present case, it is rather fortunate that the correction by the molar activity coefficient $y_{\text{O},s}$, eqn. (21), is of minor importance due to its relatively small value. It may also be noted that similar activity coefficients, formally introduced for the intermediates in the reaction scheme, are eliminated together with the corresponding “concentrations” in the derivation of the overall rate constant.

(iv) It is interesting to make a comparison between the present results and those of a similar study on the Zn(II) reduction performed earlier by Andreu et al. [1]. To this end, we reconsidered the data on Zn(II) applying the corrections for the Debye-Hückel effect and the change in the Zn(II) mole fraction, as described in Section (III.2). This resulted in somewhat higher values of the number of water molecules released stepwise and involved in the overall process. The reduction mechanism of Zn(II) becomes



The two mechanisms are compared in Table 5.

Because the rate constants of the electron-transfer steps for zinc are 250 and 80 times lower than those for cadmium, a chemical step in the mechanism of the Zn(II) reduction could not possibly be detected if its rate constant were of the same order of magnitude as that for Cd(II). The numbers of water molecules exchanged in a fast preceding equilibrium (homogeneous or heterogeneous), i.e. 12.5 and 11.6 for Cd(II) and Zn(II) respectively, are remarkably close. So, the main difference which remains is that the Zn(I) intermediate seems to be dehydrated completely before the second electron transfer, whereas Cd(I) is only partially dehydrated. The dehydration number in the zinc case, however, bears an uncertainty of ± 4 aq., which is

large in comparison with the Cd(II) reduction. This is so because for Cd(II) the values of $k_{s,1}$ and $k_{s,2}$ are much closer than those for Zn(II) (see Table 4).

From the present analysis it seems that the “chemical” step in the mechanism of the Cd(II) reduction cannot be identified with a dehydration. If so, then the chemical step can only represent the creation of some spatial configuration at the interface which strongly promotes the probability of electron transfer or even is a prerequisite for it.

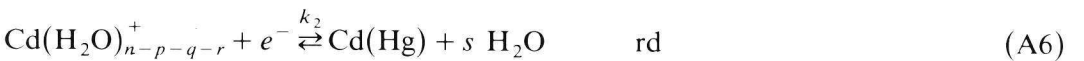
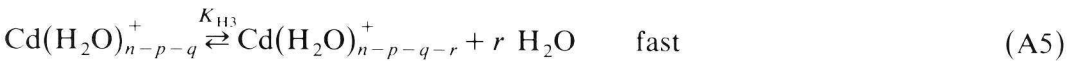
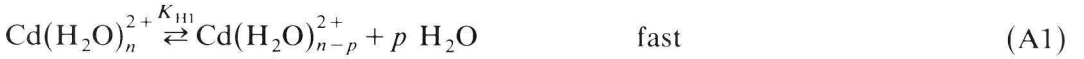
ACKNOWLEDGEMENT

The authors wish to express their gratitude to Professor Dr. J.A.A. Ketelaar for his interest and valuable suggestions.

APPENDIX

Derivation of the expression for the reciprocal forward rate constant in terms of the molar activity coefficients y

Assume the following reaction scheme:



In this reaction scheme we find three rate-determining (rd) steps which are preceded by fast dehydration equilibria. The fluxes for the rate-determining steps are:

$$v_c = k_c \left(y_{\text{Cd}(\text{H}_2\text{O})_{n-p}^{2+}} c_{\text{Cd}(\text{H}_2\text{O})_{n-p}^{2+}} - K_c y_{\text{Cd}(\text{H}_2\text{O})_{n-p}^{2+*}} c_{\text{Cd}(\text{H}_2\text{O})_{n-p}^{2+*}} \right) \quad (\text{A7})$$

$$v_1 = k_1 \left(y_{\text{Cd}(\text{H}_2\text{O})_{n-p-q}^{2+*}} c_{\text{Cd}(\text{H}_2\text{O})_{n-p-q}^{2+*}} - K_1 y_{\text{Cd}(\text{H}_2\text{O})_{n-p-q}^+} c_{\text{Cd}(\text{H}_2\text{O})_{n-p-q}^+} \right) \quad (\text{A8})$$

$$v_2 = k_2 \left(y_{\text{Cd}(\text{H}_2\text{O})_{n-p-q-r}^+} c_{\text{Cd}(\text{H}_2\text{O})_{n-p-q-r}^+} - K_2 y_{\text{Cd}(\text{Hg})} c_{\text{Cd}(\text{Hg})} a_{\text{H}_2\text{O}}^s \right) \quad (\text{A9})$$

For the dehydration equilibria given by reactions (A1), (A3) and (A5), we define the equilibrium constants K_{H1} , K_{H2} and K_{H3} by

$$K_{H1} = \frac{y_{Cd(H_2O)_n^{2+}} \cdot c_{Cd(H_2O)_n^{2+}}}{y_{Cd(H_2O)_{n-p}^{2+}} \cdot c_{Cd(H_2O)_{n-p}^{2+}} \cdot a_{H_2O}^p} \quad (A10)$$

$$K_{H2} = \frac{y_{Cd(H_2O)_{n-p}^{2+}} \cdot c_{Cd(H_2O)_{n-p}^{2+}}}{y_{Cd(H_2O)_{n-p-q}^{2+}} \cdot c_{Cd(H_2O)_{n-p-q}^{2+}} \cdot a_{H_2O}^q} \quad (A11)$$

$$K_{H3} = \frac{y_{Cd(H_2O)_{n-p-q}^+} \cdot c_{Cd(H_2O)_{n-p-q}^+}}{y_{Cd(H_2O)_{n-p-q-r}^+} \cdot c_{Cd(H_2O)_{n-p-q-r}^+} \cdot a_{H_2O}^r} \quad (A12)$$

The way to find the equation for the reciprocal forward rate constant is to start with eqn. (A9) and to eliminate all intermediate concentrations and molar activity coefficients by substituting eqns. (A7), (A8) and (A10)–(A12). Assuming equality of fluxes, $v_c = v_1 = v_2 = v$, and with the thermodynamic relationship

$$K_{H1} K_c K_{H2} K_1 K_{H3} K_2 = e^\varphi \quad (A13)$$

we get

$$\begin{aligned} v \left(1 + \frac{k_2}{k_c K_c K_{H2} K_1 K_{H3} a_{H_2O}^{p+q+r}} + \frac{k_2}{k_1 K_1 K_{H3} a_{H_2O}^r} \right) \\ = \frac{k_2 y_{O,s}}{K_{H1} K_c K_{H2} K_1 K_{H3} a_{H_2O}^{p+q+r}} \left\{ c_{Cd(H_2O)_{h_0}^{2+}} - c_R e^\varphi \frac{y_R}{y_{O,s} a_{H_2O}^{-h_0}} \right\} \end{aligned} \quad (A14)$$

with $h_0 = p + q + r + s = n$, $y_{O,s} = y_{Cd(H_2O)_{h_0}^{2+}}$ and $y_R = y_{Cd(Hg)}$.

From eqn. (A14) we easily obtain the reciprocal forward rate constant by introducing

$$k_1 = k_{s,1} \exp\left(-\frac{1}{2}\alpha_1\varphi\right) \quad (A15)$$

and

$$k_2 = k_{s,2} \exp\left(-\frac{1}{2}\alpha_2\varphi\right) \quad (A16)$$

for the rate constant of the electrochemical steps and

$$K_1 = \exp\left(\frac{\varphi}{2} + F(E^\circ - E_1^\circ)/RT\right) \quad (A17)$$

$$K_2 = \exp\left(\frac{\varphi}{2} + F(E^\circ - E_2^\circ)/RT\right) \quad (A18)$$

with

$$\varphi = \frac{2F}{RT}(E - E^\circ) \quad (A19)$$

The final expression for $1/k_f$ then reads

$$\frac{1}{k_f} = \frac{1}{y_{O,s}} \left\{ \frac{a_{H_2O}^p}{k_c} + \frac{a_{H_2O}^{p+q} e^{1/2\alpha_1\varphi}}{k_1'} + \frac{a_{H_2O}^{p+q+r} e^{1/2(\alpha_2+1)\varphi}}{k_2'} \right\} \quad (A20)$$

with the following abbreviations:

$$k'_c = k_c K_{H1}^{-1} K_{H2}^{-1} \quad (A21)$$

$$k'_1 = k_{s1} K_{H1}^{-1} K_{H2}^{-1} \quad (A22)$$

$$k'_2 = k_{s2} K_c^{-1} K_{H1}^{-1} K_{H2}^{-1} K_{H3}^{-1} \quad (A23)$$

From eqn. (A20) it follows that the real rate constants are obtained by dividing the observed values by the molar activity coefficient

$$y_{O,s} = \frac{f_O^{DH} m_O / c_O}{1 + 0.018(2 - h_s) m_s}$$

(see eqn. 21) of the hydrated Cd ion for each base electrolyte concentration.

REFERENCES

- 1 R. Andreu, M. Sluyters-Rehbach, A.G. Remijnse and J.H. Sluyters, *J. Electroanal. Chem.*, 175 (1984) 251.
- 2 C.P.M. Bongenaar, A.G. Remijnse, M. Sluyters-Rehbach and J.H. Sluyters, *J. Electroanal. Chem.*, 111 (1980) 139, 155.
- 3 J. Struys, M. Sluyters-Rehbach and J.H. Sluyters, *J. Electroanal. Chem.*, 171 (1984) 177.
- 4 J. Struys, M. Sluyters-Rehbach and J.H. Sluyters, *J. Electroanal. Chem.*, 146 (1983) 263.
- 5 G.J. Brug, M. Sluyters-Rehbach and J.H. Sluyters, *J. Electroanal. Chem.*, 176 (1984) 297.
- 6 C.J. van Velzen, M. Sluyters-Rehbach and J.H. Sluyters, *Electrochim. Acta*, 32 (1987) 815.
- 7 R.A. Robinson and R.H. Stokes, *Electrolyte Solutions*, Butterworths, London, 1965.
- 8 B.B. Damaskin, A.N. Frumkin, V.F. Ivanov, N.I. Melekhova and V.F. Khonina, *Elektrokhimiya*, 4 (1968) 1336.
- 9 H. Wroblowa, Z. Kovac and J.O'M. Bockris, *Trans. Faraday Soc.*, 61 (1965) 1523.
- 10 R. Payne, *J. Phys. Chem.*, 70 (1966) 204.
- 11 R. Parsons and R. Payne, *Z. Phys. Chem., N.F.*, 98 (1975) 9.
- 12 C.P.M. Bongenaar, M. Sluyters-Rehbach and J.H. Sluyters, *J. Electroanal. Chem.*, 109 (1980) 23.
- 13 J. Struys, M. Sluyters-Rehbach and J.H. Sluyters, *J. Electroanal. Chem.*, 143 (1983) 37, 61.
- 14 D.M. Mohilner in A.J. Bard (Ed.), *Electroanalytical Chemistry*, Vol. 1, Marcel Dekker, New York, 1966, pp. 241-409.
- 15 J. Newman, *J. Electroanal. Chem.*, 15 (1969) 309.
- 16 J. Koryta, J. Dvorák and V. Bokácková, *Electrochemistry*, Methuen, London, 1970.
- 17 E.A. Moelwijn-Hughes, *Physical Chemistry*, Pergamon Press, Oxford, 1961.
- 18 T. Jacobsen and E. Skou, *Electrochim. Acta*, 22 (1977) 161.
- 19 Chai-fu Pan, *J. Phys. Chem.*, 25 (1978) 2699.
- 20 M. Sluyters-Rehbach and J.H. Sluyters in E. Yeager, J.O'M. Bockris, B.E. Conway and S. Sarangapani (Eds.), *Comprehensive Treatise of Electrochemistry*, Vol. 9, Plenum Press, New York, 1984, pp. 177-292.
- 21 M. Sluyters-Rehbach and J.H. Sluyters in C.M. Bamford and R.G. Compton (Eds.), *Comprehensive Chemical Kinetics*, Vol. 26, Elsevier, Amsterdam, 1986, pp. 203-354.
- 22 J.E. Enderby and G.W. Neilson in F. Franks (Ed.), *Water, a Comprehensive Treatise*, Vol. 6, Plenum Press, New York, 1979, pp. 1-46.
- 23 A.H. Narten, F. Vaslov and H.A. Levy, *J. Chem. Phys.*, 58 (1973) 5017.
- 24 J.R. Newsome, G.W. Neilson, J.E. Enderby and M. Sandström, *Chem. Phys. Lett.*, 82 (1981) 399.
- 25 G. Licheri, G. Paschina, G. Piccaluga and G. Pina, *J. Chem. Phys.*, 81 (1984) 6059.

- 26 R.M. Souto, M. Saakes, M. Sluyters-Rehbach and J.H. Sluyters, *J. Electroanal. Chem.*, 245 (1988) 167.
- 27 R.M. Reeves in J.O'M. Bockris, B.E. Conway and E. Yeager (Eds.), *Comprehensive Treatise of Electrochemistry*, Vol. 1, Plenum Press, New York and London, 1980, pp. 83-134.
- 28 J. Goodisman, *Electrochemistry: Theoretical Foundations*, John Wiley, New York and Toronto, 1987, pp. 136-144, 225-232.
- 29 L. Gierst in E. Yeager (Ed.), *Transactions of the Symposium on Electrode Processes*, Philadelphia, 1959, John Wiley, New York, 1961, p. 109.
- 30 C.W. de Kreuk, M. Sluyters-Rehbach and J.H. Sluyters, *J. Electroanal. Chem.*, 28 (1970) 391; 33 (1971) 267.

CHAPTER 3

THE REACTION PATHWAY OF THE Cd(II) REDUCTION IN MIXED (0.8 - x) M NaClO₄ + x M NaF BASE ELECTROLYTES

A theory is developed of how to obtain the reaction pathway(s) and the kinetic parameters of a metal ion reduction if the reduction proceeds in several heterogeneous steps and via several co-existing metal complexes in a so-called scheme of squares.

The theory is applied successfully to the results obtained using the demodulation technique on the reduction of Cd(II) from aqueous NaClO₄ + NaF mixed base electrolyte at a dropping mercury electrode.

(1) INTRODUCTION

The pronounced effects of anions on the rate of simple electrode reactions are generally recognized. Quantitatively, these effects show up in the well-known compilations by Tanaka and Tamamushi of the standard heterogeneous rate constants of reactions occurring at mercury electrodes [1]. However, these are the standard rate constants, i.e. pertaining (in principle) to the formal standard potential in a given medium, sometimes corrected for the non-specific double-layer effect and sometimes not.

In studies intended especially to explain anion effects, several models have been proposed. Most accepted seems to be the idea that the catalytic activity of halides and anions like thiocyanate should be due to their specific adsorption in the electrical double layer [2-7]. Still, it is not clear whether there is one common mechanism by which this catalysis is exerted. Anions like ClO₄⁻ and NO₃⁻ are also specifically adsorbed at mercury, but they do not bring about an acceleration of charge-transfer processes as do the halides. On the contrary, an inhibition of the stepwise reduction of Cu²⁺ to Cu(Hg) by NO₃⁻ has been reported [8].

An important aspect, hitherto scarcely considered, is the fact that cationic reactants may form complexes with the anions of the supporting electrolyte, and thus are distributed over various species bearing different charges. In the early

fifties, Gerischer reported some interesting studies [9,10] on the reduction of Zn(II) and Cd(II) in different complexing media, showing that the charge transfer proceeds via a minority species instead of the dominating species, e.g. via $\text{Zn}(\text{OH})_2$ instead of the dominating $\text{Zn}(\text{OH})_4^{2-}$ and via $\text{Cd}(\text{CN})_2$ or $\text{Cd}(\text{CN})_3^-$ instead of the dominating $\text{Cd}(\text{CN})_4^{2-}$ complex. Remarkably, the reacting complex was frequently found to be a neutral one.

Recently, the Zn(II)/Zn(Hg) and Cd(II)/Cd(Hg) reactions have been the subject of several studies in which anion effects were considered in connection with the mechanism of the charge-transfer process, which can be deduced from the potential dependence of the forward reduction rate constant [7,11–13]. For zinc, this mechanism is controlled by the two separate electron-transfer steps (EE mechanism); for cadmium, at least one co-rate-determining heterogeneous “chemical” reaction step is found to exist in all the cases studied so far (CEE mechanism). A detailed investigation of this reaction in a series of $(1-x) M \text{F}^- + x M \text{Cl}^-$ mixtures [13] even gave rise to the surmise of more of such chemical steps (CECEC mechanism).

The possible role of specific complex species in such mechanisms has not been considered thus far. A suitable system for this purpose appears to be the Cd(II)/Cd(Hg) reaction in mixtures of F^- and ClO_4^- at constant ionic strength, for which it may be assumed that only the fluoride ion forms complexes with Cd(II), whereas only the perchlorate ion is specifically adsorbed; however, presumably without having a specific influence on the reduction rate of Cd(II), opposite to the Cl^- ion.

In the present paper we describe an experimental study of this system, using demodulation measurements in view of the expected high rate constants [14,15]. It will be shown that the results can be interpreted in terms of the CEE mechanism, the formalism of which is extended in order to account for the existence of parallel reaction paths via different Cd(II)–fluoride complexes. A discussion of the most probable pathway, and the implications for the earlier studies involving the fluoride anion, will be given as well.

(II) EXPERIMENTAL

The measurements were performed using a three-electrode cell comprising a DME made from a drawn-out capillary as the working electrode, a mercury pool as the counter-electrode, and a sodium saturated calomel electrode (SSCE) as the reference electrode. The latter was connected to the cell via a salt bridge filled with cell solution. The cell was thermostated at $25.0 \pm 0.1^\circ \text{C}$.

A series of cell solutions was prepared, containing $(0.8-x) M \text{NaClO}_4 + x M \text{NaF}$, and 1 mM CdSO_4 , dissolved in freshly twice-distilled water. The values of x were 0, 0.2, 0.4, 0.6 and 0.8. The ionic strength was chosen to be $0.8 M$ in order not to exceed the limited solubility of NaF. Oxygen was removed by bubbling argon gas.

Sampled dc voltammograms were obtained as usual by means of the automatic Network Analyzer system [16], which was also used to measure the values of the differential double-layer capacitance of the DME in the supporting electrolyte. The

latter values were needed both for the analysis of the demodulation voltammograms and for the estimation of double-layer parameters (see Sections III.2 and III.3). All measurements were taken at exactly 4 s after drop birth.

In addition, the potentials of zero charge (pzc) in the supporting electrolytes were determined by measuring the charging current at a fast DME with a typical natural drop life of about 1 ms. The current vs. potential traces were displayed on an oscilloscope, enabling us to obtain E_{pzc} with an accuracy of 1 mV.

To determine the kinetics of the Cd(II) reduction, the demodulation method was applied, using the instrument described earlier [15]. The high frequency was 100 kHz and the low frequency 122 Hz. The current density (peak to peak) of the high frequency perturbation at the moment of measurement was kept constant at about 0.25 A cm^{-2} . The drops of the DME were knocked off mechanically, in this case at exactly 4 s time intervals. The demodulation voltammograms were measured in a dc potential range as wide as possible.

(III) DATA ANALYSIS

(III.1) Dc data

From the limiting currents of the dc voltammograms the diffusion coefficient, D_O , of Cd(II) was calculated using the expression accounting for diffusion to an expanding sphere, proposed by Newman [17]. Using the D_O values, the reversible half-wave potential, $E_{1/2}^r$, could be derived from the measured half-wave potentials. However, as the demodulation voltammograms are quite sensitive to the value of $E_{1/2}^r$, more accurate results were obtained from kinetic analysis of the latter (see Section III.3). The values of D_O and $E_{1/2}^r$ as a function of the fluoride concentration x are listed in Table 1.

The diffusion coefficient D_R of the cadmium in the amalgam was taken from the literature [18]: $D_R = 10 \times 10^{-6} \text{ cm}^2 \text{ s}^{-1}$. The formal standard potential, E_f° , could then be calculated as usual. The value of E_f° , also reported in Table 1, becomes more negative with increasing x , which indicates the presence of Cd(II)-fluoride complexes. The stability constants may be defined as

$$\beta_{O,j} = c_{\text{CdF}_j^{2-j}} / c_{\text{Cd}^{2+}} c_{\text{F}^-}^j \quad j = 1, 2, 3 \quad (1)$$

$$\beta_{O,0} = 1$$

The amount of data in Table 1 is not sufficient to deduce the set of β_j values unambiguously. However, combined with the E_f° values obtained in 1 M F^- and 1 M ClO_4^- [11-14], the following values were assigned: $\beta_{O,1} = 3 \text{ mol}^{-1} \text{ dm}^3$, $\beta_{O,2} = 2 \text{ mol}^{-2} \text{ dm}^6$, and $\beta_{O,3} = 6 \text{ mol}^{-3} \text{ dm}^9$.

(III.2) Double-layer data

The potentials of zero charge are also tabulated in Table 1. Their values for $x = 0, 0.6$ and 0.8 are in good agreement with the corresponding data reported in the literature [19,20]. The capacity vs. potential curves measured at $-450 > E > -1000$ mV (vs. SSCE) are represented in Fig. 1.

TABLE 1

Values of D_{O_2} and $E_{1/2}^r$ for Cd(II) in $x M$ NaF + $(0.8 - x) M$ NaClO₄ at the indicated values of x (x : concentration of NaF) The potentials of zero charge are also given

$x / \text{mol l}^{-1}$	$10^6 D_{O_2} / \text{cm}^2 \text{ s}^{-1}$	$E_{1/2}^r / \text{mV}$ (vs. SSCE)	E_{zc}^o / mV (vs. SSCE)	E_{pzc} / mV (vs. SSCE)
0	8.0	-570	-572	-510
0.2	8.0	-578	-580	-500
0.4	7.9	-584	-586	-490
0.6	7.0	-589	-592	-474
0.8	6.9	-593	-596	-433

By integration of these curves the charge density σ^M as a function of the potential was obtained. In order to calculate the potential profile in the diffuse double layer, it is necessary to estimate the charge density σ^1 in the inner layer due to specifically adsorbed ClO₄⁻. These data are not directly available in the literature for our mixtures at a total concentration of 0.8 M, but a satisfactory estimation, in view of our purpose, could be made by combining the data reported by Payne for 1 M (ClO₄⁻ + F⁻) mixtures [19] and by Parsons and Payne for pure ClO₄⁻ solutions [20]. We constructed plots of σ^1 vs. ClO₄⁻ concentration at constant σ^M for both systems as shown in Fig. 2. Clearly the presence of fluoride suppresses the specific ClO₄⁻ adsorption. The isotherms for $(0.8 - x) M$ ClO₄⁻ + $x M$ F⁻ were drawn just intuitively as shown in Fig. 2. In this way, the interpolated σ^1 values for $x = 0.2, 0.4$ and 0.6 were obtained.

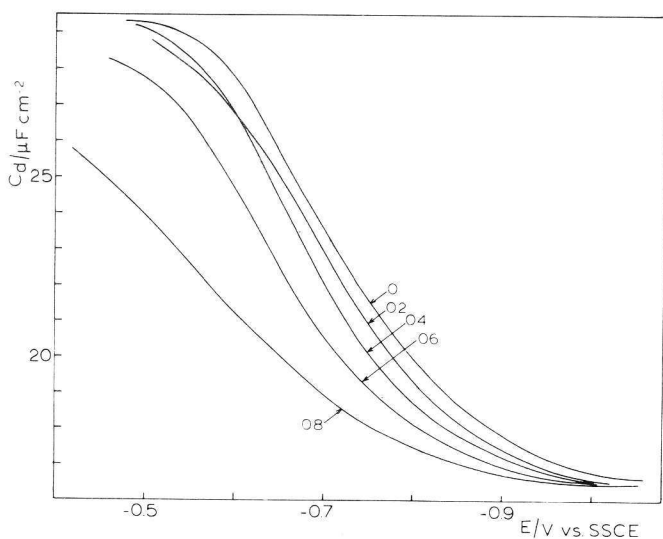


Fig. 1. Interfacial capacitance of aqueous solutions of $x M$ NaF + $(0.8 - x) M$ NaClO₄. The values of x are indicated.

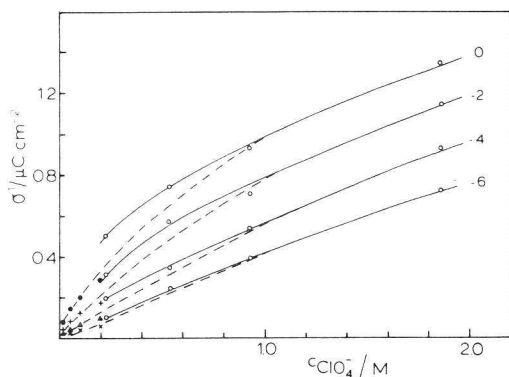


Fig. 2. The specifically adsorbed charge as a function of the ClO_4^- concentration, at surface charge densities $\sigma^M = 0, -2, -4$ and $-6 \mu\text{C cm}^{-2}$ (indicated in the figure). The drawn curves and open circles are for pure HClO_4 solutions, taken from ref. 19. The dashed curves connect the points at $c_{\text{ClO}_4^-} = 1 \text{ M}$ on the drawn lines with the experimental points for mixtures of $1 \text{ M } (\text{NH}_4\text{ClO}_4 + \text{NH}_4\text{F})$, taken from ref. 18 at various charge densities $\sigma^M/\mu\text{C cm}^{-2}$: (●) 0; (+) -2; (▲) -4; (×) -6.

From the values of $\sigma^M + \sigma^1$ the potentials ϕ_2 at the outer Helmholtz plane (OHP) were calculated assuming the validity of the Gouy–Chapman theory [21]. In view of the discussions to follow, the potentials $\phi_{1,\text{H}_2\text{O}}$, pertaining to a plane 0.28 nm remote from the OHP, were also computed. The data thus obtained in the faradaic regions of the Cd(II) reduction at all values of x are listed in Table 2.

(III.3) The kinetic analysis

The way to analyse the demodulation voltammograms has been extensively described before [14,15] and the most essential parameters and expressions have

TABLE 2

Values of ϕ_2 and $\phi_{1,\text{H}_2\text{O}}$ as a function of the potential for $x \text{ M NaF} + (0.8 - x) \text{ M NaClO}_4$

E/mV (vs. SSCE)	$x = 0$		$x = 0.2$		$x = 0.4$		$x = 0.6$		$x = 0.8$	
	ϕ_2/mV	$\phi_{1,\text{H}_2\text{O}}/\text{mV}$	ϕ_2/mV	$\phi_{1,\text{H}_2\text{O}}/\text{mV}$	ϕ_2/mV	$\phi_{1,\text{H}_2\text{O}}/\text{mV}$	ϕ_2/mV	$\phi_{1,\text{H}_2\text{O}}/\text{mV}$	ϕ_2/mV	$\phi_{1,\text{H}_2\text{O}}/\text{mV}$
-480	-38.9	-16.4	-32.4	-13.9	-25.2	-10.9	-15.8	-6.9	-6.1	-2.7
-500	-38.9	-16.4	-32.4	-13.9	-25.7	-11.1	-16.8	-7.3	-8.5	-3.7
-520	-38.9	-16.4	-32.5	-13.9	-26.2	-11.3	-17.8	-7.8	-10.8	-4.7
-540	-38.9	-16.4	-32.6	-13.9	-26.8	-11.6	-18.9	-8.2	-12.9	-5.6
-560	-38.9	-16.4	-32.9	-14.0	-27.5	-11.8	-20.3	-8.8	-15.1	-6.6
-580	-39.0	-16.5	-33.3	-14.2	-28.2	-12.1	-21.5	-9.3	-17.1	-7.5
-600	-39.1	-16.5	-33.7	-14.4	-29.1	-12.5	-22.9	-9.9	-19.1	-8.3
-620	-39.3	-16.6	-34.1	-14.5	-29.9	-12.8	-24.1	-10.4	-21.0	-9.1
-640	-39.5	-16.7	-34.8	-14.8	-30.8	-13.2	-25.5	-11.0	-22.9	-9.9
-660	-39.8	-16.8	-35.6	-15.1	-31.7	-13.6	-26.9	-11.6	-24.6	-10.6
-680	-40.2	-16.9	-36.4	-15.5	-32.7	-14.0	-28.2	-12.1	-26.3	-11.3
-700	-40.7	-17.1	-37.2	-15.8	-33.8	-14.4	-29.4	-12.6	-27.9	-12.0
-720	-41.3	-17.4	-38.1	-16.1	-35.0	-14.9	-30.7	-13.2	-29.4	-12.6

been recalled in a previous study concerning the reduction of Cd(II) [22]. As argued there, it is necessary to adopt a mechanism a priori which prescribes the potential dependence of the reduction rate constant k_f . Also in the present work the CEE mechanism was adopted, and a possible non-specific double-layer correction was accounted for. This means that k_f is given by the expression

$$\frac{\exp\left[-\frac{zF}{RT}\phi_r\right]}{k_f} = \frac{1}{k_f^t} = \frac{1}{k_{s,0}^c} + \frac{\exp\frac{1}{4}\phi_r'}{k_{s,1}} + \frac{\exp\frac{3}{4}\phi_r'}{k_{s,2}} \quad (2)$$

with

$$\phi_r' = (2F/RT)(E - E_f^0 - \phi_r) \quad (3)$$

where z is the charge of the reacting Cd(II) species and ϕ_r is the potential of the

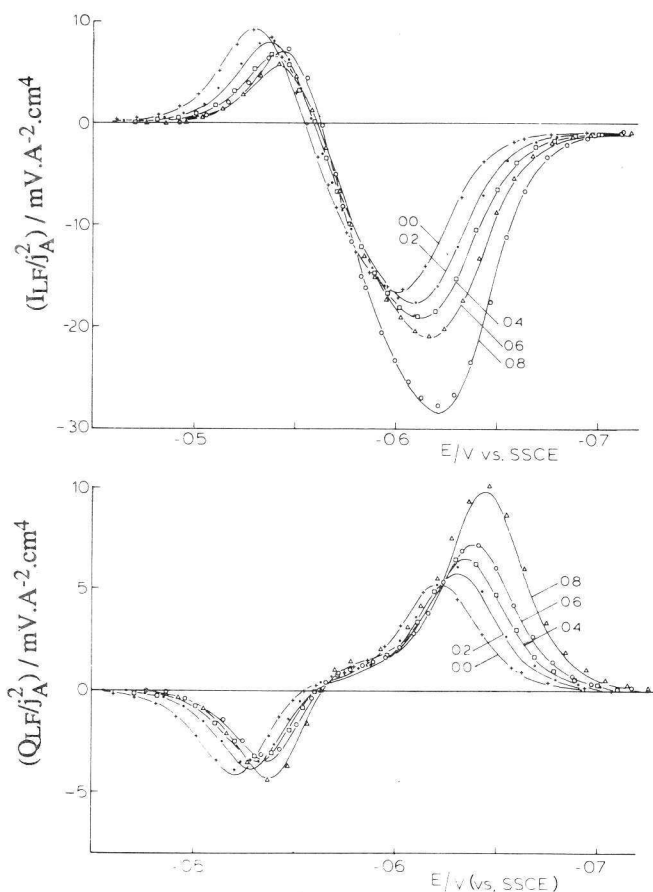


Fig. 3. (a) In-phase and (b) quadrature demodulation voltammograms of 1 mM Cd(II) in the same solutions as in Fig. 1. (+, ●, □, ○, △) Experimental data; (—) theoretical voltammograms obtained with $\phi_r = \phi_{1,H_2O}$.

reaction plane towards which the reactant has to move prior to the first reaction step. The three terms on the right-hand side of eqn. (2) correspond to the three subsequent steps in the CEE mechanism, i.e. the preceding chemical reaction and the two electron-transfer steps.

In contradistinction to our study in the perchlorate solutions [22], in the presence of fluoride the Cd(II) will be distributed over various complexes with charges + 2, +1, 0 and -1. Therefore, in eqn. (2), z has to represent the so-called "effective charge" [13]. The implications of this will be dealt with in Section (IV).

As before, the demodulation data were analysed three times, choosing $\phi_r = 0$, $\phi_r = \phi_2$ and $\phi_r = \phi_{1,H_2O}$, respectively. The fit to eqn. (2) was equally good in all cases, thus establishing again the validity of the CEE mechanism. In Fig. 3 the quality of the fits is demonstrated by plotting the experimental and the theoretical demodulation voltammograms (taking $\phi_r = \phi_{1,H_2O}$).

This analysis yielded the values of $k_{s,0}^c$, $k_{s,1}$ and $k_{s,2}$ for all the solution compositions, and from these values the corresponding "Tafel plots" of $\ln k_f$ vs. potential were calculated. These results will be discussed in the sections to follow.

(IV) RESULTS AND DISCUSSION

(IV.1) The kinetic parameters

The primary results from the kinetic analysis are the values for $k_{s,0}^c$, $k_{s,1}$ and $k_{s,2}$ referred to the formal standard potential E_f° pertaining to each solution composition. These results are given in Table 3.

The fits taking $\phi_r = 0$ actually yield the apparent individual rate constants [22]. For $x = 0.8$, i.e. the 0.8 M NaF solution, the results are reasonably close to those reported earlier for 1 M KF [13,14]. For $x = 0$, i.e. the 0.8 M NaClO₄ solution, all the rate constants are higher than those reported before by Struijs et al. [14]. However, in ref. 14 some inconsistency with the CEE mechanism was reported, which was absent in the present results.

TABLE 3

Values of $k_{s,0}^c$, $k_{s,1}$ and $k_{s,2}$ using $\phi = 0$, ϕ_{1,H_2O} and ϕ_2 for x M NaF + (0.8 - x) M NaClO₄ at the indicated standard potentials. Accuracies are typically 3 in the final digits

x	E_f° /mV (vs. SSCE)	$\phi_r = 0$			$\phi_r = \phi_{1,H_2O}$			$\phi_r = \phi_2$		
		$k_{s,0}^c$ / cm s ⁻¹	$k_{s,1}$ / cm s ⁻¹	$k_{s,2}$ / cm s ⁻¹	$k_{s,0}^c$ / cm s ⁻¹	$k_{s,1}$ / cm s ⁻¹	$k_{s,2}$ / cm s ⁻¹	$k_{s,0}^c$ / cm s ⁻¹	$k_{s,1}$ / cm s ⁻¹	$k_{s,2}$ / cm s ⁻¹
0	-572	4.5	0.75	8.3	1.2	0.288	5.5	0.18	0.079	3.3
0.2	-580	1.4	0.58	3.7	1.0	0.299	5.5	0.20	0.126	5.3
0.4	-586	1.6	0.37	3.6	0.9	0.293	4.6	0.29	0.167	5.0
0.6	-592	1.6	0.27	3.7	1.3	0.273	5.3	0.65	0.230	5.0
0.8	-596	1.1	0.20	2.1	1.1	0.243	2.8	0.86	0.270	4.2

Some discussions about the formalism to be used to account for the non-specific double-layer effect (“Frumkin correction”) were recently raised in papers from this laboratory dealing with the Zn(II) and the Cd(II) reduction [13,22,23]. First, in view of the large size of the metal ion as compared with Na^+ , in pure ClO_4^- solutions, it was considered unlikely that it would move towards the outer Helmholtz plane prior to the onset of the reduction process. Therefore it was proposed that the reaction plane be situated at a distance of 0.28 nm (i.e. the diameter of one water molecule) from the OHP towards the solution. The potential at this location was indicated by $\phi_{1,\text{H}_2\text{O}}$ [22,23]. In the case of both the Zn(II) and the Cd(II) reduction, this resulted in a better consistency of the corrected rate constants obtained under variation of the NaClO_4 concentration.

In the present study, the nature of the Cd(II) species will change when ClO_4^- is replaced by F^- . Most probably, the fluoride complexes are less strongly hydrated, or even not hydrated at all. This may allow them to move closer to the OHP, and consequently equating ϕ_r with ϕ_2 becomes plausible. In order not to speculate too much on this point, we decided to consider the results of both possibilities, i.e. of fits taking $\phi_r = \phi_2$ and $\phi_r = \phi_{1,\text{H}_2\text{O}}$, respectively.

Another point is the variance of the charges of the cadmium–fluoride complexes. As it was concluded (see Section III.1) that the species Cd^{2+} , CdF^+ , CdF_2 and CdF_3^- are present in significant amounts, the corresponding Boltzmann factors needed to calculate the concentrations in the reaction plane have to be adapted. Following the derivation given in our study of the Cd(II) reduction in $\text{F}^- + \text{Cl}^-$ mixtures [13], we can express the total concentrations of the Cd(II) species, c_{OT} , by

$$\frac{c_{\text{OT}}}{c_{\text{Cd}^{2+}}} = 1 + \beta_{\text{O},1}x + \beta_{\text{O},2}x^2 + \beta_{\text{O},3}x^3 = F_{\text{O}}(x) \quad (4)$$

x being the F^- concentration, and $\beta_{\text{O},1}$, $\beta_{\text{O},2}$, $\beta_{\text{O},3}$ the stability constants, derived from the dc data (Section III.1).

Similarly, the total Cd(II) concentration, c_{OT}^{\dagger} , in the reaction plane, will be related to the concentration, $c_{\text{Cd}^{2+}}^{\dagger}$, of the aquo ion in the reaction plane by

$$\frac{c_{\text{OT}}^{\dagger}}{c_{\text{Cd}^{2+}}^{\dagger}} = 1 + \beta_{\text{O},1}y + \beta_{\text{O},2}y^2 + \beta_{\text{O},3}y^3 = F_{\text{O}}(x, \phi_r) \quad (5)$$

where y is the F^- concentration in the reaction plane:

$$y = x \exp(f\phi_r) \quad (6)$$

with $f = F/RT$.

Because $c_{\text{Cd}^{2+}}^{\dagger}/c_{\text{Cd}^{2+}} = \exp(-2f\phi_r)$, the ratio of the total concentrations becomes

$$\frac{c_{\text{OT}}^{\dagger}}{c_{\text{OT}}} = \frac{F_{\text{O}}(x, \phi_r)}{F_{\text{O}}(x)} \exp[-2f\phi_r] \quad (7)$$

and this leads to the definition of the “effective charge” [13]:

$$z_{\text{eff}} = 2 - \frac{1}{f\phi_r} \ln \frac{F_{\text{O}}(x, \phi_r)}{F_{\text{O}}(x)} \quad (8)$$

TABLE 4

Values of z_{eff} as a function of the potential for $x M \text{ NaF} + (0.8 - x) M \text{ NaClO}_4$ using $\phi_r = \phi_{1, \text{H}_2\text{O}}$

E/mV (vs. SSCE)	z_{eff}				
	$x = 0$	$x = 0.2$	$x = 0.4$	$x = 0.6$	$x = 0.8$
-480	2	1.59	1.16	0.68	0.23
-500	2	1.59	1.16	0.69	0.26
-520	2	1.59	1.16	0.70	0.28
-540	2	1.59	1.17	0.71	0.30
-560	2	1.59	1.17	0.72	0.33
-580	2	1.59	1.17	0.73	0.35
-600	2	1.60	1.18	0.74	0.37
-620	2	1.60	1.18	0.75	0.39
-640	2	1.60	1.19	0.76	0.40
-660	2	1.60	1.19	0.78	0.42
-680	2	1.60	1.20	0.79	0.44
-700	2	1.61	1.21	0.80	0.45
-720	2	1.61	1.21	0.81	0.47

The parameter z occurring in eqn. (2) has to be replaced by z_{eff} . It is clear that where ϕ_r is dependent on the electrode potential E , z_{eff} will also be potential-dependent. It is instructive to have an idea of the magnitude of the effect, for which purpose the compilations in Table 4 have been prepared.

Strictly, relations (4)–(7) should be written in terms of activities rather than concentrations and, even more strictly, it should be realized that activity coefficients at the reaction plane may differ from those in the bulk. The effect of neglecting this is probably not essential in the analysis to follow.

(IV.2) Tafel plots

It is also instructive to inspect the dependence of the reaction rate on the solution composition visualized by the plots of $\ln k_f$ vs. the potential difference between the electrode and the reaction plane for the compositions indicated, given in Fig. 4.

As is already known from the literature [14], the apparent rate constant, k_f , is considerably higher in the pure ClO_4^- solution than in the pure F^- solution. The plots pertaining to the mixtures lead to the conclusion that in the entire faradaic region the reduction rate constant increases with decreasing x . One could say that ClO_4^- "catalyses" the reduction of Cd(II) , or that F^- "inhibits" this reduction.

A comparison of "Frumkin-corrected" Tafel plots in the two electrolytes has thus far never been made. Remarkably, taking $\phi_r = \phi_2$ leads to an inversion of the reaction rate dependence on the fluoride concentration at potentials more negative than ca. -0.5 V (vs. SSCE). This means that now the fluoride appears to "catalyse" at $E < -0.5 \text{ V}$ and to "inhibit" at $E > -0.5 \text{ V}$. This could be ascribed to (some of) the fluoride complexes taking part in the reaction with rate constants different from those pertaining to the aquo ion.

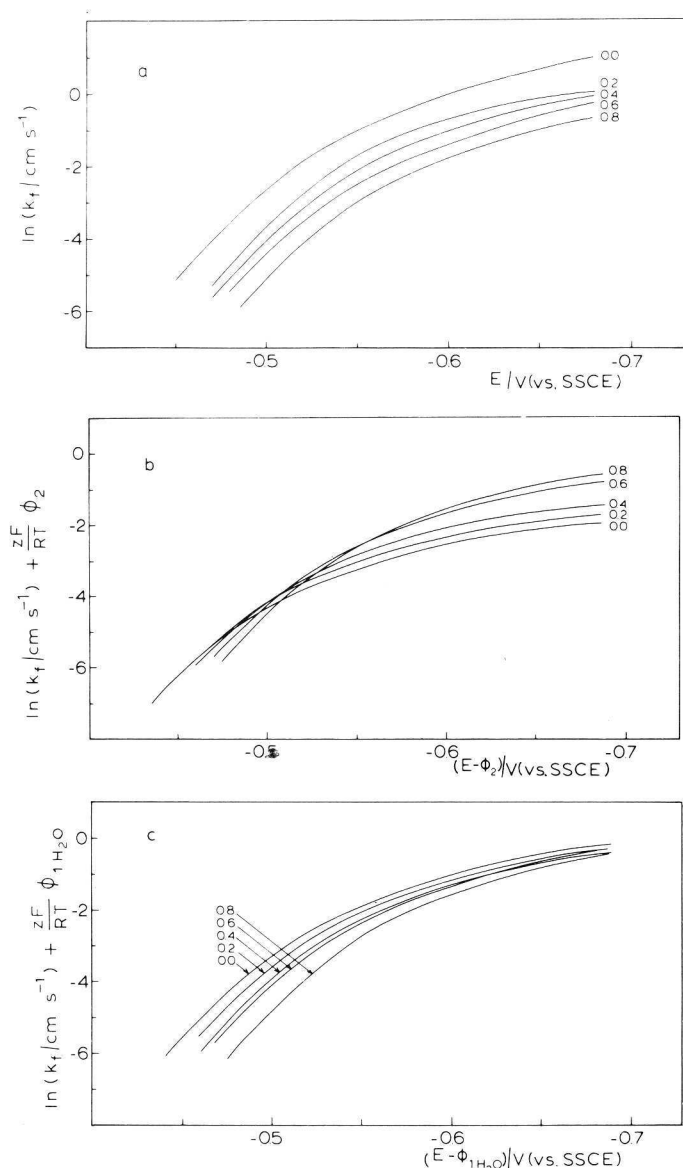


Fig. 4. Potential dependence of $\ln k_f$ calculated for the same solutions as in Fig. 3 taking the reaction plane (a) at the electrode surface, (b) in the outer Helmholtz plane and (c) 0.28 nm more remote from the outer Helmholtz plane.

Finally, with $\phi_r = \phi_{1, \text{H}_2\text{O}}$, an outstanding regular series of $\ln k_f^{\ddagger}$ vs. $E - \phi_r$ plots is obtained. They have the tendency to coincide at the most negative potentials. Note that there the chemical reaction step in the CEE mechanism is predominantly rate-determining. Indeed, the value for $k_{s,0}^c$ (see Table 3) is fairly independent of the fluoride concentration.

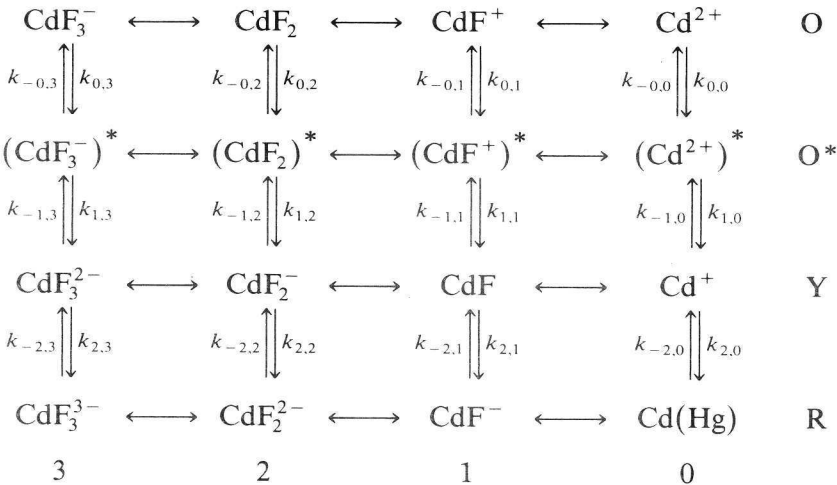
(IV.3) The possibility of parallel reaction pathways

The expressions used in the foregoing analysis imply, in fact, that the overall rate equation for the charge-transfer process is of the general form [24,25]

$$v = k_f [c_{OT}^t - c_R \exp \varphi_f'] \quad (9)$$

with φ_f' given by eqn. (3) and $v = j_F/nF$; c_R is the surface concentration of the metal amalgam and c_{OT}^t is the total concentration of all the oxidized species present at the reaction plane. In other words, it is assumed that fast equilibria exist between the several metal ion complexes and the aquo ion, thus supplying the species that undergoes the reduction reaction infinitely fast. This principle was elaborated by Gerischer, who showed in an elegant way that it can be deduced from the dependence of the exchange current density on the ligand concentration which of the complexes is the reacting species [9,10]. This analysis was found to work quite well if there was only one reducible species; in a few cases, however, it appeared that there were at least two [10]. In later studies in the literature [2,26], the idea of all species being reducible in principle was adopted to derive expressions for the apparent and the true standard rate constant, k_{sh} , of an electrode reaction as a function of the ligand concentration, x . Naturally, such expressions are polynomials in x .

To our knowledge, the implications of several complexes being reduced via a mechanism of consecutive elementary steps have not yet been considered. Here we will give such a treatment focused on the cadmium-fluoride system, reduced by a CEE mechanism. The following reaction scheme is supposed to apply:



The vertical arrows represent the rate-determining steps of the CEE mechanism (all reactions are heterogeneous). Each step may proceed via four parallel reactions involving an uncomplexed reactant, and the three complexed reactants respectively. The horizontal double-sided arrows indicate that the substances in the same state of

reduction are in equilibrium, i.e. they can be converted into each other infinitely fast. The conversions from state O* to Y and from state Y to R involve one electron each. The horizontal conversions, of course, all involve the transfer of one fluoride ion.

Only Cd(Hg) and CdF₃⁻, CdF₂, CdF⁺, Cd²⁺ are considered as *stable species*. For their concentrations in the reaction plane the following expressions will hold:

$$c_{\text{Cd(Hg)}}^t = c_{\text{Cd(Hg)}} \quad (10)$$

$$\begin{aligned} c_{\text{CdF}_j^{2-j}}^t &= c_{\text{CdF}_j^{2-j}} \exp[-(2-j)f\phi_r] \\ &= c_{\text{Cd}^{2+}} \beta_{\text{O},j} x^j \exp[-(2-j)f\phi_r] \\ &= \beta_{\text{O},j} y^j c_{\text{Cd}^{2+}} \exp[-2f\phi_r] \\ &= \beta_{\text{O},j} y^j c_{\text{Cd}^{2+}}^t \end{aligned} \quad (11)$$

with $f = F/RT$. The concentrations without the superscript t are “surface concentrations”, i.e. the concentrations that would occur at the reaction plane if its potential difference with the solution were zero. The stability constants, $\beta_{\text{O},j}$, are defined by eqn. (1), and the “true” concentration, y , of F⁻ in the reaction plane by eqn. (6). The different versions of the right-hand side of eqn. (11) are equivalent, but the last is the more convenient one for our purpose.

In an analogous way, the concentrations of the intermediate complexes can be related to the concentration of the uncomplexed intermediate with which they are in equilibrium. The relevant expressions are

$$c_{(\text{CdF}_j^{2-j})^*}^t = \beta_{\text{O}^*,j} y^j c_{\text{Cd}^{2+}}^t \quad (12)$$

$$c_{\text{CdF}_j^{1-j}}^t = \beta_{\text{Y},j} y^j c_{\text{Cd}^+}^t \quad (13)$$

$$c_{\text{CdF}_j^{-j}}^t = \beta_{\text{R},j} y^j c_{\text{Cd(Hg)}}^t \quad (14)$$

Let us first consider the situation of equilibrium, i.e. the net rate of the whole process equals zero. In this case, the concentrations of the species connected by vertical arrows obey the equilibrium condition, e.g. $c_{\text{Cd}^{2+}}/c_{(\text{Cd}^{2+})^*} = k_{-0,0}/k_{0,0} = K_{0,0}$, etc. From corresponding equilibria it is easily derived that, in general, the following relationships hold:

$$\frac{k_{-0,j}}{k_{0,j}} = \frac{k_{-0,0}}{k_{0,0}} \frac{\beta_{\text{O},j}}{\beta_{\text{O}^*,j}} = K_{0,0} \frac{\beta_{\text{O},j}}{\beta_{\text{O}^*,j}} \quad (15a)$$

$$\frac{k_{-1,j}}{k_{1,j}} = \frac{k_{-1,0}}{k_{1,0}} \frac{\beta_{\text{O}^*,j}}{\beta_{\text{Y},j}} = K_{1,0} \frac{\beta_{\text{O}^*,j}}{\beta_{\text{Y},j}} \quad (15b)$$

$$\frac{k_{-2,j}}{k_{2,j}} = \frac{k_{-2,0}}{k_{2,0}} \frac{\beta_{\text{Y},j}}{\beta_{\text{R},j}} = K_{2,0} \frac{\beta_{\text{Y},j}}{\beta_{\text{R},j}} \quad (15c)$$

Furthermore, it is important to note that

$$K_{0,0}K_{1,0}K_{2,0} = \exp[(2F/RT)(E - E^\circ - \phi_r)] = \exp(\varphi') \quad (16)$$

where E° is the standard potential of the redox couple $\text{Cd}^{2+}/\text{Cd}(\text{Hg})$.

If the equilibrium is perturbed, the overall reaction will proceed with a net rate v . We can define the net rates of the partial reactions v_0 , v_1 and v_2 for the conversions of O into O^* , O^* into Y, and Y into R respectively, in the following form:

$$v_0 = c_{\text{Cd}^{2+}}^t \sum_{j=0}^3 k_{0,j} \beta_{\text{O},j} y^j - c_{(\text{Cd}^{2+})^*}^t \sum_{j=0}^3 k_{-0,j} \beta_{\text{O}^*,j} y^j \quad (17a)$$

$$v_1 = c_{(\text{Cd}^{2+})^*}^t \sum_{j=0}^3 k_{1,j} \beta_{\text{O}^*,j} y^j - c_{\text{Cd}^+}^t \sum_{j=0}^3 k_{-1,j} \beta_{\text{Y},j} y^j \quad (17b)$$

$$v_2 = c_{\text{Cd}^+}^t \sum_{j=0}^3 k_{2,j} \beta_{\text{Y},j} y^j - c_{\text{Cd}(\text{Hg})}^t \sum_{j=0}^3 k_{-2,j} \beta_{\text{R},j} y^j \quad (17c)$$

Because all the intermediates are unstable (they do not diffuse into the solution, neither adsorb at the interface to a significant amount) it is required that $v_0 = v_1 = v_2 = v$. With this it is possible to eliminate the unknown concentrations $c_{(\text{Cd}^{2+})^*}^t$ and $c_{\text{Cd}^+}^t$ from eqns. (17a)–(17c), and using eqns. (15a)–(15c) and (16) this leads to

$$v \left\{ \frac{1}{\sum_{j=0}^3 k_{0,j} \beta_{\text{O},j} y^j} + \frac{K_{0,0}}{\sum_{j=0}^3 k_{1,j} \beta_{\text{O}^*,j} y^j} + \frac{\exp\left[\frac{2F}{RT}(E - E^\circ - \phi_r)\right]}{\sum_{j=0}^3 k_{-2,j} \beta_{\text{R},j} y^j} \right\} = c_{\text{Cd}^{2+}}^t - c_{\text{Cd}(\text{Hg})}^t \exp[(2F/RT)(E - E^\circ - \phi_r)] \quad (18)$$

The rate constants $k_{0,j}$ of the chemical steps are assumed to be potential-independent. The rate constants $k_{1,j}$ and $k_{-2,j}$ are assumed to depend on the potential according to [14,24,25]

$$k_{1,j} = k_{s1,j} \exp[-(F/2RT)(E - E^\circ - \phi_r)] \quad (19a)$$

$$k_{-2,j} = k_{s2,j} \exp[(F/2RT)(E - E^\circ - \phi_r)] \quad (19b)$$

i.e. the symmetry factors of both electron-transfer steps are taken equal to 0.5. On this basis, and using the abbreviation in eqn. (16), eqn. (18) becomes

$$v \left\{ \frac{1}{k'_{s,0}} + \frac{\exp(\frac{1}{4}\varphi')}{k'_{s,1}} + \frac{\exp(\frac{3}{4}\varphi')}{k'_{s,2}} \right\} = c_{\text{Cd}^{2+}}^t - c_{\text{Cd}(\text{Hg})}^t \exp(\varphi') \quad (20)$$

with

$$k'_{s,0} = \sum_{j=0}^3 k_{0,j} \beta_{\text{O},j} y^j = \sum_{j=0}^3 a_{0,j} y^j \quad (21a)$$

$$k'_{s,1} = \sum_{j=0}^3 \frac{k_{s1,j}}{K_{0,0}} \beta_{O^*,j} y^j = \sum_{j=0}^3 a_{1,j} y^j \quad (21b)$$

$$k'_{s,2} = \sum_{j=0}^3 k_{s2,j} \beta_{R,j} y^j = \sum_{j=0}^3 a_{2,j} y^j \quad (21c)$$

If desired, the concentration $c_{Cd^{2+}}^t$ can be replaced by $c_{OT}^t/F_O(x, \phi_r)$. This leads to the rate equation

$$v = k_f^t [c_{OT}^t - c_{Cd(Hg)} \exp(\varphi_r')] \quad (22)$$

with

$$\frac{1}{k_f^t} = \left\{ \frac{1}{k'_{s,0}} + \frac{\exp(\frac{1}{4}\varphi_r')}{k'_{s,1}} + \frac{\exp(\frac{3}{4}\varphi_r')}{k'_{s,2}} \right\} F_O(x, \phi_r) \quad (23)$$

The version with the apparent rate constant can also be reconstructed, using $c_{OT}^t = c_{OT} F_O(x, \phi_r)/F_O(x) \cdot \exp(-2f\phi_r)$:

$$v = k_f^a [c_{OT} - c_{Cd(Hg)} \exp \varphi_r] \quad (24)$$

with

$$\frac{1}{k_f^a} = \left\{ \frac{1}{k'_{s,0}} + \frac{\exp(\frac{1}{4}\varphi_r')}{k'_{s,1}} + \frac{\exp(\frac{3}{4}\varphi_r')}{k'_{s,2}} \right\} F_O(x) \exp(2f\phi_r) \quad (25)$$

In the next section, the applicability of eqn. (23) to the data sets of Table 3 will be examined.

(IV.4) Interpretation in terms of the CEE mechanism with parallel pathways

The formulation in Section (IV.3) is such that the potential E is referred to a common reference potential E° for all solutions. E° is the standard potential of the redox couple $Cd^{2+}/Cd(Hg)$. The primary kinetic data collected in Table 3 are the rate constants appearing in eqn. (2), where the potential E has been referred to the formal potential E_f° for each solution. Identifying eqn. (2) with eqn. (23) and using eqns. (3) and (16), it follows that

$$k_{s,0}^c = k'_{s,0}/F_O(x, \phi_r) \quad (26)$$

$$k_{s,1} \exp\left[\frac{1}{2} \frac{F}{RT} (E_f^\circ - E^\circ)\right] = k'_{s,1}/F_O(x, \phi_r) \quad (27)$$

$$k_{s,2} \exp\left[\frac{3}{2} \frac{F}{RT} (E_f^\circ - E^\circ)\right] = k'_{s,2}/F_O(x, \phi_r) \quad (28)$$

These relations enable us to calculate the primed rate constants from the data in Table 3. The value of E° is equal to the E_f° value measured for the 0.8 M $NaClO_4$ solution, i.e. $E^\circ = -0.572$ V (vs. SSCE). For ϕ_r , the value of either ϕ_2 or ϕ_{1,H_2O} at $E = -0.572$ V (vs. SSCE) in each solution was taken. The data sets thus obtained are compiled in Table 5.

TABLE 5

Data collected for the analysis in terms of the CEE mechanism with parallel pathways (for explanation see text). Accuracies are typically ± 3 in the final digits

(a) $\phi_r = \phi_2$

x	ϕ_2 /mV	y	$F_O(x, \phi_2)$	$k'_{s,0}$ - /cm s ⁻¹	$k'_{s,1}$ /cm s ⁻¹	$k'_{s,2}$ /cm s ⁻¹
0	-39	0	1	0.181	0.079	3.3
0.2	-33	0.0551	1.173	0.235	0.116	3.75
0.4	-28	0.134	1.454	0.42	0.184	3.2
0.6	-21	0.265	2.046	1.32	0.319	5.3
0.8	-16	0.429	3.129	2.68	0.528	3.3

(b) $\phi_r = \phi_{1,H_2O}$

x	ϕ_{1,H_2O} /mV	y	$F_O(x, \phi_{1,H_2O})$	$k'_{s,0}$ /cm s ⁻¹	$k'_{s,1}$ /cm s ⁻¹	$k'_{s,2}$ /cm s ⁻¹
0	-16.5	0	1	1.16	0.288	5.5
0.2	-14	0.116	1.384	1.30	0.322	4.6
0.4	-12	0.251	1.972	1.69	0.409	3.9
0.6	-9	0.423	3.078	3.90	0.563	4.9
0.8	-7	0.609	4.925	5.86	0.801	3.8

Strictly, this procedure is not entirely correct, because the potential profile, and thus $F_O(x, \phi_r)$, is in principle dependent on E . However, it happens that in our systems ϕ_2 and ϕ_{1,H_2O} vary only slightly with the electrode potential, so that the results in Table 5 will not be significantly different from the values that would have been obtained in a more rigorous way, i.e. fitting of the demodulation voltammograms to eqn. (23) or (25).

The next step is to examine the validity of expressions (21a)–(21c) for $k'_{s,i}$, i.e. to evaluate the polynomial coefficients $a_{i,j}$ ($i=0$ to 2, $j=0$ to 3). This part of the analysis is most conveniently discussed “step by step”:

(i) The values of $k'_{s,2}$ are, within experimental error, *independent* of the solution composition. Their average gives the following result:

$$\text{for } \phi_r = \phi_2 \quad : \quad k'_{s,2} = 3.8 \text{ cm s}^{-1}$$

$$\text{for } \phi_r = \phi_{1,H_2O} : \quad k'_{s,2} = 4.3 \text{ cm s}^{-1}$$

This means that the second electron is transferred solely to the non-complexed intermediate Cd^+ .

(ii) The values of $k'_{s,1}$ can be well described by a second-degree polynomial in y . Even if a third polynomial is admitted, $a_{1,3}$ attains a value close to zero. So, we have

$$\text{for } \phi_r = \phi_2 \quad : \quad k'_{s,1} = 0.08 + 0.51y + 1.25y^2 \text{ cm s}^{-1}$$

$$\text{for } \phi_r = \phi_{1,H_2O} : \quad k'_{s,1} = 0.29 + 0.20y + 1.09y^2 \text{ cm s}^{-1}$$

This means that the first electron is transferred to the three species (Cd^{2+})*,

(CdF⁺)^{*} and (CdF₂)^{*}. At high fluoride concentration, the latter species is favoured.

(iii) The rate constants obtained for the chemical step lead to $k'_{s,0}$ values with the remarkable behaviour of being quadratic functions of y :

$$\text{for } \phi_r = \phi_2 \quad : \quad k'_{s,0} = 0.18 + 13.7y^2 \quad \text{cm s}^{-1}$$

$$\text{for } \phi_r = \phi_{1,\text{H}_2\text{O}} : \quad k'_{s,0} = 1.16 + 12.7y^2 \quad \text{cm s}^{-1}$$

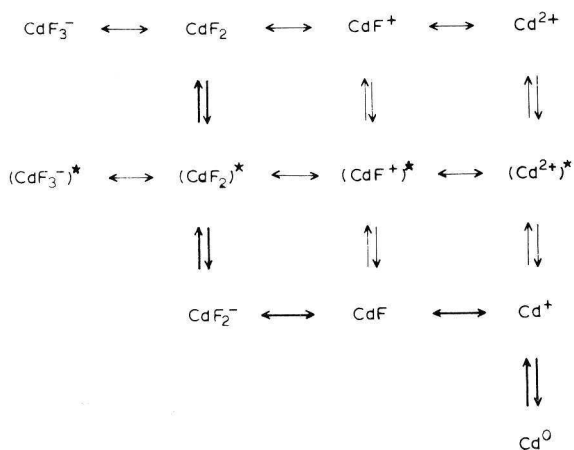
This means that in any case the species Cd²⁺ and CdF₂ undergo a chemical reaction preceding charge transfer. The complex species is highly favoured at a high fluoride concentration.

Some reservation has to be made here. The experimental accuracy of $k'_{s,0}$ is (much) less than that of $k'_{s,1}$. Therefore, a third-degree polynomial cannot be excluded. In fact, for $\phi_r = \phi_{1,\text{H}_2\text{O}}$ the rate constant $k^c_{s,0}$ itself is independent of the solution composition (see Table 3). This may imply that all the Cd(II) species present undergo the chemical reaction with exactly the same rate constant, and from a physical point of view this idea seems attractive.

(IV.5) Discussion and conclusions

Returning to the apparent reduction rate of Cd(II) in the mixtures of F⁻ and ClO₄⁻, it will be clear that three effects are responsible for the distances between the Tafel plots shown in Fig. 4a. Firstly, the potential of the reaction plane is less negative in fluoride than in perchlorate, so that in the presence of fluoride the reaction via Cd²⁺ is decelerated through the Boltzmann factor. Secondly, and in addition, the concentration of the free Cd²⁺ is lowered through the complex formation. Thirdly, however, this effect is partly counteracted by the fact that the complex species also appear to be electroactive. Both the chemical step and the first electron-transfer step show a tendency to proceed faster via the uncharged CdF₂ species, although for the chemical step it can also be concluded that all the complexes present react with the same rate constant. Concerning the second electron transfer, the conclusion is that any monovalent Cd(I) bound to F⁻ has to dissociate before the final reduction step can take place.

The whole picture is visualized by the following "reduced scheme of squares":



The bold arrows indicate the route preferably being followed at high fluoride concentration. It may be noticed that qualitatively, these conclusions hold irrespective of the choice of the reaction plane.

The present study is the fourth one in a series from this laboratory concerning the Cd(II) reduction being influenced by the solution composition. In the first one, thiourea (TU) was added to 1 M KF, and its extremely high accelerating effect was explained by surmising that the reduction proceeded via adsorbed Cd(II) complexes [12]. This is not unreasonable if indeed the CdF₂ is the faster reacting species. In the second study, mixtures of F⁻ + Cl⁻ were employed as the supporting electrolyte [13]. Only the chemical reaction and the first electron-transfer step were found to be accelerated by Cl⁻. A correlation with adsorbed Cl⁻ was sought, but in the light of the present results it seems also that the complex formation of Cd(II) with chloride, which is rather strong, has to be considered. It might well be that CdCl₂ and CdFCl complexes are able to react relatively fast, either via the adsorbed state or not.

Finally, from the work in pure ClO₄⁻ solutions with varied ionic strength, it was concluded that the reaction mechanism also comprises fast reaction steps in which the hydration shell of the aquo Cd²⁺ is repelled in a stepwise manner. It is fair to believe that the water activity will not change significantly if only the ClO₄⁻ is replaced by F⁻ at a constant ionic strength of 0.8 M as was done in the present paper. Then the Cd(II)-fluoride complexes will be less strongly hydrated, and therefore the intrinsic rate constant of a parallel pathway, e.g. CdF₂ ↔ (CdF₂)^{*} ↔ CdF₂⁻, can be larger than that of the reaction proceeding via the "free", but hydrated Cd²⁺.

We conclude that complexation appears to have an important influence on the rate of reduction, in this case of Cd(II). We hope that more examples of this effect, with other suitable metal ions and/or ligands, can be found and investigated.

REFERENCES

- 1 N. Tanaka and R. Tamamushi, *Electrochim. Acta*, 9 (1964) 963; R. Tamamushi, *Kinetic Parameters of Electrode Reactions of Metallic Compounds*, IUPAC additional publications, Butterworths, London, 1975.
- 2 P. Teppema, M. Sluyters-Rehbach and J.H. Sluyters, *J. Electroanal. Chem.*, 16 (1968) 165.
- 3 M. Sluyters-Rehbach, J.S.M.C. Breukel and J.H. Sluyters, *J. Electroanal. Chem.*, 19 (1968) 85.
- 4 B. Timmer, M. Sluyters-Rehbach and J.H. Sluyters, *J. Electroanal. Chem.*, 19 (1968) 73 and refs. cited therein.
- 5 R. Parsons, *J. Electroanal. Chem.*, 21 (1969) 35.
- 6 R. de Levie, *J. Electrochem. Soc.*, 118 (1971) C 185.
- 7 R. Andreu, M. Sluyters-Rehbach and J.H. Sluyters, *J. Electroanal. Chem.*, 171 (1984) 139.
- 8 A.W.M. Verkroost, M. Sluyters-Rehbach and J.H. Sluyters, *J. Electroanal. Chem.*, 47 (1973) 323.
- 9 H. Gerischer, *Z. Phys. Chem.*, 202 (1953) 292; 302.
- 10 H. Gerischer, *Z. Elektrochem.*, 57 (1953) 604.
- 11 C.P.M. Bongenaar, A.G. Remijnse, E. Temmerman, M. Sluyters-Rehbach and J.H. Sluyters, *J. Electroanal. Chem.* 111 (1980) 155.
- 12 R.M. Souto, M. Sluyters-Rehbach and J.H. Sluyters, *J. Electroanal. Chem.*, 201 (1986) 33.
- 13 R.M. Souto, M. Saakes, M. Sluyters-Rehbach and J.H. Sluyters, *J. Electroanal. Chem.*, 245 (1987) 167.

- 14 J. Struijs, M. Sluyters-Rehbach and J.H. Sluyters, *J. Electroanal. Chem.*, 171 (1984) 157, 171.
- 15 J. Struijs, M. Sluyters-Rehbach and J.H. Sluyters, *J. Electroanal. Chem.*, 146 (1983) 263.
- 16 C.P.M. Bongenaar, M. Sluyters-Rehbach and J.H. Sluyters, *J. Electroanal. Chem.*, 109 (1980) 23.
- 17 J. Newman, *J. Electroanal. Chem.*, 15 (1967) 309.
- 18 F. van der Pol, M. Sluyters-Rehbach and J.H. Sluyters, *J. Electroanal. Chem.*, 58 (1975) 177.
- 19 R. Payne, *J. Phys. Chem.*, 70 (1966) 204.
- 20 R. Parsons and R. Payne, *Z. Phys. Chem.*, 98 (1975) 9.
- 21 D.M. Mohilner in A.J. Bard (Ed.), *Electroanalytical Chemistry*, Vol. 1, Marcel Dekker, New York, 1966, p. 241-409.
- 22 M. Saakes, M. Sluyters-Rehbach and J.H. Sluyters, *J. Electroanal. Chem.*, 259 (1989) 265.
- 23 R. Andreu, M. Sluyters-Rehbach and J.H. Sluyters, *J. Electroanal. Chem.*, 134 (1982) 101.
- 24 M. Sluyters-Rehbach and J.H. Sluyters in E. Yeager, J.O'M. Bockris, B.E. Conway and S. Saranagapani (Eds.), *Comprehensive Treatise of Electrochemistry*, Vol. 9, Plenum Press, New York, 1984, pp. 177-292.
- 25 M. Sluyters-Rehbach and J.H. Sluyters in C.M. Bamford and R.G. Compton (Eds.), *Comprehensive Chemical Kinetics*, Vol. 26, Elsevier, Amsterdam, 1986, pp. 203-354.
- 26 J. Blackledge and N.S. Hush, *J. Electroanal. Chem.*, 5 (1963) 435.

CHAPTER 4

THE INHIBITION OF Cd(II) REDUCTION AT THE DME FROM AQUEOUS 1 M NaClO₄ BY SUCROSE

It is shown that the steps in the earlier established CEE mechanism for the charge transfer process of Cd(II) reduction all are slowed down upon addition of sucrose. An attempt is made to correlate the individual standard rate constants with (i) the surface coverage by sucrose, and (ii) the viscosity of the solution layer adjacent to the electrode surface. No clear relationships are obtained, thus leaving the physical nature of the effects unexplained.

(I) INTRODUCTION

Gradually more and more evidence is found in the literature of the complexity of factors that may influence the rate of even simple electrode reactions. They can be divided into interfacial effects such as adsorption of ionic or neutral species, and bulk effects like complexation or solvation. In several recent papers [1-4], attention was paid to a possible correlation between the standard rate constant of so-called "outer-sphere" reactions and the viscosity of the electrolyte solution. The causality of this correlation is supposed to be the influence of the longitudinal solvent relaxation time, τ_L , on the pre-exponential factor in the theoretical expression for the rate constant [5-9]. Mostly [1-3,8,9] this influence was demonstrated by comparing results obtained with different solvents; in a communication by Zhang et al. [4], however, the viscosity was varied by adding increasing amounts of dextrose or sucrose, which were thought to have minor effects on e.g. interfacial properties. In all these publications reactions involving solution-soluble reactants and products were studied, and mechanistic complications were assumed to be absent.

Because the multi-step character of many electrode reactions that were formerly supposed to be simple, has become accessible to precise and detailed experimental studies [10-18], it might be worthwhile to see to what extent the separate steps in the mechanism are sensitive to changes in viscosity. This question is especially

interesting with respect to the potential-independent, so-called "chemical" steps, the nature of which is still unclear.

The reduction of Cd(II) to its amalgam from aqueous solutions has been shown to involve such a chemical step, preceding the two electron transfer steps (CEE mechanisms) under many circumstances [10,13,15-18]. From a study in which the water activity was varied by varying the NaClO₄ supporting electrolyte concentration [17] it became clear that the chemical step cannot be identified with a slow desolvation. In fact, it was found that the reaction mechanism does comprise several dehydration steps, but these were all shown to proceed immeasurably fast.

The hypothesis left is the idea that some more or less improbable configuration has to develop spontaneously at the interface, in which the probability for electron transfer is large. If so, then in a mathematical description, that configuration can act as an intermediate, e.g. in the stationary state approximation of the CEE mechanism. It seems reasonable to believe that if this hypothesis makes sense, especially the rate of the chemical step should slow down with increasing viscosity. Also, though the overall reaction $\text{Cd(II)} + 2 e^- \rightarrow \text{Cd(Hg)}$ is not of the "outer sphere" category, at least the first electron transfer step could be considered as such, thus making it sensible to compare its behaviour with that of the simple one-electron reactions.

To this end we have chosen to investigate the reduction of Cd(II) to Cd(Hg) from aqueous 1 M NaClO₄ solutions, with additions of sucrose in the concentration range $0 \leq x \leq 1$ M. With this system, a considerable change in the viscosity of the bulk solution can be achieved. A complication, however, is the fact that sucrose is also adsorbed at the mercury/electrolyte solution interface [19,20]. This brings on the question, whether any relation between electrochemical reaction rate and a (dynamic) solution property, should be examined in terms of the value of this property at the interface rather than its bulk value.

In the present communication, the results of a preliminary study of the above-mentioned systems are dealt with, paying explicit attention to the questions raised in the foregoing.

(II) EXPERIMENTAL

All experiments were performed in a three-electrode cell configuration. The working electrode was a dropping mercury electrode made from a drawn-out capillary. A mercury pool served as the counter electrode and the reference electrode was a sodium chloride saturated calomel electrode (SSCE), connected to the cell via a salt bridge filled with cell solution. The cell solutions were prepared from freshly twice-distilled water and p.a. chemicals, and freed from oxygen by passing through argon. The cell was thermostatted at $25.0 \pm 0.1^\circ \text{C}$ and all measurements were made at 4 s after drop birth.

Sampled dc and ac voltammograms of solutions containing 2×10^{-3} M CdSO₄, 1 M NaClO₄ and x M sucrose, $0 \leq x \leq 1$, were obtained with the network analyzer system described before [21]. Also, the values of the differential double layer

capacity in the 1 M NaClO₄ + x M sucrose solutions were measured, at a fixed frequency of 1020 Hz, after having established that frequency dispersion of the capacity was virtually absent.

The reduction of Cd(II) in the absence of sucrose is too fast to allow a precise kinetic study with the impedance method. Therefore the rate constant data for this case were obtained by means of demodulation voltammetry in the same way as described previously [17].

Potentials of zero charge were measured with an accuracy of 1 mV from charging currents at a rapidly dropping mercury electrode.

The viscosities of the 1 M NaClO₄ + x M sucrose solutions were measured with a capillary viscosimeter (type Ubbelohde, Schott Geräte GmbH), for x = 0, 0.25, 0.5, 1.0, 1.5 and 2.0, at 25°C.

(III) RESULTS

(III.1) Double layer analysis

The potential of zero charge, E_{pzc} , was found to become more positive on increasing the sucrose concentration, c_s^* . The values of E_{pzc} are reported in Table 1. A similar trend can be inferred from the interfacial tension data published by Krishnan and de Levie for the ternary system NaCl + H₂O + sucrose, although these authors do not mention the effect explicitly [20]. Parsons and Peat [19] did not observe a shift of E_{pzc} for the system NaF + H₂O + sucrose up to x = 1 M. This may suggest that sucrose has a slight influence on the specific adsorption of ClO₄⁻ or Cl⁻, as indeed could not be excluded by the authors of ref. 20.

TABLE 1
Primary data as a function of sucrose concentration

$x/\text{mol dm}^{-3}$	$E_{pzc}/\text{mV vs. SSCE}$	η/η_0^a	$10^6 D_0/\text{cm}^2 \text{s}^{-1}$	$-E_f^\circ/\text{mV vs. SSCE}$	$k_{s,0}^c/\text{cm s}^{-1}$	$k_{s,1}/\text{cm s}^{-1}$	$k_{s,2}/\text{cm s}^{-1}$
0	-508	1.043	8.0	570	1.4	0.32	4 -5
0.001		(1.050)		570	0.57	0.31	4 -5
0.002	-500	(1.051)		570	0.48	0.25	3 -4.5
0.004		(1.052)		570	0.41	0.21	3 -4
0.006		(1.054)		570	0.375	0.16	3 -4
0.010	-490	(1.056)		569	0.29	0.12	3 -5
0.025	-483	(1.065)		568	0.265	0.065	3 -5
0.050	-478	(1.083)		568	0.26	0.042	2.5-5
0.100	-472	(1.125)	8.0	565	0.282	0.030	≥ 2
0.250	-467	1.328	7.2	562	0.185	0.023	0.7
0.500	-461	1.798	6.0	558	0.165	0.017	0.4
1.000	-462	3.537	3.3	548	0.100	0.0097	≥ 0.5
1.500		8.884	1.4				
2.000		32.13	0.6				

^a Numbers between brackets obtained by interpolation.

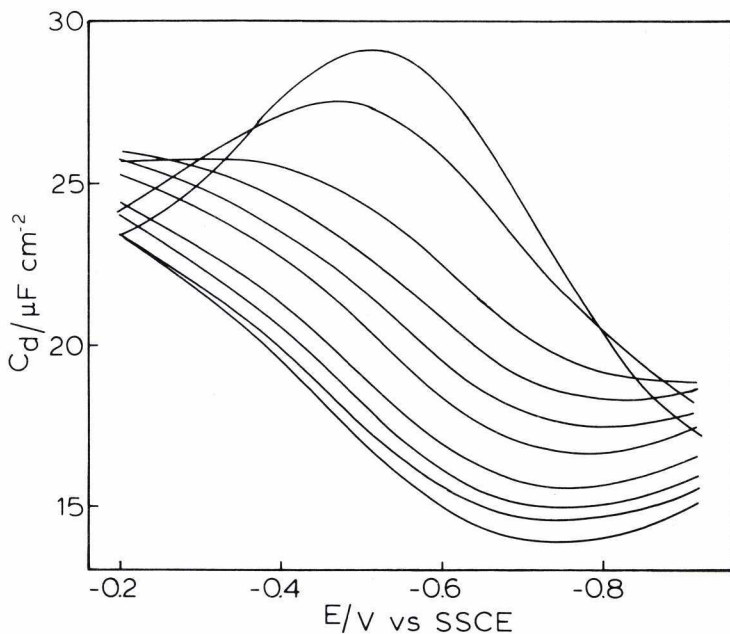


Fig. 1. Double layer capacity as a function of potential; DME in contact with aqueous 1 M NaClO₄. Sucrose concentration, from top to bottom: 0, 0.002, 0.010, 0.025, 0.050, 0.100, 0.250, 0.500, 1.000 and 2.000 M.

The capacity-potential curves, shown in Fig. 1, were integrated to give the charge density, σ^M , as a function of potential, shown in Fig. 2. A common intersection point is observed at $\sigma^M = -2.1 \pm 0.05 \mu\text{C cm}^{-2}$, $E = -0.580 \pm 0.001 \text{ V vs. SSCE}$. It can be concluded that sucrose adsorption is maximal at this potential. Obviously, with NaF as the electrolyte, the maximum adsorption occurs at the pzc [19], i.e. at a substantially more positive potential.

The data in Fig. 2 are needed in the first place to estimate the potential profile in the diffuse double layer. An exact estimation is actually hampered by the uncertainty about the specific adsorption of ClO₄⁻ in the presence of sucrose, as mentioned above. Since the effect is probably weak [20] and since also the ClO₄⁻ adsorption is weak in the potential region of our interest, $-0.5 < E < -0.65 \text{ V vs. SSCE}$, we decided to assume that the amount of ClO₄⁻ adsorbed remains the same at constant charge density throughout the range of sucrose concentrations, $0 < x < 1 \text{ M}$. A possible error thus made, is discussed further on. The data on the specifically adsorbed charge density, σ^1 , as a function of σ^M were taken from the literature [22]. Accidentally, the Outer Helmholtz Plane potential, ϕ_2 , varies only slightly from ca. -37 mV at $E = -0.46$ to -38 mV at $E = -0.66 \text{ V}$, and this behaviour is almost the same for all sucrose concentrations. Accordingly, the potential $\phi_{1\text{H}_2\text{O}}$ at a distance of 0.28 nm from the OHP, takes values ranging from -14.2 mV at $E = -0.46$ to -14.7 mV at $E = -0.66 \text{ V vs. SSCE}$.

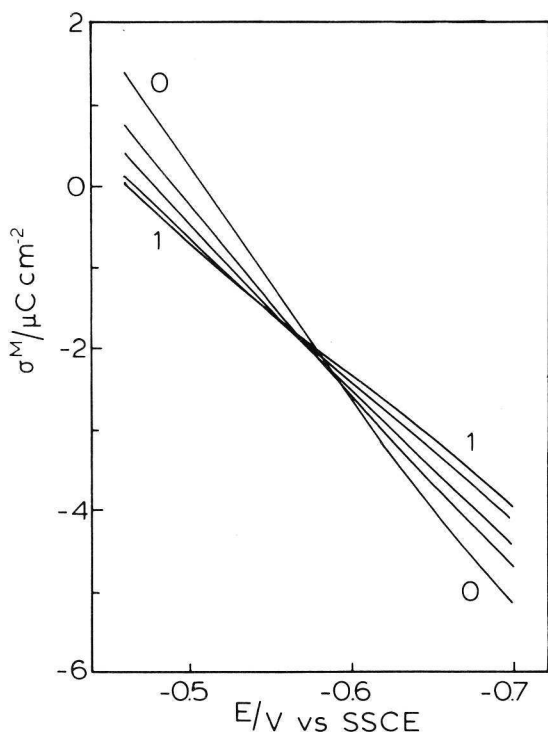


Fig. 2. Surface charge densities as a function of potential. Sucrose concentrations: 0, 0.01, 0.05, 0.25 and 1 M. (0 and 1 M are indicated.)

A second problem is the estimation of the surface excess, Γ , of adsorbed sucrose. Krishnan and de Levie concluded from their own results with the system $\text{NaCl} + \text{H}_2\text{O} + \text{sucrose}$ that the sucrose adsorption is (almost) independent of the NaCl activity, which was varied from 0.01 to 1 mol kg^{-1} . However, their data on the relative surface excess, Γ_{OW} , differ largely from those obtained by Parsons and Peat with the system $\text{NaF} + \text{H}_2\text{O} + \text{sucrose}$. This means that either the presence of specifically adsorbed Cl^- does affect the sucrose adsorption, or the estimation of Γ_{OW} from interfacial tension data, obtained directly [20] or indirectly [19], involved systematic errors.

As for our purposes it is sufficient to know the relative surface coverage, $\theta = \Gamma/\Gamma_s$, we decided to estimate this quantity directly from the capacity data in the potential region $-0.460 < E < -0.700$ V, which is symmetrical around the potential of maximum adsorption, E_m . It can be assumed safely that in this region the adsorption coefficient follows the quadratic relationship

$$\ln \beta = \ln \beta_m - b(E - E_m)^2 \quad (1)$$

and, if θ obeys an isotherm with only β as potential-dependent parameter,

$$\theta = \theta_m - g(E - E_m)^2 \quad (2)$$

where θ_m is the surface coverage at $E = E_m$. Following thermodynamic reasoning, it can be shown that at fixed potential E :

$$C_d(E) - C_d^\circ(E) = RT \frac{d^2 \ln \beta}{dE^2} \Gamma + RT \frac{d \ln \beta}{dE} \frac{d\Gamma}{dE}$$

$$= -RT \{ 2b\Gamma - 4bg(E - E_m)^2 \Gamma_s \} \quad (3)$$

in which $C_d^\circ(E)$ is the double layer capacity in the base electrolyte solution without sucrose. At $E = E_m$ we have

$$C_d(E_m) - C_d^\circ(E_m) = -RT \cdot 2b\Gamma_m \quad (4)$$

A capacity $C_d^1(E_m)$ may be defined, pertaining to saturation coverage, $\theta_m = 1$, or $\Gamma_m = \Gamma_s$:

$$C_d^1(E_m) - C_d^\circ(E_m) = -RT \cdot 2b\Gamma_s \quad (5)$$

Dividing eqn. (3) by eqn. (5) gives

$$\frac{C_d(E) - C_d^\circ(E)}{C_d^1(E_m) - C_d^\circ(E_m)} = \theta - 2g(E - E_m)^2 \quad (6a)$$

$$= \theta_m - 3g(E - E_m)^2 \quad (6b)$$

Using eqn. (6b), θ_m and g may be evaluated by fitting of the right-hand side to the left-hand side.

In the present case, the value of $C_d^1(E_m)$ is difficult to obtain experimentally. Attempts to extrapolate the measured C_d values at $E = E_m$ beyond the highest concentration employed (2 M sucrose) reveal that $C_d^1(E_m)$ can have any value below $13.5 \mu\text{F cm}^{-2}$. Following Parsons and Peat [19], a "theoretical" value can be calculated assuming that a monolayer of adsorbed sucrose has a thickness of 0.5 nm, and a dielectric constant $\epsilon = 5.3$ [23]. This leads to $C_d^1(E_m) \cong 9.5 \mu\text{F cm}^{-2}$. Adopting this value, the values of θ plotted in Fig. 3 were obtained.

The results in Fig. 3 fit rather poorly to the Frumkin isotherm. However, the isotherm

$$\beta c = \theta / (1 - \theta)^n \quad (7)$$

proposed as an alternative [20,24], gives a very good fit. At $E = E_m = -0.58 \text{ V vs. SSCE}$, the values of the parameters are $\ln \beta_m = 4.8 \pm 0.1$ and $n = 4.72 \pm 0.15$. Theoretically, n equals the number of adsorbed water molecules (in the compact layer) replaced by an adsorbed sucrose molecule.

(III.2) Dc polarography

The dc polarograms showed reversible behaviour up to the highest sucrose concentration. From the limiting current values the diffusion coefficients D_0 of Cd(II) were calculated, using Newman's diffusion layer model including a correction for sphericity [25]. The results are reported, together with the values of the

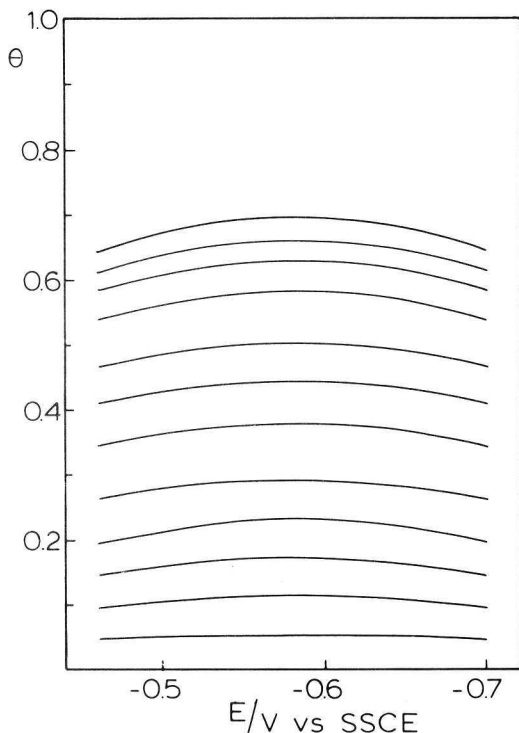


Fig. 3. Fractional surface coverage by sucrose, calculated from capacity data using $C_d^1 = 9.5 \mu\text{F cm}^{-2}$ (see text). Sucrose concentration, from bottom to top: 0.001, 0.002, 0.004, 0.006, 0.010, 0.025, 0.050, 0.100, 0.250, 0.500, 1.000 and 2.000 M.

relative viscosity, η/η_0 , in Table 1. Clearly a correlation exists between these two quantities; the relationship is not the simple linear one predicted by the Einstein-Stokes law, however.

From the experimental half-wave potentials the standard formal potential, E_f° , was calculated as a function of the sucrose concentration, using the relationship

$$E_{1/2} = E_f^\circ + (RT/nF) \ln(D_R/\delta_R)(\delta_O/D_O) \quad (8)$$

with the appropriate expressions for δ_R and δ_O , the diffusion layer thickness [10,25]. The value of D_R was taken from the literature [26]. The E_f° values thus obtained were used as starting values for a precise fit of the Warburg coefficients as a function of potential, which eventually gives E_f° with a precision of ± 1 mV. The latter values are reported in Table 1.

At sucrose concentrations higher than 0.025 M, the formal standard potential is seen to become more positive. This can be ascribed to the expected decrease of the water activity, in the same way as was discussed in our study on Cd(II) reduction at varying NaClO_4 concentration [17]. Indeed, it has been shown that the water activity of concentrated sucrose solutions is decreased as a consequence of hydration of the dissolved sucrose molecules [27].

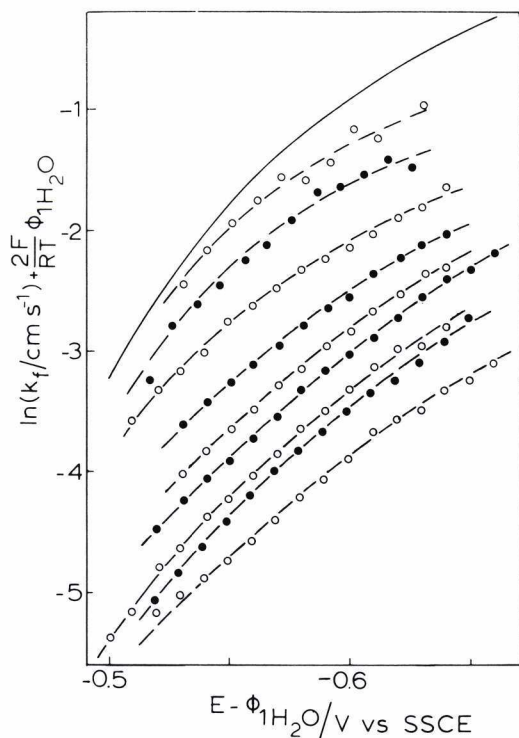


Fig. 4. Corrected Tafel plots at fixed sucrose concentrations, from top to bottom: 0, 0.001, 0.004, 0.010, 0.025, 0.050, 0.100, 0.250, 0.500, 1.000 M. The plots for 0.002 and 0.006 M have been omitted for clarity.

(III.3) The kinetic analysis

The impedance data were analyzed by fitting to the expressions valid in the case of Randles' behaviour [28,29], giving the values of the Warburg coefficient, σ , and the irreversibility quotient, p' , at dc potentials with 10 mV intervals. From p' , the value of the apparent reduction rate constant, k_f^a , was calculated as a function of potential. In view of our earlier experiences [17] these data were converted directly to the Frumkin corrected $\ln k_f$ vs. E plot, assuming the reaction plane to be situated 0.28 nm away from the Outer Helmholtz Plane. These plots are reproduced in Fig. 4 for sucrose concentrations $0.001 < x < 1$ M. It should be mentioned here that the curve for $x = 0$ was calculated from the rate constants obtained by fitting of the demodulation voltammograms to the expressions describing the CEE mechanism shown to apply previously [17].

The curves in Fig. 4 were also analyzed in terms of the CEE mechanism found to apply before [10,12,15-18], by fitting to the expression

$$\frac{1}{k_f} = \frac{1}{k_{s,0}^c} + \frac{\exp\left[\frac{1}{2}\alpha_1\varphi'\right]}{k_{s,1}} + \frac{\exp\left[\frac{1}{2}(1 + \alpha_2)\varphi'\right]}{k_{s,2}} \quad (9)$$

$$\varphi' = (2F/RT)(E - \phi_{1H_2O} - E_f^\circ) \quad (10)$$

taking $\alpha_1 = \alpha_2 = 0.5$. The quality of the fits gave good evidence that the CEE mechanism also applies in the presence of sucrose. The values of the individual standard rate constants, referred to the tabulated formal standard potentials, are also reported in Table 1. It should be realized that the second electron transfer step is relatively fast, especially at the higher sucrose concentrations. Therefore, the $k_{s,2}$ values are mostly found to be in a certain range. Also, at the highest sucrose concentrations, the overall accuracy is somewhat less, because then the analysis suffers from a high ohmic resistance, typically ca. 100 Ω instead of the usual value of ca. 30 Ω .

(IV) DISCUSSION

(IV.1) Rate constants and sucrose concentration

The effect of sucrose on the Cd(II) reduction is clearly an inhibition of all three steps in the mechanism, as follows from the standard rate constants in Table 1, and also from the plots in Fig. 4. At low sucrose concentration, the chemical step appears to be inhibited more strongly than the electron transfer steps, which might fit to the expectation formulated in the introduction.

An overall picture of the inhibition of the separate steps is given in Fig. 5. It should be realized that at the higher sucrose concentrations ($x > 0.1$ M) the water activity will be decreased to a significant extent, thus promoting the desolvation of the Cd(II)-aquo complex. From our previous results at varying NaClO₄ concentration [17] it can be inferred that this has an accelerating effect, thus counteracting the

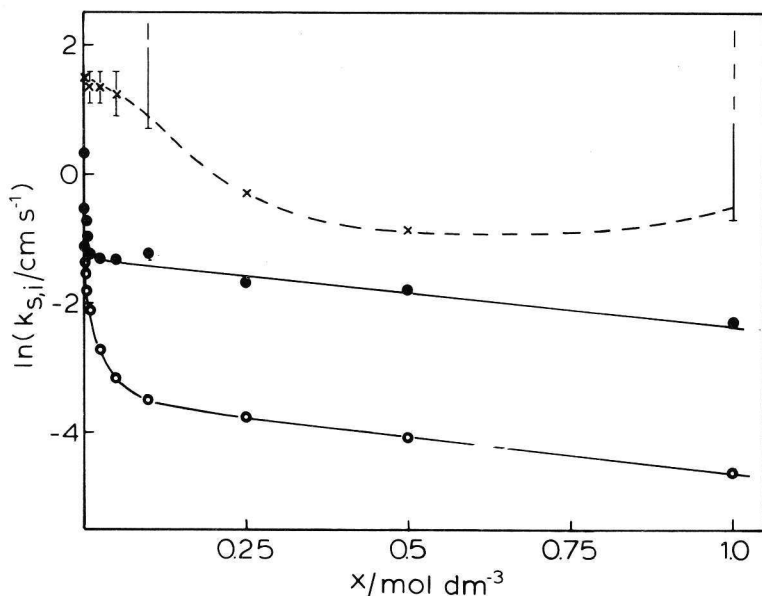


Fig. 5. The individual standard rate constants, logarithmically plotted vs. sucrose concentration: (●) $k_{s,0}^c$, (○) $k_{s,1}$ and (×) $k_{s,2}$.

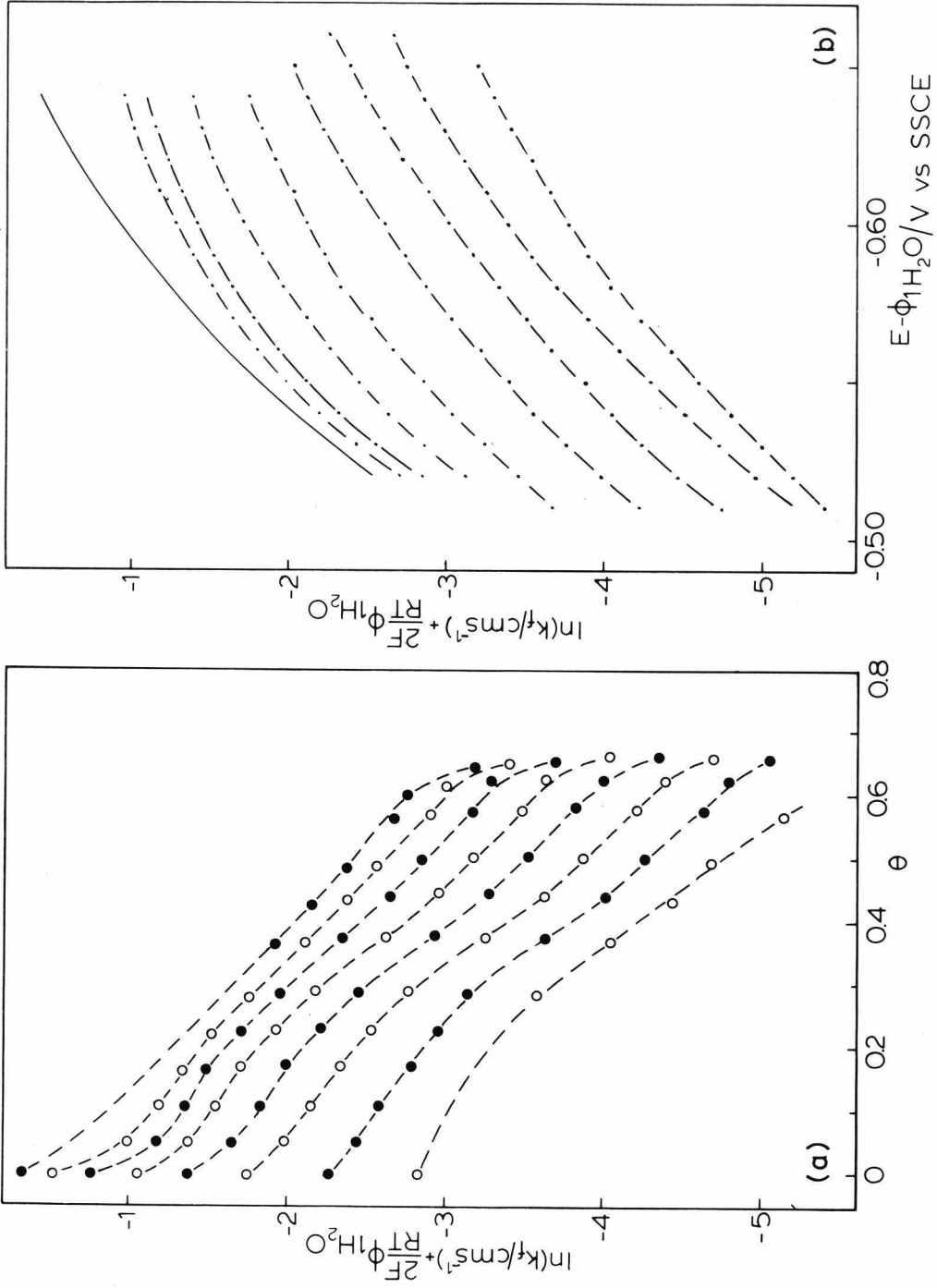


Fig. 6. (a) Rate constants plotted against surface coverage, at fixed potentials, $E - \phi_{\text{H}_2\text{O}}$. From bottom to top: $-0.51, -0.53, -0.55, -0.57, -0.59, -0.61, -0.63, -0.65$ V vs. SSCE. (b) Corrected Tafel plots at fixed surface coverage, θ , from top to bottom: $\theta = 0, 0.05, 0.1, 0.2, 0.3, 0.4, 0.5, 0.6$ and 0.65 .

inhibition. However, its magnitude can be estimated to be relatively low, and the general shape of the curves in Fig. 5 is essentially not affected. Therefore, no quantitative correction for the desolvation effect will be attempted.

In Fig. 5 it can be seen that the rate of the chemical step especially decreases dramatically upon addition of quite small amounts of sucrose, i.e. in the range $0 < x \leq 0.1$ M. As the viscosity hardly changes in this concentration range, a direct correlation with this quantity evidently does not exist.

(IV.2) Rate constants and sucrose adsorption

The data in Figs. 3 and 4 were combined to construct plots of $\ln k_f$ vs. θ at fixed potential (Fig. 6a) and of $\ln k_f$ vs. potential at fixed values of θ (Fig. 6b).

It is not surprising that the curves in Fig. 6b can also be fitted to the CEE mechanism, because θ is only slightly potential dependent. The values of the individual standard rate constants, this time referred to a common reference potential, -0.570 V vs. SSCE, are reported in Table 2. Plots of $k_{s,i}$ and $\ln k_{s,i}$ against θ are shown in Fig. 7. The individual rate constants appear to decrease more or less exponentially with the surface coverage, which might be interpreted in terms of a linear relation between the activation energy and the surface coverage.

A remark has to be made here about the reliability of this conclusion, in view of the more or less intuitive procedure followed to determine the fractional surface coverage (Section III.1). The actual values of θ , of course, depend on the value of $C_d^1(E_m)$ inserted into eqn. (6). We repeated, therefore, the analysis taking $C_d^1(E_m) = 13.5 \mu\text{F cm}^{-2}$, i.e. its highest possible value. The results obtained are qualitatively similar to those in Figs. 7, showing also a more or less linear dependence of $\ln k_{s,i}$ on θ .

As we argued before, an appreciable increase in the viscosity in the interfacial layer can be expected as a consequence of sucrose adsorption. In a very rough manner, the extent of such an effect is estimated here as follows. It is assumed that a maximum surface coverage ($\theta = 1$) a monolayer of adsorbed sucrose occupies the layer adjacent to the mercury. From the molar density of sucrose it follows that this

TABLE 2

Rate constants at fixed surface coverage, and corresponding values of "interphasial viscosity"

θ	$k_{s,0}^c/\text{cm s}^{-1}$	$k_{s,1}/\text{cm s}^{-1}$	$k_{s,2}/\text{cm s}^{-1}$	η_{int}/η_0
0	1.4	0.32	4.9	1.04
0.05	0.56	0.325	3.75	1.3
0.1	0.49	0.27	3.75	1.8
0.2	0.38	0.19	3 - 4	3.2
0.3	0.275	0.120	2.5-4	6.5
0.4	0.248	0.060	2.5-4	18
0.5	0.200	0.036	2 - 3	65
0.6	0.160	0.023	0.9	500
0.65	0.085	0.017	1.0	1600

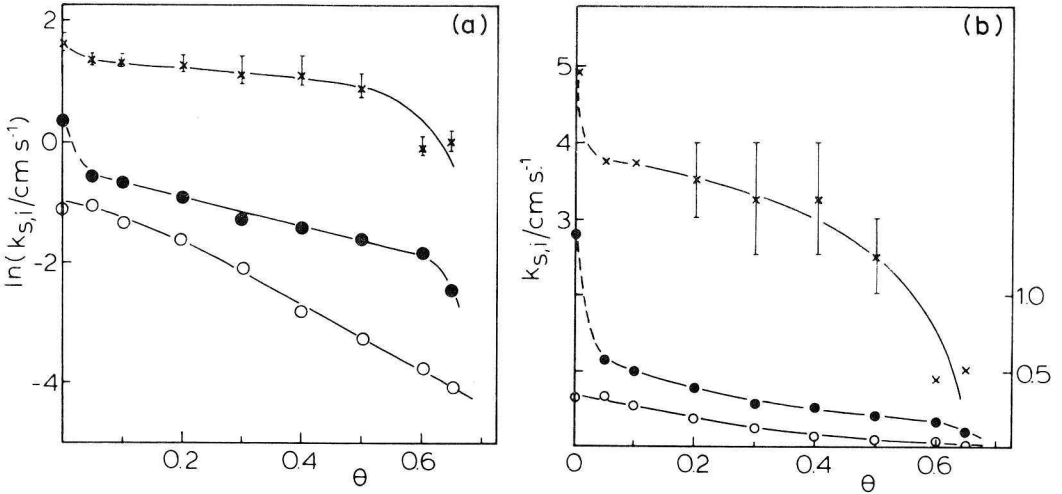


Fig. 7. Correlation of the individual standard rate constants with surface coverage; (a) $\ln k_{s,i}$ vs. θ , (b) $k_{s,i}$ vs. θ . (●) $k_{s,0}^c$, (○) $k_{s,1}$ (right-hand scale), (×) $k_{s,2}$ (left-hand scale).

layer corresponds to a concentration $x_s = \text{ca. } 4.5 \text{ M}$. At lower coverages the “interphasial concentration” of sucrose is then calculated as $x_{\text{int}} = \theta x_s$. Next, it is assumed that the viscosity in the interphasial region is equal to that of a bulk solution of sucrose having the same concentration. Following this quite tentative reasoning, we obtained the numbers for η_{int}/η_0 listed in Table 2, using our own data (Table 1) as well as tabulated data for higher sucrose concentrations [30].

In order to see whether a correlation with the viscosity in the interphasial layer exists, the individual standard rate constants of Table 2 are plotted against

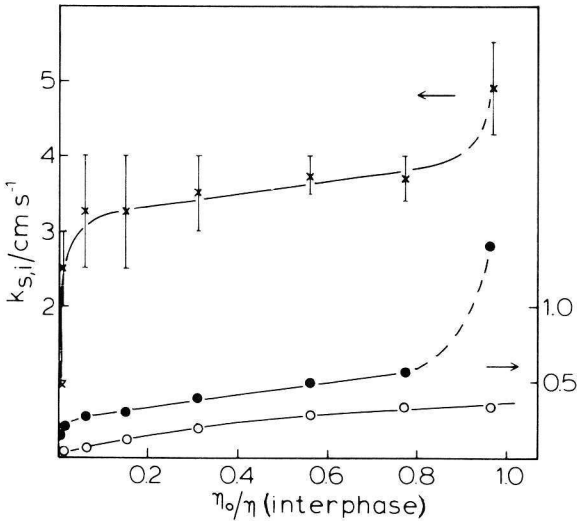


Fig. 8. Correlation of the individual standard rate constants with the reciprocal of the “interphase viscosity” (see text): (●) $k_{s,0}^c$, (○) $k_{s,1}$ (right-hand scale), (×) $k_{s,2}$ (left-hand scale).

$(\eta_{\text{int}}/\eta_0)^{-1}$ in Fig. 8. None of them shows the proportionality expected theoretically and the data points for $k_{s,0}^c$ and $k_{s,2}$ corresponding to $(\eta_{\text{int}}/\eta_0)^{-1} = 0.96$, i.e. zero sucrose concentration, are exceptionally high. Moreover, no special behaviour of the chemical step is observed. It has to be concluded that, on the basis of the simplistic approach in the previous paragraph, there is no reason to prefer the correlation with "interphasial viscosity" above the more usual correlation with the relative surface coverage (Fig. 7).

(V) CONCLUSION

Although in this paper the properties θ and η_{int} were estimated rather than determined exactly, it appears justified to conclude that the inhibition of Cd(II) reduction by sucrose should be interpreted as an interfacial effect. However, no clear decision can be made as to whether it is the frequency factor or the activation energy that is affected by the change in interfacial structure. It could be argued that both of them may be involved, thus making the analysis virtually impossible at the present state of knowledge. On the other hand, our attempt to derive the interfacial viscosity from bulk solution data is most probably not realistic, as the mobility of the sucrose molecules being fixed to the electrode surface is apt to be much lower than in the free solution.

Remarkably, the CEE mechanism remains valid throughout the range of sucrose concentrations. Kisova and co-workers [31,32], in a study of the inhibition of cadmium ion reduction by aliphatic alcohols and fatty acids, concluded that the EE mechanism would hold. The presence of the chemical step, however, shows up unquestionably in the Tafel plots (Figs. 4 and 6) at the more negative potentials. More work is needed to understand its physical meaning.

REFERENCES

- 1 A. Kapturkiewicz and B. Behr, *J. Electroanal. Chem.*, 179 (1984) 187.
- 2 T. Gennet, D.F. Milner and M.J. Weaver, *J. Phys. Chem.*, 89 (1985) 2787.
- 3 M.J. Weaver and T. Gennet, *Chem. Phys. Lett.*, 113 (1985) 213.
- 4 X. Zhang, J. Leddy and A.J. Bard, *J. Am. Chem. Soc.*, 107 (1985) 3719.
- 5 D.F. Calef and P.G. Wolynes, *J. Phys. Chem.*, 87 (1983) 3387.
- 6 D.F. Calef and P.G. Wolynes, *J. Phys. Chem.*, 78 (1983) 470.
- 7 W. Harrer, G. Grampp and W. Jaenicke, *Chem. Phys. Lett.*, 112 (1984) 263.
- 8 M. Opallo and A. Kapturkiewicz, *Electrochim. Acta*, 30 (1985) 1301.
- 9 W.R. Fawcett and C.A. Foss, *J. Electroanal. Chem.*, 252 (1988) 221.
- 10 C.P.M. Bongenaar, A.G. Remijnse, M. Sluyters-Rehbach and J.H. Sluyters, *J. Electroanal. Chem.*, 111 (1980) 139.
- 11 J. Struys, M. Sluyters-Rehbach and J.H. Sluyters, *J. Electroanal. Chem.*, 146 (1983) 263.
- 12 J. Struys, M. Sluyters-Rehbach and J.H. Sluyters, *J. Electroanal. Chem.*, 171 (1984) 177.
- 13 G.J. Brug, M. Sluyters-Rehbach and J.H. Sluyters, *J. Electroanal. Chem.*, 176 (1984) 297.
- 14 M. Sluyters-Rehbach and J.H. Sluyters, *Electrochim. Acta*, 33 (1988) 983.
- 15 R.M. Souto, M. Sluyters-Rehbach and J.H. Sluyters, *J. Electroanal. Chem.*, 201 (1986) 33.
- 16 R.M. Souto, M. Sluyters-Rehbach and J.H. Sluyters, *J. Electroanal. Chem.*, 245 (1987) 167.
- 17 M. Saakes, M. Sluyters-Rehbach and J.H. Sluyters, *J. Electroanal. Chem.*, 259 (1989) 265.

- 18 M. Saakes, M. Sluyters-Rehbach and J.H. Sluyters, *J. Electroanal. Chem.*, 264 (1989) 217.
- 19 R. Parsons and R. Peat, *J. Electroanal. Chem.*, 122 (1981) 299.
- 20 M. Krishnan and R. de Levie, *J. Electroanal. Chem.*, 131 (1982) 97.
- 21 C.P.M. Bongenaar, M. Sluyters-Rehbach and J.H. Sluyters, *J. Electroanal. Chem.*, 109 (1980) 23.
- 22 R. Parsons and R. Payne, *Z. Phys. Chem.*, 98 (1975) 9.
- 23 R. Parsons, *J. Electroanal. Chem.*, 59 (1975) 229.
- 24 H.P. Dhar, B.E. Conway and K.M. Joshi, *Electrochim. Acta*, 18 (1973) 789.
- 25 J. Newman, *J. Electroanal. Chem.*, 15 (1967) 309.
- 26 F. van der Pol, M. Sluyters-Rehbach and J.H. Sluyters, *J. Electroanal. Chem.*, 58 (1975) 177.
- 27 R.A. Robinson and R.H. Stokes, *J. Phys. Chem.*, 65 (1961) 1954.
- 28 M. Sluyters-Rehbach and J.H. Sluyters in A.J. Bard (Ed.), *Electroanalytical Chemistry*, Vol. 4, Marcel Dekker, New York, 1970, pp. 1-128.
- 29 M. Sluyters-Rehbach and J.H. Sluyters in E. Yeager, J.O'M. Bockris, B.E. Conway and S. Sarangapani (Eds.), *Comprehensive Treatise of Electrochemistry*, Vol. 9, Plenum Press, New York, 1984, pp. 177-292.
- 30 R.C. Weast, *Handbook of Chemistry and Physics*, 55th ed., CRC Press, Cleveland, OH, 1974, p. D-231.
- 31 L. Kisova, M. Goledzinowski and J. Lipkowski, *J. Electroanal. Chem.*, 95 (1979) 29.
- 32 M. Goledzinowski, L. Kisova, J. Lipkowski and Z. Galus, *J. Electroanal. Chem.*, 95 (1979) 43.

CHAPTER 5

THE INVESTIGATION OF THE ADSORPTIVE BEHAVIOUR OF ELECTROACTIVE SPECIES BY MEANS OF DEMODULATION VOLTAMMETRY

I. Introduction

The great significance of the impedance method for studying the adsorption of electroactive species at the electrode/electrolyte interface has been outlined before [1-6]. It was shown that the information obtained with this technique is highly detailed, due to the fact that in the faradaic potential region the charge transfer process and the adsorption process are coupled [1], while moreover, the surface concentration of the adsorbing species changes rapidly with the change in the applied electrode potential. In the case of a higher order technique we can expect an even more sensitive behaviour of the measured response of the processes at the electrode/electrolyte interface to the effects of adsorption of the electroactive species. As an example of a higher order technique we will consider here the demodulation technique which was developed in our laboratory [7]. This technique measures the second order, non-linear, voltage response of an electrochemical cell due to a perturbation with a high frequency sine wave current (carrier wave) modulated by a low frequency cosine wave. In several studies [8, 9, this thesis, Chapter 2 and 3] this technique has proven to give detailed information on the mechanism of charge transfer. Compared with the a.c. technique the demodulation technique is not only more sensitive to mechanistic details but also provides information in a larger potential range. Because of this, promising results are to be expected from a theoretical study investigating the potentialities of the demodulation technique for studies of the adsorption of electroactive species. In order to keep the necessary derivations limited we will assume that both the charge transfer and the adsorption/desorption process are infinitely fast.

Furthermore we will assume only the ox-component in the simple electrode reaction $O + ne^- \leftrightarrow R$ to be adsorbed.

II. Theory

II.1 Survey of first order thermodynamic relations

Following the restrictions mentioned in the introduction only two independent variables are necessary namely the potential E and the parameter ψ defined by

$$\psi = D_O^{1/2} c_O(0,t) + D_R^{1/2} c_R(0,t) \quad (1)$$

where D_O and D_R are the diffusion coefficients, and $c_O(0,t)$ and $c_R(0,t)$ are the surface concentrations of O and R respectively.

The parameter ψ occurs in the thermodynamic relation for the first order derivative of the surface excess Γ_O (only the ox-component is assumed to be adsorbed) with respect to the potential E.

In general Γ_O will be a function of the product $\beta_O c_O(0,t)$, where β_O is the adsorption coefficient. From this definition the relation follows [5]:

$$\left(\frac{\partial \Gamma_O}{\partial \psi}\right)_E = \left(\frac{\partial \Gamma_O}{\partial E}\right)_\psi \frac{1}{\bar{\psi}} \left\{ \frac{nF}{RT} \frac{1}{1+e^\zeta} + \frac{d \ln \beta_O}{dE} \right\}^{-1} \quad (2)$$

can be derived, in which $\zeta = (nF/RT)(E - E_{1/2}^r)$, $E_{1/2}^r$ is the reversible halfwave potential and $\bar{\psi}$ is the mean value of ψ . The charge density q on the electrode is related to the surface excess Γ_O and the adsorption coefficient β_O via [5]:

$$q = q^0(E) + RT \Gamma_O \frac{d \ln \beta_O}{dE} \quad (3)$$

where q^0 is the charge density in the absence of the species O. From this relation two useful expressions can be derived showing the dependence of q with respect to E (with ψ constant) and ψ (with E constant):

$$\left(\frac{\partial q}{\partial E}\right)_\psi = \frac{dq^0}{dE} + RT \left\{ \left(\frac{\partial \Gamma_O}{\partial E}\right)_\psi \frac{d \ln \beta_O}{dE} + \Gamma_O \frac{d^2 \ln \beta_O}{dE^2} \right\} \quad (4)$$

$$\left(\frac{\partial q}{\partial \psi}\right)_E = RT \left(\frac{\partial \Gamma_O}{\partial \psi}\right)_E \frac{d \ln \beta_O}{dE} \quad (5)$$

The quantity dq^0/dE is identical to the differential double layer capacity, C_d^0 , pertaining to the supporting electrolyte. The relations given here are the starting point for deriving equations for the second order partial derivatives of both Γ_O and q with respect to E and ψ .

II.2 Survey of second order thermodynamic relations

Using the relations in Section II.1 the second order partial derivatives of Γ_{O} and q with respect to E and ψ can easily be found.

In Table 1 we have given all the possible first and second order partial derivatives and some abbreviations (γ_{E} and γ_{ψ}) introduced before [5]. Note two new abbreviations given in Table 1 namely q_{E} and q_{ψ} .

Table 1 Possible first and second order partial derivatives of Γ_{O} and q with respect to E and ψ .

$\Gamma_{\text{O}}(E, \psi)$	$q(E, \psi)$
$(\partial\Gamma_{\text{O}}/\partial E)_{\psi} \equiv \gamma_{\text{E}}$	$(\partial q/\partial E)_{\psi} \equiv q_{\text{E}}$
$(\partial\Gamma_{\text{O}}/\partial\psi)_{\text{E}} \equiv \gamma_{\psi}$	$(\partial q/\partial\psi)_{\text{E}} \equiv q_{\psi}$
$(\partial^2\Gamma_{\text{O}}/\partial E^2)_{\psi}$	$(\partial^2 q/\partial E^2)_{\psi}$
$(\partial^2\Gamma_{\text{O}}/\partial\psi^2)_{\text{E}}$	$(\partial^2 q/\partial\psi^2)_{\text{E}}$
$(\partial^2\Gamma_{\text{O}}/\partial E\partial\psi)$	$(\partial^2 q/\partial E\partial\psi)$

It was shown before [1] that the product $\beta_{\text{O}}c_{\text{O}}(0,t)$ can also be regarded as the product $\epsilon_{\text{O}}\psi$ with ϵ_{O} equal to

$$\epsilon_{\text{O}} = \frac{\beta_{\text{O}} D_{\text{O}}^{-1/2}}{1 + e^{-\zeta}} \quad (6)$$

From eqn. (6) it follows that

$$\frac{d \ln \epsilon_{\text{O}}}{dE} = \frac{d \ln \beta_{\text{O}}}{dE} + \frac{nF}{RT} \frac{1}{1 + e^{\zeta}} \quad (7)$$

Using eqns (2) and (7) the second order partial derivatives of Γ_{O} can be derived:

$$\left(\frac{\partial^2 \Gamma_{\text{O}}}{\partial \psi^2} \right)_{\text{E}} = \left(\frac{d \ln \epsilon_{\text{O}}}{dE} \right)^{-1} \left\{ \frac{1}{\bar{\psi}} \frac{\partial^2 \Gamma_{\text{O}}}{\partial E \partial \psi} - \frac{1}{\bar{\psi}^2} \left(\frac{\partial \Gamma_{\text{O}}}{\partial E} \right)_{\psi} \right\} \quad (8)$$

and

$$\begin{aligned} \frac{\partial^2 \Gamma_O}{\partial E \partial \Psi} &= \left\{ \left(\frac{\partial^2 \Gamma_O}{\partial E^2} \right)_{\Psi} - \bar{\Psi} \frac{d^2 \ln \epsilon_O}{dE^2} \left(\frac{\partial \Gamma_O}{\partial \Psi} \right)_E \right\} / \left(\bar{\Psi} \frac{d \ln \epsilon_O}{dE} \right) \\ &= \left\{ \left(\frac{\partial^2 \Gamma_O}{\partial E^2} \right)_{\Psi} - \left(\frac{d \ln \epsilon_O}{dE} \right)^{-1} \frac{d^2 \ln \epsilon_O}{dE^2} \left(\frac{\partial \Gamma_O}{\partial E} \right)_{\Psi} \right\} / \left(\bar{\Psi} \frac{d \ln \epsilon_O}{dE} \right) \end{aligned} \quad (9)$$

From the relations existing between the ten partial derivatives given in Table 1, we find that there are only two independent parameters to be made explicit namely $(\partial \Gamma_O / \partial E)_{\Psi}$ and $(\partial^2 \Gamma_O / \partial E^2)_{\Psi}$. This can only be done if an adsorption isotherm is adopted as will be shown later on. How these two partial derivatives will determine the demodulated signal will be the subject of the next sections.

III. Solving the diffusion problem

The way in which the concentration of an electroactive species varies with time and distance x from the electrode surface is found by solving Fick's laws.

In more complex situations like in the case of adsorption of the electroactive species the diffusion problem is most easily solved by means of the method of Laplace transforms.

The second law of Fick then becomes:

$$D \frac{\partial^2 \overline{c(x,s)}}{\partial x^2} = s \overline{c(x,s)} - c(x,0) \quad (10)$$

where s is the Laplace parameter. Using as boundary conditions in the time domain

$$c(x,0) = c^* \quad \text{and} \quad c(\infty,t) = c^*$$

and the boundary condition in the Laplace domain

$$\overline{c(\infty,s)} = c^*/s$$

eqn. (10) can be solved, leading to

$$\overline{c(x,s)} = \frac{c^*}{s} + M(s) \exp\left(-x \frac{s^{1/2}}{D^{1/2}}\right) \quad (11)$$

Taking the partial derivative of $\overline{c(x,s)}$ with respect to x gives $M(s)$ which can be inserted into eqn. (11). Taking $x=0$ then gives

$$D \left(\frac{\partial \overline{c(0,s)}}{\partial x} \right)_{x=0} = -D^{1/2} s^{1/2} \left(\overline{c(0,s)} - \frac{c^*}{s} \right) \quad (12)$$

Since demodulation voltammetry is concerned with a sinusoidal perturbation with small amplitude eqn. (12) has to be formulated in terms of changes given by Δ ($\Delta c^*=0$):

$$D \left(\frac{\partial \overline{\Delta c(0,s)}}{\partial x} \right)_{x=0} = -D^{1/2} s^{1/2} \overline{\Delta c(0,s)} \quad (13)$$

III.2 Flux equations describing the mass transfer of ox and red

The flux of the ox and red component (in $\text{molcm}^{-2}\text{s}^{-1}$) towards the electrode surface, in case only adsorption of the ox component is considered, is given by

$$-\frac{1}{nF} j_F = D_O \left(\frac{\partial c_O}{\partial x} \right)_{x=0} - \frac{d\Gamma_O}{dt} \quad (14a)$$

and

$$\frac{1}{nF} j_F = D_R \left(\frac{\partial c_R}{\partial x} \right)_{x=0} \quad (14b)$$

Because the diffusion problem was solved in the Laplace domain eqns. (14a,b) have to be Laplace transformed and in terms of the small amplitude perturbation ($\overline{\Delta c(s)} \equiv \overline{\Delta c(0,s)}$):

$$-\frac{1}{nF} \overline{\Delta j_F(s)} + s \overline{\Delta \Gamma_O(s)} = -s^{1/2} D_O^{1/2} \overline{\Delta c_O(s)} \quad (15a)$$

and

$$\frac{1}{nF} \overline{\Delta j_F(s)} = -s^{1/2} D_R^{1/2} \overline{\Delta c_R(s)} \quad (15b)$$

Summarizing eqns. (15a) and (15b) results into

$$-s^{1/2} \overline{\Delta \Gamma_O(s)} = D_O^{1/2} \overline{\Delta c_O(s)} + D_R^{1/2} \overline{\Delta c_R(s)} \quad (16)$$

Using the Laplace transform of eqn. (1) for a perturbation Δ :

$$\overline{\Delta\psi(s)} = D_O^{1/2} \overline{\Delta c_O(s)} + D_R^{1/2} \overline{\Delta c_R(s)} \quad (17)$$

Substituting eqn. (17) into eqn. (16) gives

$$\overline{\Delta\psi(s)} = -s^{1/2} \overline{\Delta\Gamma_O(s)} \quad (18)$$

The latter expression is valid for first and higher order perturbations.

Eqn. (18) can be rewritten by substituting the first order expansion of $\overline{\Delta\Gamma_O(s)}$:

$$\overline{\Delta\Gamma_{O,1}(s)} = \left(\frac{\partial\Gamma_O}{\partial E}\right)_\psi \overline{\Delta E_1(s)} + \left(\frac{\partial\Gamma_O}{\partial\psi}\right)_E \overline{\Delta\psi_1(s)} \quad (19)$$

leading to:

$$\overline{\Delta\psi_1(s)} = -\frac{s^{1/2}}{1 + \gamma_\psi s^{1/2}} \gamma_E \overline{\Delta E_1(s)} \quad (20)$$

with

$$\gamma_\psi = \left(\frac{\partial\Gamma_O}{\partial\psi}\right)_E \quad \text{and} \quad \gamma_E = \left(\frac{\partial\Gamma_O}{\partial E}\right)_\psi \quad [\text{see Table 1}]$$

IV. Nernst equation: first and second order expansion

Because of the assumption of reversible charge transfer the concentrations $c_O(0,t)$ and $c_R(0,t)$ will virtually obey the equilibrium relationship, i.e. they will be related via the Nernst equation:

$$\frac{c_O(0,t)}{c_R(0,t)} = \exp\left(\frac{nF}{RT}(E-E^0)\right) = \exp(\varphi) \quad (21)$$

where E^0 is the standard potential.

To deal with the several order contributions we assume that the quantities c_O , c_R and φ can be considered as a superposition of a mean value \bar{c}_O , \bar{c}_R and $\bar{\varphi}$ and their sinusoidal fluctuations Δc_O , Δc_R and $\Delta\varphi$ around these values. Furthermore we assume that the fluctuations are additively composed of the several order contributions. Expanding to second order gives:

$$\Delta\phi = \Delta\phi_1 + \Delta\phi_2 \quad (22a)$$

$$\Delta c_O = \Delta c_{O,1} + \Delta c_{O,2} \quad (22b)$$

$$\Delta c_R = \Delta c_{R,1} + \Delta c_{R,2} \quad (22c)$$

Introducing eqns. (22a-c) into eqn. (21), and making use of the second order Taylor expansion $\exp(x) = 1 + x + \frac{1}{2}x^2$, results into a first order part of the Nernst equation given by:

$$\frac{\Delta c_{R,1}}{\bar{c}_R} + \Delta\phi_1 - \frac{\Delta c_{O,1}}{\bar{c}_O} = 0 \quad (23a)$$

and a second order part

$$\frac{\Delta c_{R,2}}{\bar{c}_R} + \Delta\phi_2 - \frac{\Delta c_{O,2}}{\bar{c}_O} = -\frac{1}{2}(\Delta\phi_1)^2 - \frac{\Delta c_{R,1}\Delta\phi_1}{\bar{c}_R} \quad (23b)$$

Eqns. (23a) and (23b) can be rewritten making use of eqn. (1) in case of a perturbation Δ :

$$\Delta\psi_1 = D_O^{1/2} \Delta c_{O,1} + D_R^{1/2} \Delta c_{R,1} \quad (23c)$$

from which we obtain an expression for $\Delta c_{O,1}/\bar{c}_O$:

$$\frac{\Delta c_{O,1}}{\bar{c}_O} = \frac{\Delta\psi_1}{\bar{\psi}} \frac{\bar{\psi}}{D_O^{1/2} \bar{c}_O} - \frac{\Delta c_{R,1}}{\bar{c}_R} \frac{\bar{c}_R D_R^{1/2}}{\bar{c}_O D_O^{1/2}} \quad (23d)$$

In an analogous way $\Delta c_{O,2}/\bar{c}_O$ is found. Eqns. (23a) and (23b) are therefore identical to respectively

$$\Delta\phi_1 + \frac{\Delta c_{R,1}}{\bar{c}_R} \frac{\bar{\psi}}{\bar{c}_O D_O^{1/2}} - \frac{\Delta\psi_1}{\bar{\psi}} \frac{\bar{\psi}}{\bar{c}_O D_O^{1/2}} = 0 \quad (23e)$$

which is the first order part of the Nernst equation and

$$\Delta\phi_2 + \frac{\Delta c_{R,2}}{\bar{c}_R} \frac{\bar{\psi}}{D_O^{1/2} \bar{c}_O} - \frac{\Delta\psi_2}{\bar{\psi}} \frac{\bar{\psi}}{D_O^{1/2} \bar{c}_O} = -\frac{1}{2} (\Delta\phi_1)^2 - \frac{\Delta c_{R,1} \Delta\phi_1}{\bar{c}_R} \quad (23f)$$

The next step is to transform eqns. (23e,f) into the Laplace domain while applying eqn. (20) and the relation $\overline{\Delta\psi_2(s)} = -s^{1/2} \overline{\Delta\Gamma_2(s)}$ (see Section 4.1) which results into:

$$\frac{\overline{\Delta c_{R,1}(s)} / \bar{c}_R}{\overline{\Delta\phi_1(s)}} = -\frac{\sigma_R}{\sigma} - \frac{\sigma_O \sigma_R}{\sigma} nF \sqrt{2} \gamma_E \frac{s^{1/2}}{1 + \gamma_\psi s^{1/2}} \quad (24a)$$

and the second order part of the Nernst equation:

$$\overline{\Delta\phi_2(s)} - \frac{nF}{RT} \frac{\sigma \sqrt{2}}{s^{1/2}} \overline{\Delta j_{F,2}(s)} - \frac{n^2 F^2 \sqrt{2}}{RT} \sigma_O \overline{\Delta\psi_2(s)} = -\frac{1}{2} \overline{\Delta\phi_1^2(s)} - \frac{\overline{\Delta\phi_1} \overline{\Delta c_{R,1}(s)}}{\bar{c}_R} \quad (24b)$$

where we have introduced the Warburg parameters σ_O , σ_R and $\sigma = \sigma_O + \sigma_R$ given by

$$\sigma_O = \frac{RT}{n^2 F^2 \sqrt{2}} \frac{1}{\bar{c}_O D_O^{1/2}} \quad (25a)$$

and

$$\sigma_R = \frac{RT}{n^2 F^2 \sqrt{2}} \frac{1}{\bar{c}_R D_R^{1/2}} \quad (25b)$$

V. Explicating the surface perturbations of the ox and red component

V.1 Taking the potential perturbation equal to a sum of sinusoidal waveforms

Introducing as a perturbation a sum of sinusoidal wave forms given by:

$$\Delta E_1 = \sum_{m=1}^N E_m \sin \omega_m t \quad (26)$$

the response of the concentration of the red component at the surface will be of the form:

$$\frac{\Delta c_{R,1}}{\bar{c}_R} = \sum_{m=1}^N E_m (a_m \sin \omega_m t + b_m \cos \omega_m t) \quad (27)$$

The use of a sinusoidal perturbation is very convenient since mathematically the resulting response of the surface concentrations will always consist of sine and cosine terms.

To make the surface perturbations explicit the coefficients a_m and b_m must be solved. This can be done as follows. First eqns. (26) and (27) are transformed into the Laplace domain:

$$\overline{\Delta E_1(s)} = \sum_{m=1}^N E_m \left(\frac{\omega_m}{s^2 + \omega_m^2} \right) \quad (28)$$

and

$$\frac{\overline{\Delta c_{R,1}(s)}}{\bar{c}_R} = \sum_{m=1}^N E_m \left(\frac{\omega_m a_m + s b_m}{s^2 + \omega_m^2} \right) \quad (29)$$

The next step is to divide eqn. (29) by eqn. (28), and to insert $s = i\omega_m$ (where i is the imaginary unit):

$$\frac{\overline{\Delta c_{R,1}(s)} / \bar{c}_R}{\overline{\Delta \phi_1(s)}} = \frac{RT}{nF} (a_m + i b_m) \quad (30)$$

using $\Delta E_1 = (RT/nF) \Delta \phi_1$.

The coefficients a_m and b_m are obtained by realizing that eqn. (30) is identical to the first order expansion of the Nernst equation given by eqn. (24a). Separating the real and imaginary parts of eqn. (24a) and introducing the dimensionless parameter

$$u_m = \gamma_{\psi} (2\omega_m)^{1/2}$$

results into expressions for a_m and b_m :

$$a_m = - \frac{nF}{RT} \left[\left(\frac{\sigma_R}{\sigma} \right) + \left(\frac{\sigma_O \sigma_R}{\sigma} nF \sqrt{2} \gamma_E (2\omega_m)^{1/2} \right) \frac{u_m + 1}{u_m^2 + 2u_m + 2} \right] \quad (31a)$$

and

$$b_m = -\frac{n^2 F^2 \sqrt{2}}{RT} \frac{\sigma_O \sigma_R}{\sigma} \gamma_E (2\omega_m)^{1/2} \frac{1}{u_m^2 + 2u_m + 2} \quad (31b)$$

With an analogous procedure an explicit expression for $\overline{\Delta\psi_1(s)}$ can be found assuming the fluctuation $\Delta\psi_1$ equal to

$$\Delta\psi_1 = \sum_{m=1}^N E_m (c_m \sin \omega_m t + d_m \cos \omega_m t) \quad (32)$$

leading to expressions for c_m and d_m :

$$c_m = -\gamma_E (2\omega_m)^{1/2} \frac{u_m + 1}{u_m^2 + 2u_m + 2} \quad (33a)$$

and

$$d_m = -\gamma_E (2\omega_m)^{1/2} \frac{1}{u_m^2 + 2u_m + 2} \quad (33b)$$

V.2 Restriction of the potential perturbation to the waveform for demodulation voltammetry

The potential perturbation used in the case of demodulation voltammetry is given by [7]:

$$\Delta E_1 = \frac{E_A}{2} (\sin \omega_m t + \sin \omega_n t) \quad (34)$$

with $\omega_m = \omega_H + \omega_L$ and $\omega_n = \omega_H - \omega_L$. Only terms of $\omega_m - \omega_n$ will give rise to a response at $2\omega_L$ [7]. Using goniometric rules and keeping only terms containing $\omega_m - \omega_n$ into account we find that, introducing the condition $\omega_H \gg \omega_L$ ($\omega_m \approx \omega_n$) the coefficients $a_m \approx a_n$, $b_m \approx b_n$, $c_m \approx c_n$ and $d_m \approx d_n$.

This leads to the following simplified expressions:

$$(\Delta E_1)^2 = \left(\frac{E_A}{2}\right)^2 \cos(2\omega_L t) \quad (35a)$$

$$(\Delta\psi_1)^2 = \left(\frac{E_A}{2}\right)^2 (c_m^2 + d_m^2) \cos(2\omega_L t) \quad (35b)$$

$$\Delta E_1 \Delta \Psi_1 = \left(\frac{E_A}{2} \right)^2 c_m \cos(2\omega_L t) \quad (35c)$$

$$\frac{\Delta E_1 \Delta c_{R,1}}{\bar{c}_R} = \left(\frac{E_A}{2} \right)^2 a_m \cos(2\omega_L t) \quad (35d)$$

Laplace transformation of eqns. (35a-d) is easily done by introducing the Laplace transform \mathcal{L} of $\cos(2\omega_L t)$ given by:

$$\mathcal{L} \{ \cos(2\omega_L t) \} = \frac{s}{s^2 + (2\omega_L)^2} \quad (36)$$

VI. Second order expansion of the surface excess Γ_0 and the surface charge q

VI.1 Surface excess Γ_0

The second order expansion of the Nernst equation contains the term $\overline{\Delta \Psi_2(s)}$ which is related to $\overline{\Delta \Gamma_2(s)}$ via

$$\overline{\Delta \Psi_2(s)} = -s^{1/2} \overline{\Delta \Gamma_2(s)}$$

The second order perturbation of $\overline{\Delta \Gamma_2(s)}$ is found from a Taylor expansion:

$$\begin{aligned} \overline{\Delta \Gamma_2(s)} &= \mathcal{L}(\Delta \Gamma_2) = \gamma_E \mathcal{L}(\Delta E_2) + \gamma_\Psi \mathcal{L}(\Delta \Psi_2) + \frac{1}{2} \left(\frac{\partial^2 \Gamma_0}{\partial E^2} \right)_\Psi \mathcal{L}(\Delta E_1^2) + \\ &\frac{1}{2} \left(\frac{\partial^2 \Gamma_0}{\partial \Psi^2} \right)_E \mathcal{L}(\Delta \Psi_1^2) + \left(\frac{\partial^2 \Gamma_0}{\partial E \partial \Psi} \right) \mathcal{L}(\Delta E_1 \Delta \Psi_1) \end{aligned} \quad (37)$$

In eqn. (37) care must be taken to correctly interpret the quadratic terms $\mathcal{L}(\Delta E_1^2)$ and $\mathcal{L}(\Delta \Psi_1^2)$ and the mixed term $\mathcal{L}(\Delta E_1 \Delta \Psi_1)$ [see eqns. (35 a-c) and eqn. (36)].

VI.2 Surface charge density q

The second order expansion of the surface charge density q occurs in the condition for the net second order current Δj_2 :

$$\Delta j_2 = \Delta j_{F,2} + \Delta j_{c,2} = 0 \quad (38)$$

which equals zero in the case of demodulation voltammetry [7] via

$$\overline{\Delta j_{c,2}(s)} = s \overline{\Delta q_2(s)} \quad (39)$$

where $j_c = dq/dt$.

The expression for $\overline{\Delta q_2(s)}$ is found from a Taylor expansion:

$$\begin{aligned} \overline{\Delta q_2(s)} = \mathbf{L}(\Delta q_2) &= q_E \mathbf{L}(\Delta E_2) + q_\psi \mathbf{L}(\Delta \psi_2) + \frac{1}{2} \left(\frac{\partial^2 q}{\partial E^2} \right)_\psi \mathbf{L}(\Delta E_1^2) + \\ &\frac{1}{2} \left(\frac{\partial^2 q}{\partial \psi^2} \right)_E \mathbf{L}(\Delta \psi_1^2) + \left(\frac{\partial^2 q}{\partial E \partial \psi} \right) \mathbf{L}(\Delta E_1 \Delta \psi_1) \end{aligned} \quad (40)$$

VII. Summarizing the set of equations determining $\overline{\Delta E_2(s)}$

In the foregoing sections the complete set of equations was derived needed for obtaining $\overline{\Delta E_2(s)}$. For the sake of convenience two more abbreviations are introduced to simplify writing:

$$G_O = \frac{1}{2} \left(\frac{\partial^2 \Gamma_O}{\partial E^2} \right)_\psi \mathbf{L}(\Delta E_1^2) + \frac{1}{2} \left(\frac{\partial^2 \Gamma_O}{\partial \psi^2} \right)_E \mathbf{L}(\Delta \psi_1^2) + \left(\frac{\partial^2 \Gamma_O}{\partial E \partial \psi} \right) \mathbf{L}(\Delta E_1 \Delta \psi_1) \quad (41)$$

and

$$\underline{Q} = \frac{1}{2} \left(\frac{\partial^2 q}{\partial E^2} \right)_\psi \mathbf{L}(\Delta E_1^2) + \frac{1}{2} \left(\frac{\partial^2 q}{\partial \psi^2} \right)_E \mathbf{L}(\Delta \psi_1^2) + \left(\frac{\partial^2 q}{\partial E \partial \psi} \right) \mathbf{L}(\Delta E_1 \Delta \psi_1) \quad (42)$$

Then the basic equations describing the Laplace transformed response $\overline{\Delta E_2(s)}$ are:

$$\mathcal{L}(\Delta j_{c,2}) - sq_E \mathcal{L}(\Delta E_2) - sq_\psi \mathcal{L}(\Delta \psi_2) = s \underline{Q} \quad (43a)$$

$$\mathcal{L}(\Delta \Gamma_2) - \gamma_E \mathcal{L}(\Delta E_2) - \gamma_\psi \mathcal{L}(\Delta \psi_2) = G_O \quad (43b)$$

$$\mathcal{L}(\Delta E_2) - \sigma \sqrt{2} s^{-1/2} \mathcal{L}(\Delta j_{F,2}) - nF \sqrt{2} \sigma_O \mathcal{L}(\Delta \psi_2) = -\frac{1}{2} \frac{nF}{RT} \mathcal{L}(\Delta E_1^2) - \frac{\mathcal{L}(\Delta E_1 \Delta c_{R,1})}{\bar{c}_R} \quad (43c)$$

$$\mathcal{L}(\Delta \psi_2) + s^{1/2} \mathcal{L}(\Delta \Gamma_2) = 0 \quad (43d)$$

$$\mathcal{L}(\Delta j_{F,2}) + \mathcal{L}(\Delta j_{c,2}) = 0 \quad (43e)$$

which is a set of five linear equations from which the five unknowns $\mathcal{L}(\Delta j_{F,2})$, $\mathcal{L}(\Delta j_{c,2})$, $\mathcal{L}(\Delta \psi_2)$, $\mathcal{L}(\Delta \Gamma_2)$ and $\mathcal{L}(\Delta E_2)$ can be solved.

Eqns. (43a-b) originate from the second order expansion of the surface charge q and the surface excess Γ_O respectively.

Eqn. (43c) originates from the second order expansion of the Nernst equation. Eqn. (43d) results from the mass transfer (Fick's laws) and flux equations. Eqn. (43e) indicates that no external second order current flows in case of demodulation voltammetry.

The way of solving this set of equations (43a-e) to obtain $\overline{\Delta E_2(s)}$ is shown in Appendix A.

$$\mathcal{L}(\Delta E_2) =$$

$$\left[\sigma \sqrt{2} q_\psi G_O \frac{s}{1 + \gamma_\psi s^{1/2}} - \sigma \sqrt{2} s^{1/2} \underline{Q} - nF \sqrt{2} \sigma_O G_O \frac{s^{1/2}}{1 + \gamma_\psi s^{1/2}} - \frac{1}{2} \frac{nF}{RT} \mathcal{L}(\Delta E_1^2) - \frac{\mathcal{L}(\Delta E_1 \Delta c_{R,1})}{\bar{c}_R} \right] / \left[1 + \sigma \sqrt{2} s^{1/2} q_E - \sigma \sqrt{2} q_\psi \gamma_E \frac{s}{1 + \gamma_\psi s^{1/2}} + nF \sigma_O \sqrt{2} \gamma_E \frac{s^{1/2}}{1 + \gamma_\psi s^{1/2}} \right] \quad (44)$$

The corresponding time domain expression ΔE_2 is derived in Appendix B and is equal to:

$$\Delta E_2 = \left(\frac{E_A}{2} \right)^2 \frac{a+ib}{c+id} \quad (45)$$

with the expression for a, b, c and d given by:

$$\begin{aligned}
 a &= \sigma\sqrt{2}q_{\psi}\gamma_{\underline{}}2\omega_L\frac{u_L}{2u_L^2+2u_L+1} - \sigma\sqrt{2}q_{\underline{}}(\omega_L)^{1/2} - \\
 &\quad nF\sigma_O\sqrt{2}\gamma_{\underline{}}(\omega_L)^{1/2}\frac{2u_L+1}{2u_L^2+2u_L+1} - \frac{1}{2}\frac{nF}{RT} - a_m
 \end{aligned} \tag{46a}$$

$$\begin{aligned}
 b &= \sigma\sqrt{2}q_{\psi}\gamma_{\underline{}}2\omega_L\frac{u_L+1}{2u_L^2+2u_L+1} - \sigma\sqrt{2}q_{\underline{}}(\omega_L)^{1/2} - \\
 &\quad nF\sigma_O\sqrt{2}\gamma_{\underline{}}(\omega_L)^{1/2}\frac{1}{2u_L^2+2u_L+1}
 \end{aligned} \tag{46b}$$

$$\begin{aligned}
 c &= 1 + \sigma\sqrt{2}q_E(\omega_L)^{1/2} - \sigma\sqrt{2}q_{\psi}\gamma_E2\omega_L\frac{u_L}{2u_L^2+2u_L+1} + \\
 &\quad nF\sigma_O\gamma_E\sqrt{2}(\omega_L)^{1/2}\frac{2u_L+1}{2u_L^2+2u_L+1}
 \end{aligned} \tag{46c}$$

$$\begin{aligned}
 d &= \sigma\sqrt{2}q_E(\omega_L)^{1/2} - \sigma\sqrt{2}q_{\psi}\gamma_E2\omega_L\frac{u_L+1}{2u_L^2+2u_L+1} + \\
 &\quad nF\sigma_O\gamma_E\sqrt{2}(\omega_L)^{1/2}\frac{1}{2u_L^2+2u_L+1}
 \end{aligned} \tag{46d}$$

The Laplace parameter s is equal to $2i\omega_L$.

The eqns. (44) and (46 a-d) will be used in the next section for some model calculations.

VIII. Some numerical examples of demodulation voltammograms

VIII.1 Choice of the Langmuir isotherm

To perform model calculations it is necessary to adopt an adsorption isotherm to make the partial derivatives $(\partial\Gamma_O/\partial E)_{\psi}$ and $(\partial^2\Gamma_O/\partial E^2)_{\psi}$ explicit.

In the following part a Langmuir isotherm will be applied which has the required form $\Gamma_O = \Gamma_O(\beta_O c_O)$ ensuring the applicability of the formulae (2) and (3):

$$\frac{\Gamma_O}{\Gamma_m} = \frac{\beta_O c_O(0,t)}{1 + \beta_O c_O(0,t)} \quad (47)$$

where Γ_m is the maximum surface excess and in which the surface concentration $c_O(0,t)$ of the ox component has to be written as a function of ψ :

$$c_O(0,t) = D_O^{-1/2} \psi (1 + e^{-\zeta})^{-1} \quad (48)$$

which results into

$$\Gamma_O = \frac{\beta_O D_O^{-1/2} \psi (1 + e^{-\zeta})^{-1}}{1 + \beta_O D_O^{-1/2} \psi (1 + e^{-\zeta})^{-1}} \Gamma_m = \psi D_O^{-1/2} \Gamma_m \frac{\beta_O}{1 + e^{-\zeta} + D_O^{-1/2} \psi \beta_O} \quad (49)$$

From eqn. (46) the partial derivatives $(\partial\Gamma_O/\partial E)_\psi$ and $(\partial^2\Gamma_O/\partial E^2)_\psi$ are easily obtained in terms of the mean values of ζ and ψ (see Appendix C). The latter quantity, usually indicated by $\bar{\psi}$, is equal to

$$\bar{\psi} = D_O^{1/2} \bar{c}_O + D_R^{1/2} \bar{c}_R \quad (50a)$$

where \bar{c}_O and \bar{c}_R are the mean surface concentrations.

In order to make $\bar{\psi}$ explicit, \bar{c}_O and \bar{c}_R have to be expressed in terms of the bulk concentrations c_O^* and c_R^* , and possible other parameters, influencing the mass transfer problem in the dc sense. In the most simple approximation, it is assumed that semi-infinite linear diffusion prevails, and that the effect of reactant adsorption on the dc process is negligible. Then it follows that eqn. (50a) can be replaced by:

$$\bar{\psi} = \psi^* = D_O^{1/2} c_O^* + D_R^{1/2} c_R^* \quad (50b)$$

The potential dependence of β_O will be taken to be

$$\beta_O = \beta_O^* \exp\left(-a_O (E - E_{1/2}^r)\right) \quad (51)$$

where β_O^* is the adsorption coefficient at $E=E_{1/2}^r$ and a_O is a constant. Eqn. (51), in fact, means that the standard Gibbs energy of adsorption, ΔG_{ads} , is a linear function of the applied electrode potential. In the following sections we will consider two possibilities namely $a_O=0$ (β_O becomes potential independent) and $a_O>0$ (β_O decreases at more positive potentials).

VIII.2 Potential independent adsorption coefficient

The parameters for the numerically calculated demodulation voltammogram, taking β_O potential independent, are summarized in Table 2.

The value of β_O is varied in such a way that the product $\beta_O c_O^*$ ranges from $\beta_O c_O^* \ll 1$ to $\beta_O c_O^* \gg 1$.

Table 2 Survey of parameters used for the demodulation response calculated from eqns. (B8a-d) and (B9a-b).

n	1
v_H/Hz	100000
v_L/Hz	100
c_O^*/molcm^{-3}	10^{-7}
c_R^*/molcm^{-3}	0
$C_d^0/\mu\text{Fcm}^{-2}$	25
$\Gamma_m/\text{molcm}^{-2}$	10^{-9}
j_A/Acm^{-2}	0.20
$D_O/\text{cm}^2\text{s}^{-1}$	10^{-5}
$D_R/\text{cm}^2\text{s}^{-1}$	10^{-5}
a_O/V^{-1}	0
$\beta_O/\text{cm}^3\text{mol}^{-1}$	$0, 10^3, 10^4, 10^5, 10^6, 10^7, 10^8, 10^9$
T/K	298

The purpose of this model calculation is to see the extent to which the demodulation voltammogram (I_{LF} and Q_{LF} component) is influenced by adsorption of the electroactive species.

In Figure 1a and 1b the In-phase component (I_{LF}) and Quadrature component (Q_{LF}) are shown respectively.

The Figures 1a-b demonstrate most clearly the influence of reactant adsorption. In the special case that reactant adsorption is absent ($\beta_0=0$) we obtain the reversible demodulation voltammogram showing a symmetric In-phase and Quadrature component.

Although many other parameters can be changed for performing model calculations, the given examples in Figures 1a-b definitely prove that the demodulation technique offers a very sensitive method for studying reactant adsorption in a wide potential range.

The demodulation technique offers the possibility to study the effect of reactant adsorption as a function of the accessible dc potential range in a sensitive way at chosen values for the high and low frequency respectively (carrier wave frequency and modulating frequency) whereas the impedance technique necessitates to study the whole accessible frequency range (80 Hz-10000 Hz) at the applied dc potentials. It has become clear that the demodulation technique offers the opportunity to fit a model for reactant adsorption for the whole accessible dc range in a very accurate way.

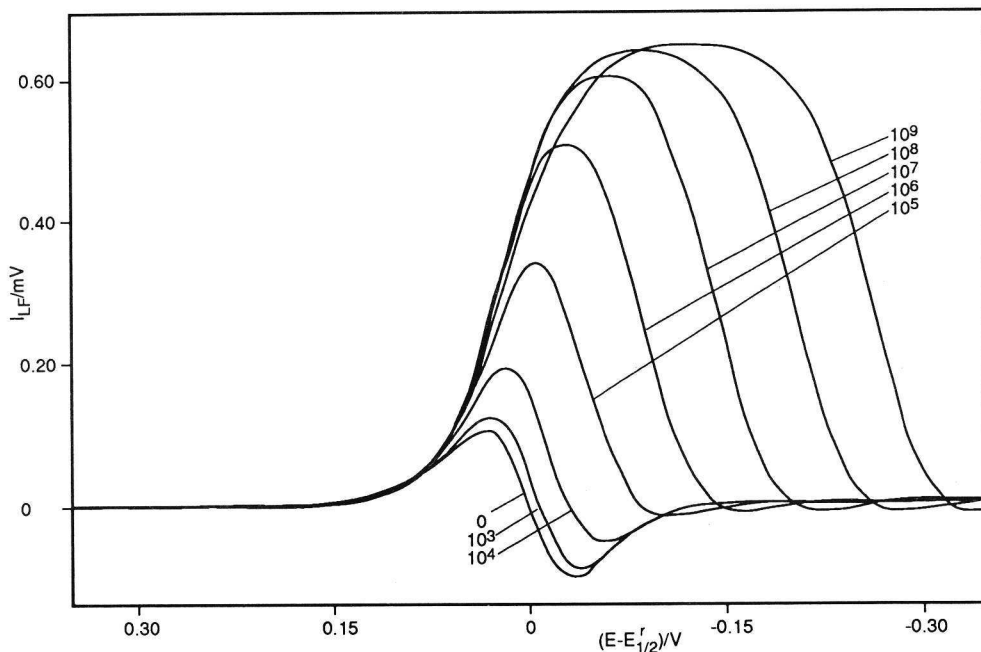


Figure 1a In-phase component I_{LF} (mV) versus $(E - E_{1/2}^r)$ (V) for $\beta_O = 0, 10^3, 10^4, 10^5, 10^6, 10^7, 10^8,$ and 10^9 ($\text{mol}^{-1}\text{cm}^3$). For other conditions see text and Table 2.

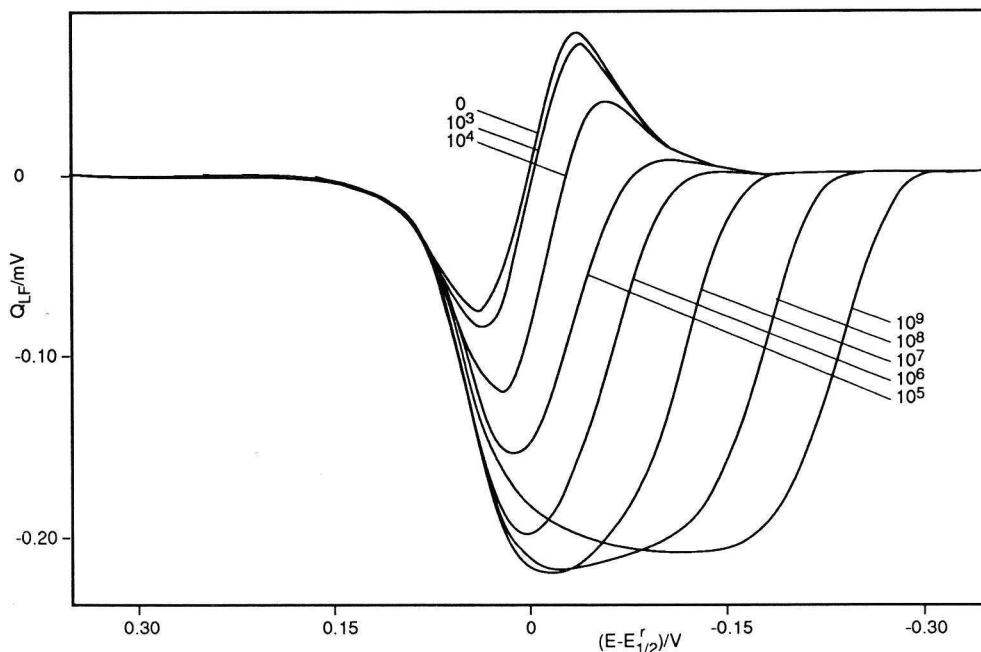


Figure 1b Quadrature component Q_{LF} (mV) versus $(E - E_{1/2}^r)$ (V) for $\beta_O = 0, 10^3, 10^4, 10^5, 10^6, 10^7, 10^8,$ and 10^9 ($\text{mol}^{-1}\text{cm}^3$). For other conditions see text and Table 2.

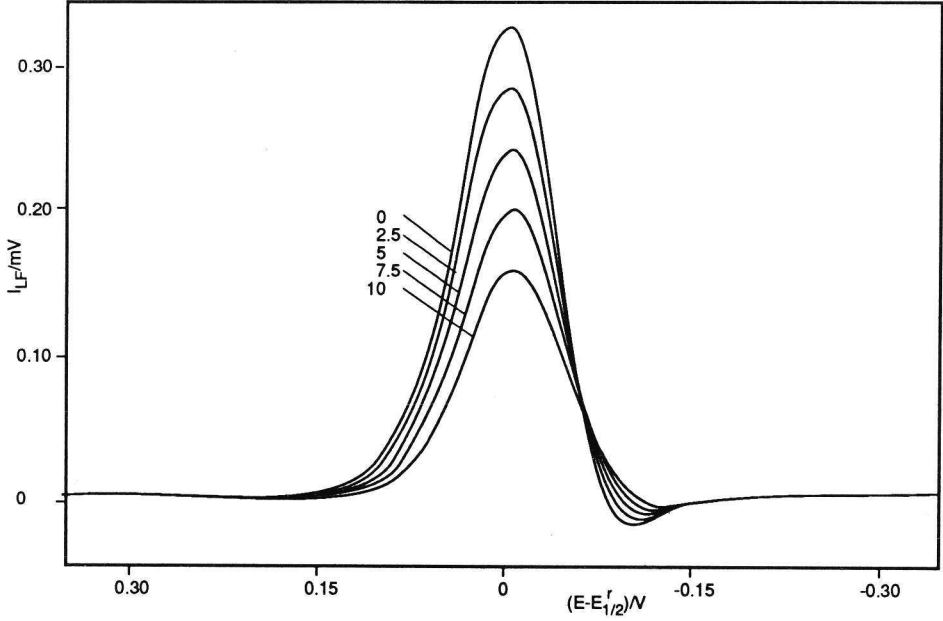


Figure 2a In-phase component I_{LF} (mV) versus $(E-E_{1/2}^r)$ (V) for $\beta_O^* = 10^5 \text{ cm}^3 \text{ mol}^{-1}$ and $a_O = 0, 2.5, 5, 7.5$ and 10 V^{-1} .
For other conditions see text and Table 2.

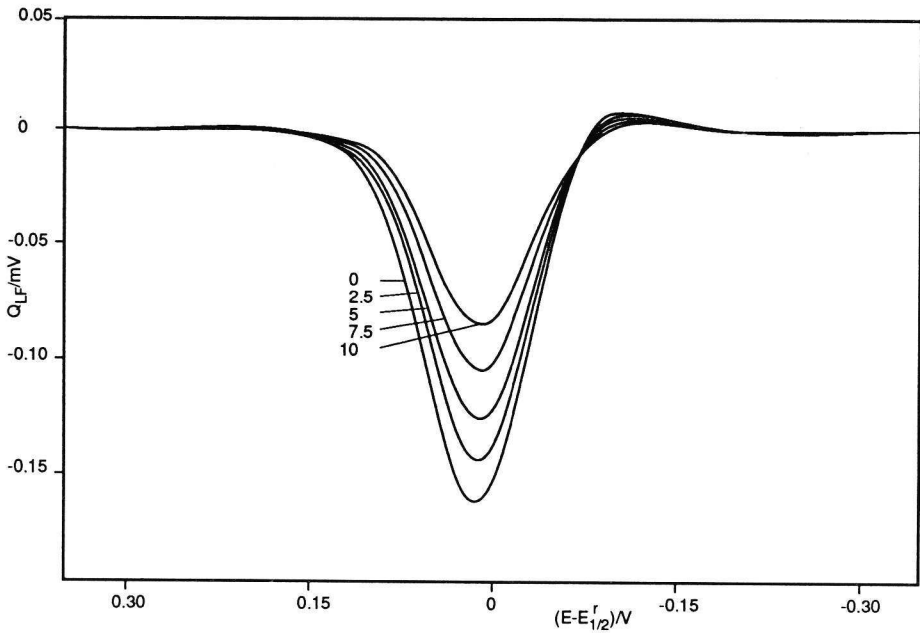


Figure 2b Quadrature component Q_{LF} (mV) versus $(E-E_{1/2}^r)$ (V) for $\beta_O^* = 10^5 \text{ cm}^3 \text{ mol}^{-1}$ and $a_O = 0, 2.5, 5, 7.5$ and 10 V^{-1} .
For other conditions see text and Table 2.

VIII.3 Potential dependent adsorption coefficient

In order to investigate the sensitivity of the demodulation voltammogram with respect to the potential dependence of β_O we have taken $\beta_O^* = 10^5 \text{ cm}^3\text{mol}^{-1}$ and $a_O = 0, 2.5, 5, 7.5$ and 10 V^{-1} respectively.

Using eqn. (51) together with eqns. (B8a-d) and (B9a-b) we have calculated the In-phase and Quadrature component as shown in Figure 2a and 2b respectively.

From Figures (2a-b) we conclude that a change in a_O gives a clear difference in the value of the I_{LF} and Q_{LF} component. In case a_O becomes smaller the phase-sensitive demodulation voltammograms show a larger amplitude and a broader curve. We conclude that the demodulation method can serve as a sensitive technique to study the potential dependence of the adsorption coefficient β_O .

IX. Conclusions

Although only a limited number of model calculations has been presented it will be clear that the demodulation technique offers a promising additional possibility to study the phenomenon of reactant adsorption in a sensitive way and in a wide potential range.

Comparing the reversible demodulation voltammogram with ($\beta_O > 0$) and without ($\beta_O = 0$) reactant adsorption it follows that reactant adsorption gives rise to an increased signal as compared with the demodulation voltammogram for $\beta_O = 0$. As no other origin for such behaviour is known such a phenomenon can safely be regarded as a criterion for reactant adsorption.

Taking into account also the sensitivity of the demodulation voltammogram towards a potential dependence of β_O we can conclude that the demodulation technique shows good promises to be used as an additional method (with the possibility to measure more sensitively and in a wider dc potential range) as compared with the ac technique to study reactant adsorption.

APPENDIX A

SOLVING THE SET OF EQNS. (43A-E) TO OBTAIN $\overline{\Delta E_2(s)}$

From eqns. (43a-e) $\overline{\Delta E_2(s)} = \mathbf{L}(\Delta E_2)$ is obtained as follows. Eqn. (43d) is substituted in eqn. (43b) from which we obtain:

$$\mathbf{L}(\Delta \Gamma_2) = \frac{\gamma_E}{1 + \gamma_\psi s^{1/2}} \mathbf{L}(\Delta E_2) + \frac{1}{1 + \gamma_\psi s^{1/2}} G_O \quad (A1)$$

Eqn. (43d) is inserted into eqns. (43a) and (43c) while $\mathbf{L}(\Delta \Gamma_2)$ is replaced by eqn. (A1).

Using eqn. (43e) we can replace $\mathbf{L}(\Delta j_{c,2})$ by $-\mathbf{L}(\Delta j_{F,2})$.

The resulting expressions are given by

$$\mathbf{L}(\Delta j_{F,2}) = -sq_E \mathbf{L}(\Delta E_2) + sq_\psi \left[\frac{s^{1/2}}{1 + \gamma_\psi s^{1/2}} \gamma_E \mathbf{L}(\Delta E_2) + \frac{s^{1/2}}{1 + \gamma_\psi s^{1/2}} G_O \right] - s\bar{Q} \quad (A2)$$

and

$$\begin{aligned} \mathbf{L}(\Delta E_2) - \frac{\sigma\sqrt{2}}{s^{1/2}} \mathbf{L}(\Delta j_{F,2}) + nF\sqrt{2} \sigma_O s^{1/2} \left[\frac{\gamma_E}{1 + \gamma_\psi s^{1/2}} \mathbf{L}(\Delta E_2) + \frac{1}{1 + \gamma_\psi s^{1/2}} G_O \right] = \\ - \frac{1}{2} \frac{nF}{RT} \mathbf{L}(\Delta E_1^2) - \frac{\mathbf{L}(\Delta E_1 \Delta c_{R,1})}{\bar{c}_R} \end{aligned} \quad (A3)$$

Substituting eqn. (A2) into eqn. (A3) results into the final expression for $\mathbf{L}(\Delta E_2)$.

APPENDIX B

TIME DOMAIN EXPRESSION OF ΔE_2

In order to find the expression of ΔE_2 in the time domain we must apply

$$\Delta E_2 = \frac{\mathbf{L}(\Delta E_2)}{\mathbf{L}(\cos(2\omega_L t))} \quad (\text{B1})$$

Eqn. (B1) consists of a real part (In-phase component) and an imaginary part (Quadrature component).

The denominator of eqn. (B1) can be found in all of the terms in the numerator of eqn. (A4).

It is convenient before giving the expression for ΔE_2 to introduce a new dimensionless parameter u_L given by

$$u_L = \gamma_\Psi (\omega_L)^{1/2} \quad (\text{B2})$$

The parameter u_L is used to simplify the following expressions occurring in ΔE_2 :

$$\left(\frac{s^{1/2}}{1 + \gamma_\Psi s^{1/2}} \right)_{s=2i\omega_L} = (\omega_L)^{1/2} \frac{2u_L + 1 + i}{2u_L^2 + 2u_L + 1} \quad (\text{B3})$$

and

$$\left(\frac{s}{1 + \gamma_\Psi s^{1/2}} \right)_{s=2i\omega_L} = (2\omega_L) \frac{u_L + i(u_L + 1)}{2u_L^2 + 2u_L + 1} \quad (\text{B3})$$

After introducing two more abbreviations

$$\underline{\gamma} = \frac{1}{2} \left(\frac{\partial^2 \Gamma_O}{\partial E^2} \right)_\Psi + \frac{1}{2} \left(\frac{\partial^2 \Gamma_O}{\partial \Psi^2} \right)_E (c_m^2 + d_m^2) + \left(\frac{\partial^2 \Gamma_O}{\partial E \partial \Psi} \right) c_m \quad (\text{B5})$$

and

$$\underline{q} = \frac{1}{2} \left(\frac{\partial^2 q}{\partial E^2} \right)_\Psi + \frac{1}{2} \left(\frac{\partial^2 q}{\partial \Psi^2} \right)_E (c_m^2 + d_m^2) + \left(\frac{\partial^2 q}{\partial E \partial \Psi} \right) c_m \quad (\text{B6})$$

the expression for ΔE_2 reads

$$\Delta E_2 = \left(\frac{E_A}{2}\right)^2 \frac{a+ib}{c+id} \quad (\text{B7})$$

with the expression for a, b, c and d as given before in Section VII.

The In-phase component I_{LF} and Quadrature component Q_{LF} are now easily obtained via

$$I_{LF} = \left(\frac{E_A}{2}\right)^2 \frac{ac + bd}{c^2 + d^2} \quad (\text{B8a})$$

$$Q_{LF} = \left(\frac{E_A}{2}\right)^2 \frac{bc - ad}{c^2 + d^2} \quad (\text{B8b})$$

Since $\omega_H \gg \omega_L$ we have to replace $(E_A/2)^2$ by $(j_A/2)^2 / |Y_H|^2$ where Y_H is the interfacial admittance pertaining to the frequency ω_H [see [5] for the expression of the admittance in case of reactant adsorption].

APPENDIX C

EXPLICIT EXPRESSIONS FOR $(\partial\Gamma_O/\partial E)_\Psi$ AND $(\partial^2\Gamma_O/\partial E^2)_\Psi$ IN CASE OF A LANGMUIR ISOTHERM

Using eqn. (46) as a starting point the partial derivatives $(\partial\Gamma_O/\partial E)_\Psi$ and $(\partial^2\Gamma_O/\partial E^2)_\Psi$ are given by

$$\left(\frac{\partial\Gamma_O}{\partial E}\right)_\Psi = D_O^{-1/2} \bar{\Psi}\Gamma_m \left\{ \frac{(1+e^{-\zeta}) \frac{d\beta_O}{dE} + \frac{nF}{RT} e^{-\zeta} \beta_O}{(1+e^{-\zeta} + \beta_O D_O^{-1/2} \bar{\Psi})^2} \right\} \quad (C1)$$

and

$$\left(\frac{\partial^2\Gamma_O}{\partial E^2}\right)_\Psi = D_O^{-1/2} \bar{\Psi}\Gamma_m \times \left\{ \frac{\frac{2d\beta_O}{dE} \left(\frac{nF}{RT} e^{-\zeta} - \frac{d\beta_O}{dE} D_O^{-1/2} \bar{\Psi} \right) - \beta_O \left(\frac{nF}{RT} \right)^2 e^{-\zeta} + (1+e^{-\zeta}) \frac{d^2\beta_O}{dE^2}}{(1+e^{-\zeta} + \beta_O D_O^{-1/2} \bar{\Psi})^2} + \frac{2\beta_O \left(-\frac{nF}{RT} e^{-\zeta} + \frac{d\beta_O}{dE} D_O^{-1/2} \bar{\Psi} \right)^2}{(1+e^{-\zeta} + \beta_O D_O^{-1/2} \bar{\Psi})^3} \right\} \quad (C2)$$

References

1. P. Delahay, J. Phys. Chem., 70 (1966) 2067, 2373.
2. B. Timmer, M. Sluyters-Rehbach and J.H. Sluyters, J. Electroanal. Chem., 18 (1968) 93; 19 (1968) 73.
3. W.H. Reinmuth and K. Balasubramanian, J. Electroanal. Chem., 38 (1972) 79, 271.
4. C.A. Wijnhorst, M. Sluyters-Rehbach and J.H. Sluyters, J. Electroanal. Chem., 85 (1977) 249; 87 (1978) 17.
5. M. Sluyters-Rehbach and J.H. Sluyters, J. Electroanal. Chem., 136 (1982) 39.
6. E. Fatas-Lahoz, M. Sluyters-Rehbach and J.H. Sluyters, J. Electroanal. Chem., 136 (1982) 59.
7. J. Struys, M. Sluyters-Rehbach and J.H. Sluyters, J. Electroanal. Chem., 143 (1983) 37.
8. J. Struys, M. Sluyters-Rehbach and J.H. Sluyters, J. electroanal. Chem., 171 (1984) 157, 171.
9. J. Struys, M. Sluyters-Rehbach and J.H. Sluyters, J. Electroanal. Chem., 146 (1983) 263.

SUMMARY

In this thesis a study on the reduction mechanism of the cadmium ion Cd(II) to cadmium amalgam Cd (Hg) at the mercury/aqueous electrolyte interface is described. This system has been considered as a simple model for the study of electrode reactions for a long time. However, during the last few years it appeared that the reaction is more complicated and actually proceeds via a three step mechanism.

A direct consequence of this discovery is that the study of the influence of some parameter on the reaction can better be done by investigating the influence on separate steps than on the overall process. This is the guiding principle of this thesis.

Several electrochemical techniques can be used to study the mechanism of reduction of an electroactive species. In this thesis the used techniques are direct current, alternating current and demodulation voltammetry.

The technique first mentioned applies a direct potential across the mercury/electrolyte interface while measuring the resulting direct current.

Alternating current voltammetry, as it largely was developed in this laboratory, superimposes an alternating potential with a low amplitude on a fixed potential. The ratio of the applied alternating potential and the resulting alternating current is measured phase sensitively as a function of the direct potential and the frequency of the alternating potential. This ratio is commonly referred to as impedance.

Demodulation voltammetry, worked out in this laboratory as a further development of alternating current voltammetry, superimposes a high frequency sinusoidal current, amplitude modulated by a low frequency cosinusoidal signal, on a direct potential. The in-phase and the quadrature component of the resulting demodulation voltage, at twice the modulation frequency, is measured as a function of the direct potential with a phase sensitive detector.

From these techniques the demodulation method is well suited for studying mechanisms of electrochemical reductions accurately in a large potential range. Moreover demodulation voltammetry allows faster reduction rates to be measured as compared with direct current and alternating current voltammetry.

Several ways can be followed to study the mechanism of reduction of Cd(II) to Cd (Hg). In this thesis three experimental investigations are presented using different ways of approach to study the mechanism of reduction. Finally a theoretical study is presented considering the possibilities of the demodulation technique for studying the reduction of electroactive species in case that the reduction process is complicated by adsorption at the interface of these species (reactant adsorption).

In Chapter 2 the role of water in the reduction mechanism of Cd^{2+} to Cd (Hg) is studied. Because of hydration of the Cd^{2+} ion in an aqueous solution and because the ultimate product is cadmium in the mercury phase, next to charge transfer necessarily also dehydration has to occur. From earlier investigations it followed that the reduction process can be described by a CEE mechanism in which a chemical step precedes two electrochemical steps. The aim of this study is to investigate whether the chemical step can be related with a dehydration process or not. This can be done by performing kinetic measurements at varied solvent activity. In order to vary the water activity measurements were done at several concentrations of the inert electrolyte NaClO_4 . From the results a detailed description of the mechanism of reduction can be given. The first step of the mechanism is the fast loss of 12.5 water molecules followed by a slow 'chemical' step which clearly is not a desolvation process. Next a slow transfer of the first electron takes place followed by a fast loss of 4 water molecules, slow transfer of the second electron and eventually fast loss of the remaining 9 water molecules.

In Chapter 3 the reduction of Cd^{2+} is studied in the presence of the fluoride anion F^- which forms three different complexes with Cd^{2+} namely CdF^+ , CdF_2 and CdF_3^- . The different forms in which Cd^{2+} can be present are in principle all reducible. Consequently it is conceivable, from a theoretical point of view, that four parallel pathways of reduction occur simultaneously. The question to be answered is whether indeed four parallel ways of reaction are followed in case of the reduction of Cd^{2+} in the presence of F^- and whether there might be preferred paths. In order to find this out experiments were performed in mixtures of $(0.8-x)$ M NaClO_4 and x M NaF as base electrolytes. From the results it follows that for all values of x ($0 \leq x \leq 0.8$) a CEE mechanism is valid. From the dependence of the individual rate constants as functions of x , using theoretical expressions derived for describing the case of a multistep parallel charge transfer process, the contribution of the four pathways, at different stages of the reduction, is calculated. As a remarkable result of our work it is found that the reduction of Cd^{2+} in the presence of F^- ($x = 0.8$) mainly proceeds via the neutral CdF_2 species although only about 15% of the total Cd^{2+} (free and complexed with F^-) is present in the CdF_2 form. After CdF_2 has reached a suitable transition state ('chemical' step) it is reduced to Cd(I)F_2^- (first electron transfer) which first releases two F^- ions before the Cd^+ ion is reduced via the second electron transfer to a Cd atom which dissolves rapidly in the mercury.

In Chapter 4 the influence of an inhibitor on the rate of reduction of Cd^{2+} is investigated, taking into account the inhibition of the separate steps in the CEE mechanism. The idea behind it is that the chemical step might be influenced more strongly than the electron transfer steps, if its nature is related to reorganization of the surroundings of the cadmium ion. As an inhibitor sucrose was chosen which was added in a concentration range

$0 < x < 1$ M to a solution containing Cd^{2+} in 1 M NaClO_4 base electrolyte. From the results it follows that the separate steps all are slowed down. Comparison of the individual rate constants with (i) the surface coverage and (ii) the 'interfacial viscosity' does not give clear relations. Possibly both the frequency factor and the activation energy are influenced which makes straightforward analysis and interpretation of the results impossible. It became clear, however, that the rate of the preceding chemical step is much more sensitive to small additions of sucrose than the two electrochemical steps which might be considered as a confirmation of the idea about the nature of the chemical step mentioned before.

From our studies a deeper understanding of the mechanism of reduction of the Cd^{2+} ion to Cd (Hg) in different electrolyte solutions has been achieved. Nevertheless there are still unsolved problems among which the question of the nature of the preceding 'chemical' step in the reduction mechanism is the most fascinating.

In the last chapter a theoretical study is presented about the potentialities of the demodulation technique for the study of adsorption of electroactive species. In the development of the mathematical description the most important assumptions made are (i) the charge transfer process is reversible (ii) the adsorption/desorption process is at equilibrium and (iii) only adsorption of the Ox form of the redox couple occurs. Describing the adsorption use is made of a Langmuir adsorption isotherm. From the theoretical study performed, using an adsorption coefficient both potential dependent and potential independent, it is found that demodulation voltammetry not only can be used for accurate kinetic measurements but can be considered as a valuable technique for reactant adsorption as well.

SAMENVATTING

In dit proefschrift wordt een studie beschreven over het mechanisme van de reductie van het cadmium ion Cd^{2+} tot cadmium amalgaam Cd (Hg) aan het grensvlak tussen kwik en een waterige elektrolietoplossing. Dit geldt al lang als een eenvoudig modelsysteem bij het bestuderen van elektrode reacties. Gedurende de laatste jaren is echter gebleken dat de reactie volgens een driestaps mechanisme verloopt.

Een direct gevolg van deze ontdekking is dat bij de bestudering van de beïnvloeding van de reactie door variatie van een experimentele parameter het beter is de invloed op de verschillende stappen te bestuderen dan die op de netto reactie. Dit is het leidende principe van deze dissertatie.

Bij de studie over het mechanisme van de reductie van een elektroactief deeltje kunnen verscheidene elektrochemische technieken gebruikt worden. In dit proefschrift worden bij de uitgevoerde experimentele studies gelijkstroom-, wisselstroom- en demodulatievoltammetrie toegepast.

De eerstgenoemde techniek bestaat uit het aanleggen van een gelijkspanning over het kwik/elektrolietoplossing grensvlak. Daarbij wordt de resulterende gelijkstroom gemeten.

Bij wisselstroomvoltammetrie, ontwikkeld in dit laboratorium, wordt een wisselspanning met kleine amplitude gesuperponeerd op een gelijkspanning. Het quotiënt van de aangelegde wisselspanning en de resulterende wisselstroom wordt fasegevoelig gemeten als functie van de gelijkspanning en de frequentie van de wisselspanning. Dit quotiënt wordt de impedantie genoemd.

De demodulatietechniek, ontwikkeld in dit laboratorium als een vervolg op en uitbreiding van de wisselstroom voltammetrie methode, superponeert een hoogfrequente sinusspanning, gemoduleerd met een laagfrequente cosinusspanning, op een gelijkspanning. De resulterende demodulatiespanning, bij de dubbele modulatiefrequentie, wordt gemeten als functie van de gelijkspanning met een fasegevoelige detector.

Van de genoemde technieken is de demodulatiemethode in het bijzonder geschikt voor het bestuderen van reductiemechanismen op een zeer nauwkeurige wijze in een groot potentiaalgebied. Bovendien kunnen met demodulatievoltammetrie snellere reducties onderzocht worden dan met gelijkstroom en wisselstroomvoltammetrie.

Bij het onderzoek van het mechanisme van de reductie van Cd^{2+} tot Cd (Hg) kunnen diverse wegen gevolgd worden. In dit proefschrift worden drie experimentele onderzoeken gepresenteerd waarbij vanuit verschillende benaderingen het reductiemechanisme wordt bestudeerd. Tenslotte wordt een theoretische studie gepresenteerd waarin de mogelijkheden van de demodulatietechniek worden bestudeerd in het geval dat de reductie van het elek-

troactieve deeltje wordt gecompliceerd door adsorptie aan het grensvlak van dit deeltje (reaktant adsorptie).

In hoofdstuk 2 wordt de rol van water in het reductiemechanisme van Cd^{2+} tot Cd (Hg) bestudeerd. Naast ladingsoverdracht zal, vanwege de hydratatie van Cd^{2+} in een waterige oplossing, tijdens het ontladingsproces ook dehydratatie plaatsvinden. Uit eerdere onderzoeken volgde dat het reductieproces beschreven kan worden met een CEE mechanisme waarin voorafgaande aan beide elektronoverdrachtstappen een chemische stap plaats heeft. Doel van deze studie is na te gaan of deze chemische stap verband houdt met een dehydratatieproces. Om de wateractiviteit te variëren werd gemeten bij verschillende concentraties van de inerte elektrolyt NaClO_4 . Uit de resultaten volgt een gedetailleerde beschrijving van het reductiemechanisme bestaand uit een CEE mechanisme en een meerstaps dehydratatieproces. De eerste stap in het mechanisme is het snel afstaan van 12,5 watermolekules gevolgd door een langzame "chemische" stap die niet met een dehydratatie geïdentificeerd kan worden. Hierna vindt een langzame overdracht van het eerste elektron plaats gevolgd door een snelle afgifte van 4 watermolekules, de langzame overdracht van het tweede elektron en tenslotte het snelle afstaan van de resterende 9 watermolekules.

In hoofdstuk 3 wordt de Cd^{2+} reductie bestudeerd in aanwezigheid van het fluoride anion F^- dat drie verschillende complexen vormt met Cd^{2+} namelijk CdF^+ , CdF_2 en CdF_3^- . De vier vormen waarin Cd^{2+} voorkomt kunnen in principe alle gereduceerd worden. Hierdoor is het mogelijk, theoretisch gezien, in totaal vier parallel naast elkaar verlopende ladingsoverdrachtprocessen te hebben. De vraag die gesteld kan worden is of er inderdaad vier parallelle reaktiewegen gevolgd worden bij de reductie van Cd^{2+} in aanwezigheid van F^- of dat er bepaalde voorkeurswegen zijn waarlangs het reductieproces verloopt. Daartoe zijn experimenten uitgevoerd in mengsels van $(0,8-x)\text{M NaClO}_4$ en $x\text{ M NaF}$ als drager elektrolyt. Uit de resultaten volgt dat voor alle waarden van x ($0 \leq x \leq 0,8$) een CEE mechanisme geldig is. Uit het verloop van de individuele reaktiesnelheidsconstanten als functie van x is, via een hiervoor opgestelde theorie, de bijdrage berekend van de diverse reaktiewegen voor de verschillende stadia van de reductie. Als opmerkelijk resultaat is gevonden dat de reductie in aanwezigheid van F^- (bij $x = 0,8$) voornamelijk verloopt via het neutrale CdF_2 hoewel dit deeltje slechts ca. 15% vormt van alle aanwezige Cd^{2+} (vrij en gecomplexeerd met F^-) ionen. Nadat CdF_2 in een geschikte overgangstoestand is gekomen ("chemische" stap) wordt het gereduceerd tot Cd(I)F_2^- (eerste elektronoverdracht) dat daarna eerst beide F^- -ionen afstaat waarna het ontstane Cd^+ -ion wordt gereduceerd via een tweede elektronoverdracht tot een Cd-atoom dat snel oplost in het kwik.

In hoofdstuk 4 wordt de invloed van een inhibitor op de snelheid van de reductie van Cd^{2+} onderzocht, waarbij de inhibitie van de afzonderlijke reaktiesnelheidsconstanten in het CEE mechanisme wordt nagegaan. Dit met het oogmerk om uit een mogelijk verschil

in remming van de voorafgaande chemische en beide elektrochemische deelstappen meer inzicht te verkrijgen in de aard van de voorafgaande chemische stap. Als inhibitor is sucrose gekozen dat in een concentratie $0 < x < 1$ M werd toegevoegd aan een oplossing bevattend Cd^{2+} en 1 M NaClO_4 als dragerelektrolyet. Uit de resultaten volgt dat de snelheid van alle afzonderlijke stappen wordt geremd. Vergelijking van de individuele reactiesnelheidsconstanten met (i) de oppervlaktebedekkingsgraad en (ii) de viscositeit aan het grensvlak levert geen duidelijke relaties op. Mogelijk wordt zowel de frequentiefactor als de aktiveringsenergie beïnvloed waardoor éénduidige analyse en interpretatie van de resultaten niet uitvoerbaar is. Wel is duidelijk geworden dat de snelheid van de voorafgaande chemische stap aanzienlijk gevoeliger is voor geringe sucrose toevoegingen dan de beide elektrochemische stappen waaruit zou kunnen worden geconcludeerd dat de chemische stap betekent het langzame ontstaan van een configuratie gunstig voor een elektron overdracht.

Uit de verrichte experimentele studies is een aantal nieuwe inzichten verkregen met betrekking tot het reductiemechanisme van het Cd^{2+} -ion tot Cd (Hg) in verschillende elektrolytoplossingen. Desalniettemin zijn er nog onopgeloste problemen zoals bijvoorbeeld een verklaring voor de voorafgaande "chemische" stap in het reductiemechanisme zodat verder onderzoek vereist is.

In het laatste hoofdstuk wordt een theoretische studie gepresenteerd waarin de mogelijkheden worden onderzocht om adsorptie van het elektroaktieve deeltje te bestuderen met demodulatievoltammetrie. Bij het ontwikkelen van de benodigde mathematische beschrijving zijn als belangrijkste fysische aannamen gebruikt dat (i) de ladingsoverdracht reversibel verloopt (ii) het adsorptie/desorptieproces in evenwicht is en (iii) alleen adsorptie van de Ox-vorm optreedt. Voor de beschrijving van de adsorptie is gebruik gemaakt van een Langmuir adsorptie isotherm. Uit de verrichte theoretische studie, waarbij de adsorptiecoëfficiënt zowel potentiaal afhankelijk als potentiaal onafhankelijk werd gekozen, volgt dat demodulatievoltammetrie niet alleen toegepast kan worden voor nauwkeurige kinetische metingen maar dat zij ook een waardevolle techniek is voor reaktant adsorptiestudies.

CURRICULUM VITAE

De schrijver van dit proefschrift werd geboren op 13 september 1960 te Waalwijk. Na het behalen van het HAVO en Atheneum B diploma aan het Willem van Oranje College te Waalwijk werd in 1979 begonnen met de studie Scheikunde aan de Rijksuniversiteit Utrecht. In mei 1984 werd het doctoraal examen scheikunde afgelegd met als specialisatie chemie van de vaste stof en als bijvak Fysische en Colloidchemie.

Op 1 juli 1984 trad hij in dienst van de Rijksuniversiteit Utrecht als medewerker bij het Van 't Hoff laboratorium voor Fysische en Colloidchemie in de werkgroep Electrochemie, waar het in dit proefschrift beschreven onderzoek werd verricht. Na beëindiging van het dienstverband aan de Rijksuniversiteit Utrecht is hij sedert 1 september 1988 werkzaam als electrochemicus bij de Nederlandse organisatie voor Toegepast Natuurwetenschappelijk Onderzoek te Delft.